NON-INVASIVE INVESTIGATION OF HUMAN FOOT MUSCLES FUNCTION

ELISABETTA FERRARI

PhD

January 2018

NON-INVASIVE INVESTIGATION OF HUMAN FOOT MUSCLES FUNCTION

ELISABETTA FERRARI

A thesis submitted in partial fulfilment of the requirements of the Manchester Metropolitan University for the Degree of Doctor of Philosophy

School of Healthcare Science

Manchester Metropolitan University

2018

Declaration

No portion of the work referred in this thesis has been submitted in support of an application for another degree or qualification at this, or any other university, or institute of learning.

Date:

Signed:

Acknowledgements

Firstly, I would like to thank my Director of Studies, Dr Emma Hodson-Tole, for her continuous and invaluable support and help in any circumstance of my PhD journey. This work would not have been possible without her support.

I would then like to thank my supervisors, Dr Glen Cooper and Professor Neil Reeves, for their precious help and feedback throughout my PhD.

I would like to thank all those people who crossed my path during this insane, yet fulfilling journey. First of all, Pete, Diego, Rachel, Kate and Maria who filled my days of laughter and happiness for the first part of my PhD.

I would then like to thank Elisa and Aron, who treated me like a real sister since I joined our lovely “Mediterranean” office on the third floor. Those were really the best times!

I would like to thank my dear Suzi, who always has nice and encouraging words for me and with whom we can be science nerds together!

I would like to thank Greg May, for his absolutely invaluable help in the lab during my data collection. I would then like to thank all of my participants, who patiently and kindly took part to my protocol.

On a more personal side, I thank from the bottom of my heart my mom and dad, who took part to this journey from a distance, but with continuous support and love.

My lifetime best friends Alessandra and Silvia, who continuously support me and are always there to listen to me.

Last, but not least, I would like to thank my beloved fiancé Fabrizio. He is my light in the darkness and I could not have done it without his support. During really tough times, he was there, and I will be forever grateful for this.

Table of Contents

List of Figures

List of Tables

Abbreviations

QP- Quadratus Plantae

TA – Tibiali anterior

FDL- Flexor digitorum brevis

LA- Longitudinal Arch

IFM – Intrinsic Foot Muscles

AH- Abductor hallucis

FDMB – Flexor Digiti minimi brevis

FHB – Flexor Hallucis Brevis

ADM – Abductor Digiti minimi

PCSA – Physiological Cross-sectional area

EFM – Extrinsic Foot Muscles

EMG – Electromyography

MU – Motor Unit

IZ – Innervation Zone

MUAP – Motor Unit Action Potential

MUAPT – Motor Unit Action Potential Train

IED – Inter- eletrode distance

MTP – Metatarsophalangeal

MVC – Maximum voluntary contraction

MLA – Medial longitudinal arch

sEMG – Surface Electromyography

CoG_E – EMG intensity based Centre of Gravity

CoG_{SE} – Sample Entropy based Centre of Gravity

CoP – Centre of Pressure

SampEn – Sample Entropy

MA – Medial Arch

ANK – Ankle

KN – Knee

RMS – Root Mean Square

Abstract

Appropriate functioning of the human foot is fundamental for good quality of life. The intrinsic foot muscles (IFM) are a crucial component of the foot, but their natural behaviour and contribution to good foot health is currently poorly understood. Recording muscle activation from IFM has been attempted with invasive techniques, but these generally only allow assessment of one muscle at a time and are not much used in many clinical populations (e.g. children, patients with peripheral neuropathy or on blood thinning medication). Here a novel application of multi-channel surface electromyography (sEMG) electrodes is presented to non-invasively, record sEMG and quantify activation patterns of IFMs from across the plantar region of the foot.

sEMG (13×5 array), kinematics and force plate data were recorded from 30 healthy adult volunteers who completed six postural balance tasks (e.g. bipedal stance, one-foot stance, two-foot tip-toe). Linear (amplitude based) and non-linear (entropy based) methodologies were used to evaluate the physiological features of the sEMG, the patterns of activation, the association with whole body and foot biomechanics and the neuromuscular drive to the IFM.

EMG signals features (amplitude and frequency) were shown to be in the physiological ranges reported in the literature (Basmajian and De Luca, 1985), with spatially clustered patterns of high activation corresponding to the *Flexor digitorum brevis* muscle. IFMs responded differently based on the direction of postural sway, with greater activations associated with sways in the mediolateral direction. Entropy based, non-linear analysis revealed that neuromuscular drive to IFM depends on the balance demand of the postural task, with greater drive evident for more challenging tasks (i.e. standing on tip-toe). Combining non-invasive measures of IFM activation and entropy based assessment of temporal organisation (or structure) of EMG signal variability is therefore revealing of IFM function and will enable a more detailed assessment of IFM function across healthy and clinical populations.

1. Introduction

The human foot is critical for a wide range of activities of daily living. However, there are many pathologies that have direct clinical implications for foot function, influencing factors such as balance and mobility, which can have a major impact on a person's quality of life (Rodriguez-Sanz et al, 2018). Issues associated with foot health can be structural (e.g. hallux valgus, pes cavus) and/or functional (hallux limitus and hallux rigidus) and can be associated with also ageing and a range of common chronic diseases, including diabetes mellitus where peripheral neuropathy and foot ulcerations are common. It is estimated to cost the NHS £14 billion pounds a year to treat diabetes and its complications, with the cost of treating complications representing the much higher proportion of the cost (Executive 2009-2010). In addition, care is required for many with conditions such as arthritis, children growing with conditions such as cerebral palsy and recreational and professional sports people who sustain foot injury, although care costs for these conditions are not well documented. Taken together, diagnosis and treatment of pathologies affecting the foot place significant clinical and economic demands to UK healthcare providers. Understanding the features of good foot health and characteristics that underpin appropriate function is therefore important in a range of health-related fields. In order to appreciate the contribution of intrinsic foot muscles to foot health it is required to study their behaviour in vivo. At the moment only limited information can be extracted from a restricted population of people. This thesis therefore lays the foundation from which wider investigation of foot function may be conducted and therefore in the future enable the relationship between function and health be probed.

The anatomy of the foot is complex, with different segments and layers of tissue interacting to provide an anatomically confined yet flexible structure that facilitates motion (Kelly et al., 2014; Bates et al., 2013; McKeon et al., 2014). In the plantar aspect of the foot there are four layers of intrinsic foot muscles arranged in a narrow compartment (McKeon et al., 2014), and their anatomical positioning provides challenges to quantifying features of anatomy and activation during weight bearing tasks. A few studies have investigated intrinsic foot muscle properties and have shown the importance of this group of muscles in supporting the arch and the foot during stance and postural tasks. However, these studies have focused on a single or small selection of muscles and tend to use invasive intramuscular electromyographic (EMG) techniques (Reeser et al, 1983; Kelly et al., 2012; Kelly et al, 2014;Fiolkowski et al 2003). Whilst providing useful insight, these approaches cannot be applied to all populations (e.g. diabetes patients, young children), where insertion of a needle is undesirable or could be contraindicated. Moreover, by recording from single channels, information about interactions between or within regions of the intrinsic foot muscles cannot be probed, although such information is required for wider aspects of foot function to be evaluated in healthy and pathological populations.

Recent advances in technology have led to the development of multi-channel electrode grids that allow the processing of myoelectric signals as topographical maps quantifying both spatial and temporal features of signals (Rojas-Martínez et al., 2013; Holtermann et al., 2009) across a region. However, to date, there have been no attempts to investigate the features of intrinsic foot muscle activation using these non-invasive approaches. In addition, while amplitude based measures of myoelectric signals provide insights into the level of engagement of these muscles, these methodologies fail to investigate the neuromuscular mechanisms underpinning motor control. Changes in the

complexity of motor patterns have recently been related to changes in motor strategies and muscle firing patterns (Rathleff et al., 2011). However, fluctuations and short-term variations within a biological signal have recently been reconsidered not as noise or disturbances, but as a way of assessing important aspects of motor control (Svendsen and Madeleine, 2010). One way to quantify these fluctuations is to use non-linear analyses such as entropy measures. To date however, there is no evidence that these approaches have been used to provide insights into control strategies underpinning healthy or pathology affected intrinsic foot muscle activation patterns.

The overarching aim of the work presented in this thesis was to investigate the potential value of non-invasively evaluating intrinsic foot muscle behaviour using multi-channel surface electrode arrays The objectives were therefore to: i) investigate the feasibility of recording reliable surface EMGs with a grid of electrodes on the plantar aspect of the foot and investigate patterns of amplitude and signal structure distribution (Chapter 4); ii) investigate the association between the medial arch and intrinsic foot muscles activation patterns (Chapter 5) and iii) investigate the neuromuscular drive properties of intrinsic foot muscles using non-linear entropy based approaches (Chapter 6).

2. Literature review

2.1. The origin of the human foot

The human foot has evolved from one similar to that of African apes, where it assisted in both arboreal and terrestrial locomotion, to a structure that reflects a shift to locomotor habits dominated by bipedalism (McKeon et al., 2014). The key events marking the evolution from African ape-like to human bipedality includes enlargement of the calcaneal tuberosity, stabilization of the calcaneocuboid and talo-navicular joints, formation of hallux and formation of a medial longitudinal arch (Figure 2.1) (Crompton, Vereecke et al. 2008).

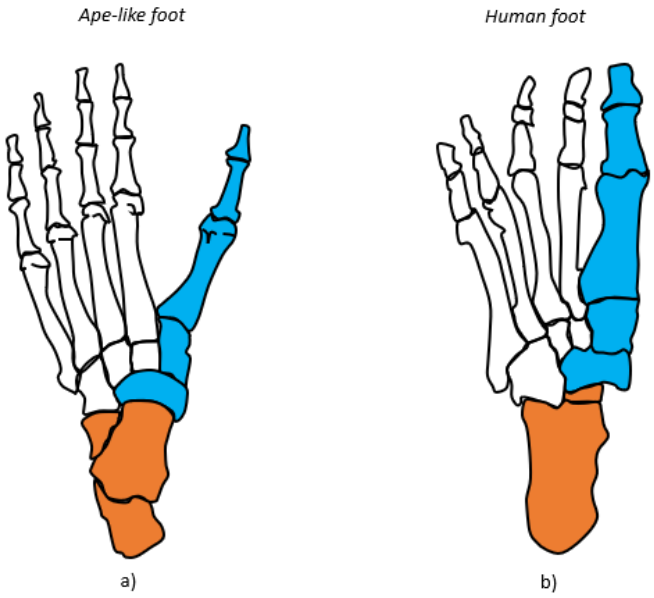

Figure 2-1 Representation of ape-like foot (a, based on (Harcourt-Smith and Aiello, 2004)) and human foot (b, based on (Kelly et al., 2012)). The calcaneus (orange shading) changed shape between the ape-like and human foot, together with the formation of the hallux (blue shading), both providing more support and stability.

Humans are the only living primates characterized by a permanently arched foot (Reeser et al., 1983) and have shorter phalanges than primates, which may be the result of reduced prehensile use of the toes (Soysa et al., 2012)

The modern foot is a multi-joint structure and, together with the lower limb, forms the ankle joint complex, a fundamental connection for the interaction of the lower limb and ground during locomotion (Leardini et al., 2007). The structure of the human foot has been functionally adapted to improve postural stability and weight-bearing capacity for upright posture and locomotion (Crompton et al., 2008) and to absorb energy of impact and transmit propulsive forces from the rest of the body to the ground (Fiolkowski et al., 2003). It adapts to movement, during walking, by changing from a compliant, shock-absorbing, supinated structure before heel-strike to a rigid lever at toe-off (Crompton et al.,2008, McKeon et al., 2014). The complexity of the foot structure makes it challenging to investigate the full functional significance of the associated musculature, which is currently still poorly understood.

To fully understand foot function, we need to understand skeletal muscle structure and function and how to best study it.

The following sections will therefore detail aspects of skeletal muscle structure and current state-of-the-art approaches for the study of in vivo activation dynamics. Then a review in more detail of the anatomy of the human foot, including current literature relating to the study of foot properties during locomotor and postural tasks will be provided.

2.2. Skeletal muscle anatomy

Muscles are defined as the active elements of the musculoskeletal system, whereas tendons are the passive elements connecting muscles to the skeleton. Tendons are primarily made of collagen fibres, bundled together in a parallel direction along the axis of the tendon. This arrangement produces a structure that is stiff and high in tensile strength, but lacking in resistance to compression or shear. On the other hand, muscles are able to actively contract, generating forces to move the skeleton and control movement.

Skeletal muscles are composed of a highly organised hierarchical structure, with the basic unit being the sarcomere. Each sarcomere is made up by parallel bands of thin filaments alternated with thick filaments along the fibre direction. The thick filament is a group of myosin proteins with tails (pointing at the centre of the sarcomere) and the head (pointing in the opposite direction) (Figure 2.2). The main component of the thin filament is a globular protein called actin, organised in chains twisted into a helix configuration. The structure is stiffened by the protein tropomyosin, with troponin proteins complexes attached along the actin filament. The Z-lines define the borders of one sarcomere, whereas the M-line defines the centre (Figure 2.2). In addition, the myosin is attached to the Z-line through a protein called titin, which is believed to act as a spring and maintain the equilibrium between the two halves of the sarcomere during contraction (Herzog et al., 2015).

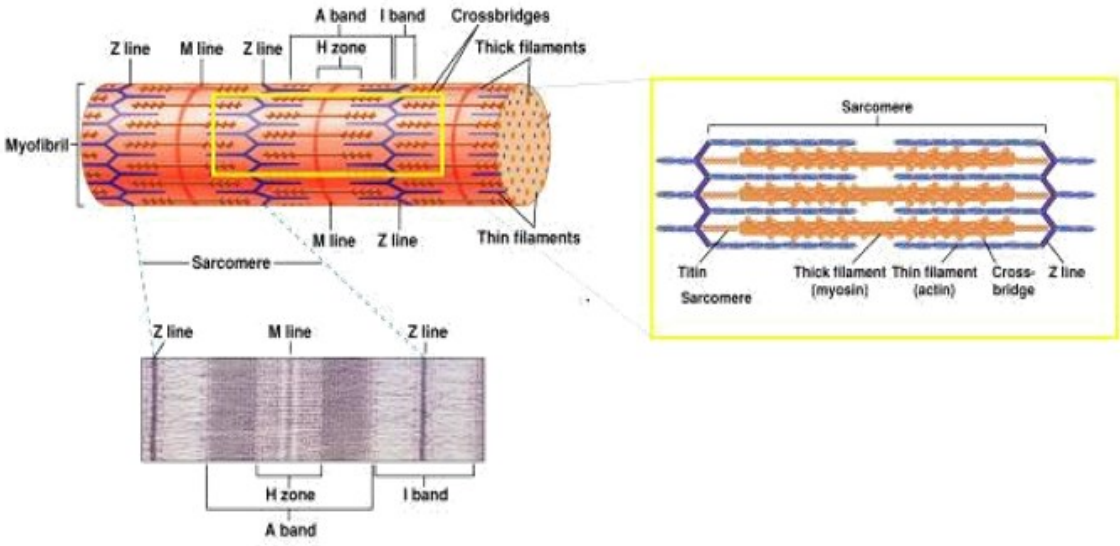

Figure 2-2 A myofibril with multiple sarcomeres. Each sarcomere is composed of actin and myosin, but also the Titin, which functions as a molecular spring which is responsible for the passive elasticity of muscle. On the bottom of the figure an electron microscope image of a single Sarcomere, where the Z-lines look like black bands defining the borders of the structure. Extracted from (Germann and Stanfield 2003). Magnification level not available.

Many sarcomeres together form a myofibril and many myofibrils compose a muscle fibre (Figure 2.3). Muscle fibre have different properties (in terms of contraction, speed, force,..) and these categories can be classified by oxidative/glycolytic enzyme levels (fast fatiguing vs. fatigue-resistant); mechanical twitch characteristics (fast vs slow twitch) and myosin heavy change composition (Type I slow twitch fibres, IIA fast oxidative fibres, IIB fast glycolytic fibres in humans) (Schiaffino and Reggiani, 2011) and these different properties enable skeletal muscles to meet the mechanical demands of the wide range of movement task completed across everyday life.

Muscle fibres are part of a more composite unit called the Motor Unit (MU), which consists of a motor neuron, its axon and all the muscle fibres innervated by the axonal

branches (Sherrington, 1925). A single motor unit may occupy a relatively large portion of a cross section of a muscle, called the motor unit territory (Figure 2.2), but can also be spatially localised (Vieira et al., 2011).

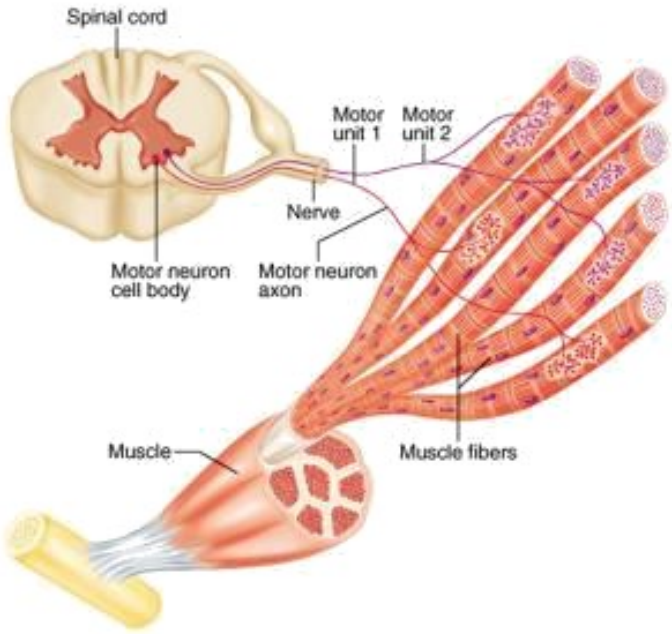

Figure 2-3 A motor unit is connected from the spinal cord to muscle fibres and transmits the signal generated at the spinal level through the muscle. The motor unit territory is represented with the dotted region on the fibres. Figures extracted from (McGinnis, 2013)

The motor neuron is a cell in the Central Nervous System made up of a nucleus in the spinal cord and the axon innervating a group of muscle fibres with synaptic connections (Figure 2.3.). At the level of the spinal cord an excitatory impulse is driven to sensory and motor afferents and then to the muscle fibres. The area where the terminal branches reach the muscle fibres is called the Innervation Zone (IZ) (Merletti and Parker, 2004). When the electrical impulse from the motor neuron reaches the muscle fibres, acetylcholine diffuses across the synaptic cleft and increases the permeability of the postsynaptic terminal to Sodium (Na+) (Figure 2.4). When the electrical impulse spreads along the fibres, calcium ions (Ca^{2+}) are released from the

sarcoplasmic reticulum into the sarcomere. The calcium attaches to troponin protein, which causes troponin structure to modify and make available an active binding site on the actin filament. This allows the myosin head to attach to the actin filament and form the so called Cross-Bridge (Huxley, 1957). This is possible as a consequence of the hydrolyzation of ATP bound to the myosin head, which releases the energy necessary to move the head and the actin filament toward the centre of the sarcomere. During a contraction, the interaction between actin and myosin is cyclic, requiring a continuous ATP supply with the amount of Ca^{2+} released in part determining the number of cross-bridges formed (Huxley, 1957).

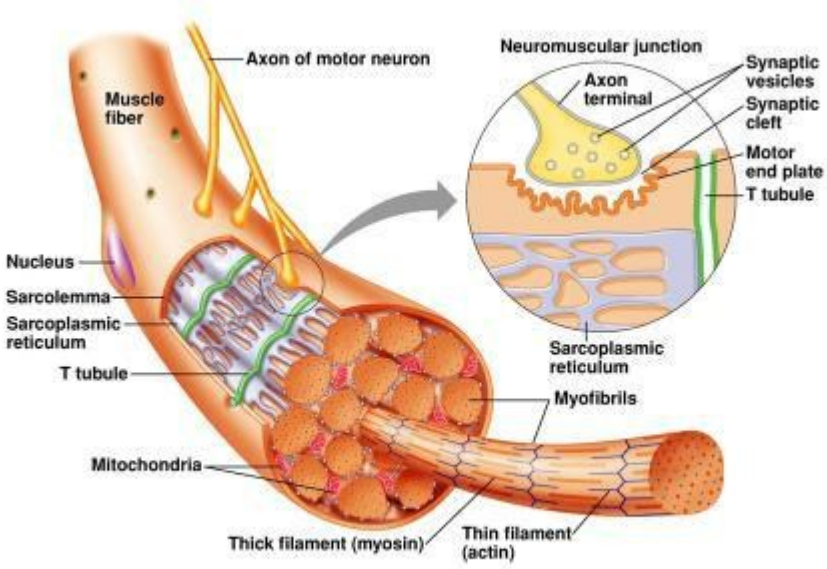

Figure 2-4 A myofibril with multiple sarcomeres. Each sarcomere is composed of actin and myosin, but also the Titin, which functions as a molecular spring which is responsible for the passive elasticity of muscle. Titin is also related to the maintenance of attached cross-bridges beyond the position initially calculated. On the bottom of the figure a microscope image of a single Sarcomere, where the Z-lines look like black bands defining the borders of the structure.

During voluntary contractions a defined pattern of motor unit recruitment is followed as the tension in the muscle increases (Henneman and Olson, 1965). The first motor units recruited are the small motor units, with a lower firing rate. These motor units have the least number of muscle fibres and a larger percentage of slow-twitch fibres (type I). As greater tension is produced, larger motor units with more fast-twitch fibres (type II) are recruited. At maximal tension, all the motor units have been recruited, and the firing rate is high. This recruitment strategy is called 'the size principle' (Henneman and Olson, 1965). In addition, smaller motor units have smaller diameter nerve axons, which result in slower action potential conduction velocities along them (Merletti and Parker, 2004). The size principle therefore predicts that, based on both contractile properties and nerve action potential conduction velocities, faster motor units will be recruited after slower motor units have been activated and will be the first motor units to be de-recruited. In the study of motor unit recruitment and activation patterns a key phenomenon is the voltage-dependent behaviour of the membrane permeability to Sodium (Na+), Potassium (K^-) and Calcium (Ca^+) ions. The dynamics of sodium and potassium conductance produces a transient membrane voltage, which is referred to as an Action Potential (Merletti and Parker, 2004). The action potential changes the permeability of the surrounding ion channels, creating a chain reaction of depolarization and repolarization along the fibre that propagates the action potential and creates trains of travelling action potentials (Pandy, 2000). These potentials can be recorded using electromyography (EMG) techniques, which are described in detail in the next section.

Motor unit recruitment patterns are still of great interest as some studies have suggested that it is not always respected. A review article (Hodson-Tole and Wakeling, 2009) highlighted that many factors (such as mechanics, sensory feedback, and

central control) could potentially affect the way motor units are recruited. During natural movements the motor unit recruitment patterns vary (not always holding to the size principle) and it is suggested that motor unit recruitment is likely related to the mechanical function of the muscles. It is therefore required to understand how recruitment is controlled during different movement tasks. For instance, when populations of motor units are studied, by analysing myoelectric signals, the presence of functional task groups of motor units within the muscle is likely to result in the identification of differential activation of motor units, therefore it does not necessarily indicate the following of the predicted motor unit recruitment pattern dictated by the size principle. Understanding this is therefore fundamental to investigate properties of muscle functions in specific body compartment and during different motor tasks.

2.3. Electromyography (EMG)

2.3.1. What is the EMG signal?

The summation of single fibre action potentials from an individual motor unit is called the Motor Unit Action Potential (MUAP). For each motor unit, it is possible to observe a series of MUAPs, the temporal summation of which is called the Motor Unit Action Potential Train (MUAPT). The electromyographic signal, or EMG, is the algebraic summation of MUAPT for different active motor units (Figure 2.5).

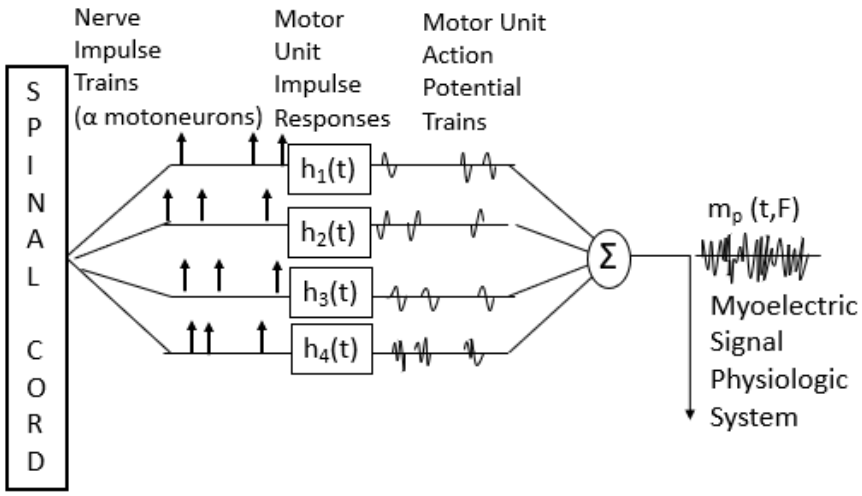

Figure 2-5 Schematic representation of EMG signal generation (based on Stashuk, 1999) . From the nucleus of the motorneuron in the spinal cord, electrical impulses are sent through the nerve axons (Nerve Impulse Trains). They reach the muscle fibres of the Motor Unit. The response of each motor unit can be modelled with a transfer function [$h_i(t)$] which is then convoluted with the Nerve Impulse Train to generate the MUAPT. The summation of MUAPT of different Motor Unit creates EMG signal.

The EMG signal is often referred to as an interference signal, as it is not a periodic signal with a defined shape such as the ECG signal. EMG represents the motor unit action potentials from the active motor units (Lindstrom and Magnusson 1977) during a contraction. By applying a detecting electrode in the proximity of the activated motor units, it is possible to record the EMG signal. The signal contains information on the timing and amplitude of motor unit activation and its frequency component is determined by the shape and conduction velocity of the motor unit action potentials. The recording, decoding and extraction of information from an EMG signal is fundamental to understanding how the signal reflects mechanisms underpinning muscle contraction and the resulting skeletal motion.

2.3.2. Recording Electromyographic Signals

EMG can be detected via the use of intramuscular or surface electrodes placed at a distance from the sources (Merletti and Parker, 2004). The tissues separating the sources and the recording electrodes acts as a so-called volume conductor. The volume conductor properties largely determine the features of the detected signals, in terms of frequency content and of distance beyond which the signal can no longer be detected, as it acts as a spatial filter between the source and the detection electrode.

Intramuscular recordings involve the insertion of a needle/fine wire electrode through the skin and into the targeted muscles, often with the help of an ultrasound scanner. The effect of tissues between electrodes and muscle fibres is therefore relatively small due to the closeness of the recording electrodes to the sources. Intramuscular electromyography is therefore well suited for the detection of changes in motor unit size and internal structure, so the objective of using intramuscular techniques is typically to study physiology and pathology at the level of individual motor units (Adrian and Bronk, 1929).

Surface recordings involve recording the superficial representation of the action potential from a portion of muscle, by a single or multi-channel electrode placed onto the skin surface. In this case, the volume conductor constitutes an important low-pass filtering effect on the EMG signal, which is therefore attenuated by the tissue in between (Basmajian and De Luca, 1985). Surface electrodes are usually better suited for studies in which information is required about the gross aspects of behaviour, such as temporal pattern of activity or fatigue (Bonato et al., 2001) of the muscle as a whole or across muscle groups. Historically, surface EMG was recorded with a one-channel system,

which allows the investigation of a limited muscle portion particularly in muscles with pennate fascicle architecture (Vieira et al., 2015). With advances in technology surface EMGs can now be recorded with multi-channel electrode arrays, comprising up to 64 channels (Masuda and Sadoyama, 1987).

While the standard single-channel bipolar recording provides a one-dimensional signal, a two-dimensional grid of electrodes performs a sampling of the muscular electrical activity over a large surface area. The recorded signal has two spatial and one temporal dimension. The characteristics of the multi-channel interference pattern can be associated with the level of muscle activation using topographical EMG representations (Figure 2.6), i.e. maps of electric potential (Kleine et al., 2007).

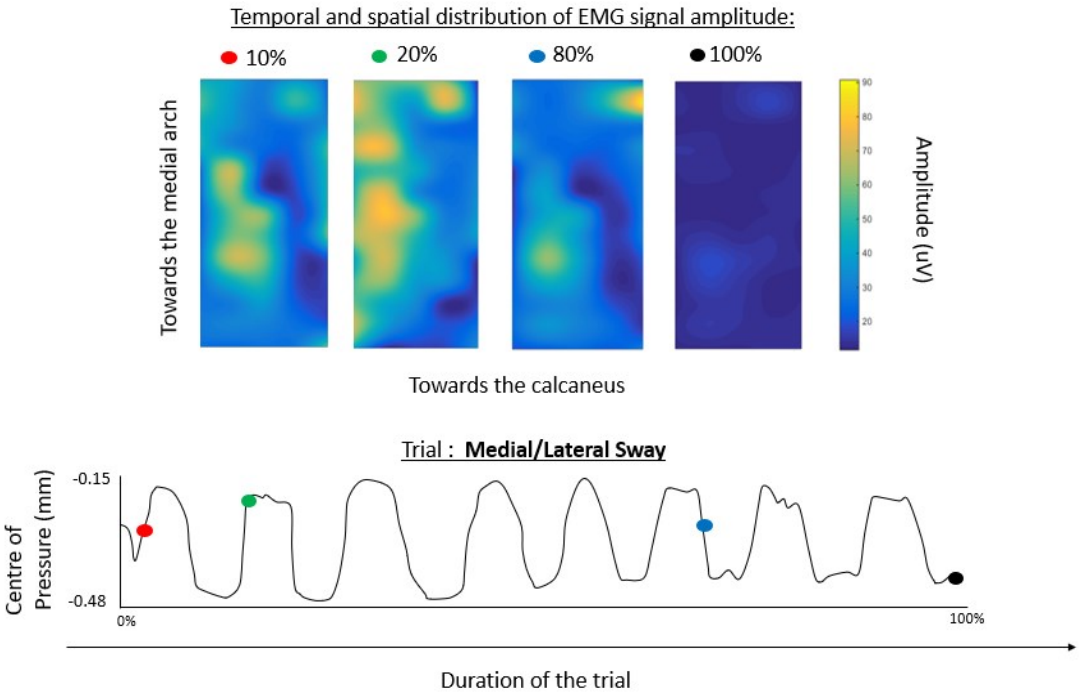

Figure 2-6 Example of temporal and spatial distribution of EMG signal amplitude for a representative participant and trial (medial/lateral sway). Each coloured dot represents a selected time point (or epoch) with a spatial ditribution of signal amplitude. Yellow regions represent high amplitude values, whereas blue regions represent low amplitude values.

2.3.3. Analysis of EMG signal

EMG feature extraction is the first step to understand the information provided by the signal on muscle function. There are a wide number of analysis methods applicable to EMG, but they can be divided in three main categories: time domain, frequency domain or time-frequency domain. Since EMG is a non-stationary signal with both time and frequency domain, the use of a methodology providing simultaneous information of time and frequency feature is the most suitable. One of these methodologies, which has been widely applied to EMG, is the Wavelet Transform. Some studies have indicated that different locomotor demand have an effect on the EMG signal at specific times and frequencies (Wakeling et al., 2002), therefore being able to simultaneously decipher time and frequency feature is essential to provide a full description of EMG information (Wakeling et al., 2002).

2.3.3.1. Wavelet analysis of EMG signal

Standard methodology to process surface EMG signal are based on analysis of amplitude parameters (Root Mean Square, Average Rectified values,…) and frequency content, usually performed with Fourier Transform. This tool requires the application of a window to the EMG signal, where the signal can be considered stationary (Wigner-Ville principle). However, by applying a window, information within the EMG signal with different time resolution, can potentially be lost. Time resolution is fundamental and has to be of the order of the physiological responses of the muscles. Von Tscharner (2000) proposed an EMG specific wavelet transform that allows the decomposition of the signal into short bursts of oscillations, with an appropriate time resolution with regard force production. Each burst of oscillations is defined by a specific frequency distribution

representing the underlying process (von Tscharner 2000). Each wavelet is a small wave defined in both time and frequency with an integral of zero. For each wavelet a central frequency is defined as:

$$f_c(k) = \frac{(k+c_1)^{c_2}}{c_3} \qquad (2.1)$$

Where c_1, c_2, c_3 are scaling factors and k is the number identifying each wavelet. The time resolution is defined by c_3, whereas c_2 defines the degree of overlap between wavelets, but the three scaling factors need to be selected based on the time resolution required and on the response time of a muscle activation process. For each wavelet analysis application, a bank of k wavelet is defined based on the sampling frequency of the EMG signal, with centre frequency calculated with Equation (2.1), with these f_c occurring at the amplitude maximum of the wavelet in the time domain. Wavelets are then convoluted with the EMG signal, which is similar to bandpass filtering the EMG signal with the same frequency characteristic of each wavelet. It is then possible to calculate the intensity spectrum of the EMG signal and an instantaneous frequency.

To obtain the EMG intensity, the power within the signal at each wavelet domain is calculated at each time point from the magnitude. The EMG intensities computed using this wavelet analysis represent the power within the EMG signal for any given time and frequency band. EMG power spectrum is calculated from the square of the Fourier-transformed EMG signal (Lindstrom et al., 1970). In contrast, root-mean-square analysis of EMG signal computes the amplitude, and not the power, of the EMG signal as a function of time. The square of such a root-mean-square value is comparable with half the intensity obtained from this wavelet analysis. The total intensity of the signal can then be calculated at a given time by summing the intensities over the k number of

wavelets selected. Moreover, a mean frequency f_m can be calculated as the mean of the instantaneous frequency. It is comparable to the mean frequency generally used in EMG studies, but with the advantage that it can be calculated at each time point as:

$$f_m = \frac{\sum_k f_c(k) i_{j;k}}{\sum_k i_{j;k}} \qquad (2.2)$$

where $i_{j;k}$ is the intensity calculated at each time point *j* and wavelet domain *k*.

Wavelet analysis has been used for investigation of motor unit recruitment patterns (Hodson-Tole and Wakeling 2007, Lee et al., 2011, Hodson-Tole et al., 2012) and the characteristics (time and level of activation) in different motor unit's recruitment patterns (Lee et al., 2011) as it provides a suitable analysis tool to gain increasing insights into the patterns of motor unit recruitment during locomotion. Moreover, being based on specific time resolution it can be applied to study muscle activation patterns with standardised protocols facilitating more robust comparison of results across different data sets.

2.3.3.2. Topographical mapping of surface EMG

The use of high-density surface EMG allows investigation of the spatial distribution of electric potentials over the skin surface during muscle contraction (Farina et al, 2008). By placing a two-dimensional electrode array a topographical representation of the electrical activity over the skin plane can be made (Farina et al., 2008) and the characteristics of this multi-channel pattern can be associated with the level of muscle activation (Merletti et al., 2008). The use of maps of electric potentials have enabled investigation of spatial information in studies on upper trapezius (Falla and Farina, 2008), upper and forearm muscles (Rojas-Martínez et al., 2012, Gallina and Botter,

2013), erector spinae (Tucker et al., 2009) and intrinsic hand muscles (Yang et al., 2011). Investigation of EMG amplitude distribution over the upper trapezius has shown the inhomogeneous distributions (Holtermann et al., 2005), that might reflect either the motor unit recruitment pattern heterogeneity or the distribution of motor units within the muscle.

One way of characterising the spatial information of the topographical maps is the calculation of an EMG amplitude-based centre of gravity (Farina et al., 2008). This analysis provides information on how the maximum EMG intensity shifts during muscle contraction and, provides potential insights into motor unit recruitment patterns (while the centroid shifts, more motor unit are recruited). Farina et al (2008) showed that the centroid of the EMG amplitude map moved in the cranial direction during submaximal contraction in the upper trapezius and this event seemed to be correlated with additional recruitment of new motor units in the cranial portion of the muscle (Falla and Farina, 2008).

In the intrinsic hand muscles, EMG maps showed that in one muscle, *Flexor digitorum superficialis*, the spatial activation depended and varied with each finger's force production and specific task (Yang et al., 2011). Martinez et al (2012) used 2-dimensional arrays to investigate the areas where EMG amplitude is maximal in the forearm and upper arm and to analyse patterns in the activation maps associating them with four movement directions at the elbow joint and with different strengths of the same movements. This allowed the extraction of features depending on the spatial distribution of motor unit action potentials and on the load-sharing between muscles, in order to have a better differentiation between tasks and effort levels. Results showed that the use of multi-channel information was able to discern between tasks and effort

levels and therefore might potentially be useful in application where identification of movement intention is needed.

2.3.3.3. Non-linear analysis techniques

Linear analysis or scale-based measures provide important information on the magnitude of a time series but ignore the temporal structure of it. With these measures interpretation of temporal changes due to adjustments of the neuromuscular control strategy are difficult to quantify (Baltich et al., 2014). Application of non-linear analysis to physiological signals, such as ECG, EMG, is a valuable tool to understand underlying mechanisms (hidden information from time series) (Richman and Moorman, 2000). As previous studies have indicated, variability is not random like noise, but reveals a degree of order that can be attributed to the operation of an adaptive control system (Slifkin and Newell, 1999). Variability within a biological data set is, therefore, not defined only by standard deviation, but through examination of the temporal pattern of variability in the movement data (Yentes et al., 2013; Svendsen and Madeleine, 2010).

Such non-linear analyses are based on entropy measures that are considered to provide a method of quantifying the complexity of a signal produced by a system (Richman and Moorman, 2000). The analysis of the variability and the short-term fluctuations within a signal can therefore be used to quantify the underlying control process (Harris and Wolpert, 1998).

Entropy measures are considered particularly suitable for biological signals (Rathleff et al., 2011), as entropy addresses the randomness and regularity of a system (Pincus, 1991) and it is a measure of the rate of information creation (Zhang et al., 2016). Entropy

quantifies the predictability of the signal investigated with higher values indicating a more complex structure and lower predictability of the time series (Richman and Moorman, 2000). There are a few entropy-based analyses, which have been applied to biological dataset and they are described in the following sections.

2.3.3.3.1. Shannon Entropy

Shannon entropy provides an indication of the structure of a signal, where a higher value suggests a random signal. Lower values indicate less randomness in the time series and a greater regularity within the signal.

Shannon entropy is defined as:

$$\sum_{i=1}^{n} p(x_i) log_a p(x_i) \quad a>1, \text{ (Eq 2.1)}$$

Where x_i is the parameter to be examined (e.g. signal amplitude) and $p(x_i)$ is the probability. The algorithm is applied for each data point *(i)*. Shannon Entropy does not check for similarity within adjacent data point but is a global measure of the whole time series or specific epochs of it. Modified versions of Shannon Entropy have been applied to surface EMG data (Farina et al., 2008). This method for estimation of the entropy of a system represented by a time series is not, however, well suited to analysis of the short and noisy data sets encountered in cardiovascular and other biological studies (Richman and Moorman, 2000). To investigate the temporal fluctuations, a measure providing an indication of the variability of the dataset could potentially provide insights into the motor control.

2.3.3.3.2. Approximate Entropy and Sample Entropy

Two entropy-based measures, which provide information about the temporal variability of a time series, are Sample entropy (SampEn) (Richman and Moorman, 2000) and Approximate entropy (ApEn) (Pincus, 1991). ApEn was first defined and is applicable to noisy and medium-sized datasets. It determines the conditional probability of similarity between a chosen data segment and the next set of segments of the same duration (Pincus, 1991). An increase in probability generates a lower value of ApEn, meaning less irregularity of the data.

ApEn is calculated as:

$$ApEn(m,r) = \frac{\sum_{i=1}^{N-m+1} \log(C_i^m(r))}{N-m+1} - \frac{\sum_{i=1}^{N-m+1} \log(C_i^{m+1}(r))}{N-m+1},$$

Where *C(r)* represents the number of data points where the absolute distance with the adjacent data point is less than a selected tolerance, *r*.

ApEn is defined as the difference of the natural logarithm of the sequence C, which counts for the similarity of respectively two sequences, of length *m* points, and two sequences when an additional data point (m+1). If no similarity is found, C will result in 0 and therefore ApEn will be undefined. For this reason, in order to provide at least one match, self-matches are accounted in ApEn, which therefore bias the result towards regularity.

Sample entropy is defined in a similar way, as the negative natural logarithm of the conditional probability that two sequences, of length *m* points, remain similar when an additional data point is introduced; however self- matches are not included in calculating the probability. This means that each data point is not checked for similarity

with itself, which would bias the result towards effected results (e.g. towards regularity) (Richman and Moorman, 2000; Donker et al., 2008; Ramdani et al., 2009; Rathleff et al., 2011, Yentes et al., 2013). Lower values of SampEn indicates more self-similarity in the time series (Richman and Moorman, 2000) and a greater regularity of the data set. In terms of physiological meaning, lower values of SampEn suggest a more predictable time series and potentially a more stable state of the motor control

SampEn is defined by three parameters *N*, *m* and *r*, which respectively indicate the length of the data set (*N*), the length of the sequence to be checked for similarity (*m*) and the tolerance (*r*). Given N data points, *x(1),…x(N),*, the first step is to create vectors of *m* consecutive *x* values ($x_m(1),\ldots\ldots,x_m(N-m+1)$. Then the distance between two vectors is defined as the absolute maximum difference between their scalar components. For each vector, each time this distance is less or equal to the tolerance *r* it is counted into the variable *B*, defined as:

$$B_i^m(r) = \frac{1}{N-m-1} B_i \qquad (2.3)$$

$$B^m(r) = \frac{1}{N-m} \sum_{i=1}^{N-m} B_i^m(r) \qquad (2.4)$$

The dimension of the array is then increased to *m+1* and each time the vector is similar to another one within the same tolerance, is counted into the variable *A*, defined as:

$$A_i^m(r) = \frac{1}{N-m-1} A_i \qquad (2.5)$$

$$A^m(r) = \frac{1}{N-m} \sum_{i=1}^{N-m} A_i^m(r) \qquad (2.6)$$

$A^m(r)$ and $B^m(r)$ are the probabilities that two sequences will match for respectively *m*+1 and *m* points and these matches will be accounted for if they are lower than a tolerance, r, which therefore indicates the dependency of A and B to r.

Sample Entropy is then defined as:

$$\text{SampEn}(m,r,N) = -ln\frac{A^m(r)}{B^m(r)} \qquad (2.7)$$

In comparison to ApEn, SampEn calculates the negative logarithm of a probability associated with the time series as a whole. ApEn calculates probabilities in a template-wise way, which

The selection of *m* and *r* could change the result of the estimate; therefore, it is fundamental to select these parameters accurately, based on the data series to be investigated. Accuracy and confidence of entropy increase as the number of lengths *m* matches increases and this can be done by selecting short templates (small *m*) and wide tolerance (large *r*). However, selecting a too small *r*, will lead to a poor conditional estimate and a too large *r* could lead to a too detailed system and sample entropy tending to zero. Also, to avoid significant noise contribution, *r* should be selected to be bigger than the noise level.

SampEn is therefore able to provide information about the variability over time of a long and noisy data series, which Shannon Entropy is not able to, and also it is not affected by self-matches, which would influence the final result.

Moreover, SampEn has recently been applied to EMG signal data to distinguish between physiological EMG and spurious noise (Zhang et al., 2016), to distinguish between different levels of chronic stroke spasticity (Roerdink et al., 2006) and to CoP in cerebral palsy patients (Donker et al., 2008). Changes in the complexity of motor patterns may be related to changes in motor strategies and may thus reveal the effects of adaptations and pathologies (Rathleff et al., 2011).

SampEn analyses has also been applied to surface EMG signal collected from multi-channel system of electrodes, to investigate complexity in force and muscle activity in diabetic patients (Suda et al., 2017). Diabetic peripheral neuropathy (DPN) generates structural and functional neuromuscular alterations, which may influence motor control and one of its components, motor variability. Therefore, by investigating the complexity of the neuromuscular system of DPN patients, it was possible to evaluate the amount and structure of variability of sEMG patterns and force data collected during isometric contractions. Results showed an increase in the amount of force variability (i.e. force signal becoming more random) corresponded to a decrease in the structure of force variability and EMG structure. Lower structure of force variability in DPN underlined the effect of the disease on motor control during isometric contractions and motor variability seemed to be affected more in moderate rather than severe subjects, suggesting that when the disease is still unstable at a moderate degree, the effects on motor control variability are most apparent. However, the averaging of both amplitude and SampEn values across a multi-channel grid, might have hindered spatial information, which could be informative of differences between DPN participants patterns and healthy participants.

SampEn is therefore a valuable tool to investigate the level of regularity of a time series and seems to be able to distinguish between a healthy state versus a pathological one (Suda et al, 2017) and between healthy patterns of motor unit firing patterns (Rathleff et al., 2011).

2.3.3.3.3. Entropy Halflife (EnHL)

However, SampEn's metric is based on probability, therefore this approach does not allow direct comparison between studies or participants. Therefore, a novel non-linear time-based method was recently developed by Zandiyeh and von Tscharner (Zandiyeh and von Tscharner, 2013) that allows for the quantification of the SampEn of a time series at different time scales providing a time-based measure of the persistence of structure within a signal. The output variable, called Entropic half-life (EnHL), indicates the time scale over which two points in the signal remain related to one another by resampling the signal and identifying the time scale at which transition from SampEn values reflecting order to those reflecting randomness occur (Baltich et al., 2014; Hodson-Tole and Wakeling, 2017).

This methodology is based on a reshape scale method, which reorganises the time series over multiple scales (number of data points) to determine the time scale over which subsequent data points remain affiliated to one another) (Figure 2.7).

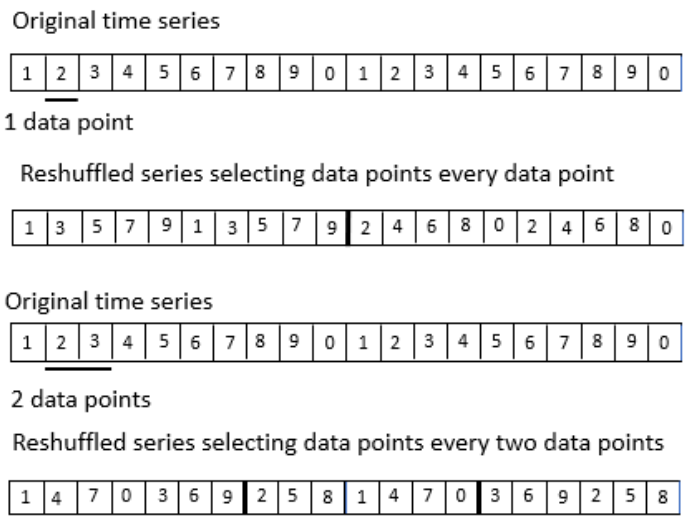

Figure 2-7 Representation of the scaling methodology applied to an example array of data. From the original series, during the first iteration, comparison is made between data points separated by one data points. On the second iter, similarity is chechked between data points seprataed by two data points (Figure based on Federolf et al, 2015).

The process started at the first element of the signal forming a first block of data and then repeating the procedure starting at the second, third, and following points until all points of the signal were organised in blocks (Figure 2.7). For each time interval, SampEn of the reshuffled block of data is calculated. The reshaped signal is then reshuffled to prevent the reordering of the elements, occurring at large scales (Enders et al., 2015). This reshaping increases the duration of the sequences that the entropy algorithm uses to evaluate whether the system is in a similar state, by unchanging its statistics (standard deviation) (Baltich et al., 2014; Enders et al., 2015; Federolf et al., 2015). Therefore, increasing the reshape scale will result in an increasingly larger time interval (τ) between adjacent points in the reshaped time series.

SampEn values are then plotted against the corresponding time interval and normalised to its maximum. This normalisation allows to identify the time point when SampEn reaches its 50%. Finally, the EnHL is defined as the scale at which the normalized SampEn equals 0.5 (Federolf et al., 2015, Enders et al., 2015, Baltich et al., 2014), or reaches the 50% of maximum entropy (Zandiyeh and von Tscharner, 2013) and transitions from being regular to more irregular.

To verify the presence of physiological significance in the reshuffled signal, the original signal is Fourier transformed and the phase randomized, so that a surrogate signal is obtained when an inverse Fourier transform is applied. The surrogate signal maintains the same power spectrum and autocorrelation as the original signal, but the structure encoded in the phase has disappeared. The EnHL from a surrogate signal should be

lower than EnHL from physiological signals, as the structure in the phase has been completely removed and therefore it should transition to random at shorter EnHL.

This novel methodology is still at an early stage of application to the investigation of neuromuscular system behaviour. It has been applied to CoP trajectories recorded during different postural balance tasks and to surface EMG during cycling (in humans) (Enders et al., 2015) and treadmill locomotion (in rats) (Hodson-Tole and Wakeling, 2017). Quantifying EnHL in myoelectric signals, recorded across multiple muscles during cycling exercise in humans, has revealed increased persistence in signal structure in response to increased cycling load (10-12 ms for 150 W cycling load, 15-22 ms for 300 W cycling load) (Enders et al., 2015). These results were suggested to indicate more structured and orderly motor unit firing patterns occurred at higher effort levels (Enders et al., 2015). As far as the recent literature goes, no studies investigated the EnHL of intrinsic foot muscles during postural tasks nor to EMGs recorded using multi-channel electrode arrays. Such work would enable a baseline of EnHL values to be established for the intrinsic foot muscles and would also provide information about spatial distribution of neuromuscular drive patterns across the plantar region of the foot. The following section therefore reviews current knowledge pertaining to foot anatomy and foot muscle function.

2.4. Human foot anatomy and function

2.4.1. Human foot anatomy (skeletal)

The foot is composed of 26 individual bones and, with the long bones of the lower limb, contains 33 joints. It can be described in three sections: i) rearfoot; ii) mid-foot and iii)

forefoot. The rearfoot forms the heel and the ankle, with the calcaneus being the largest bone in the foot (Figure 2.8).

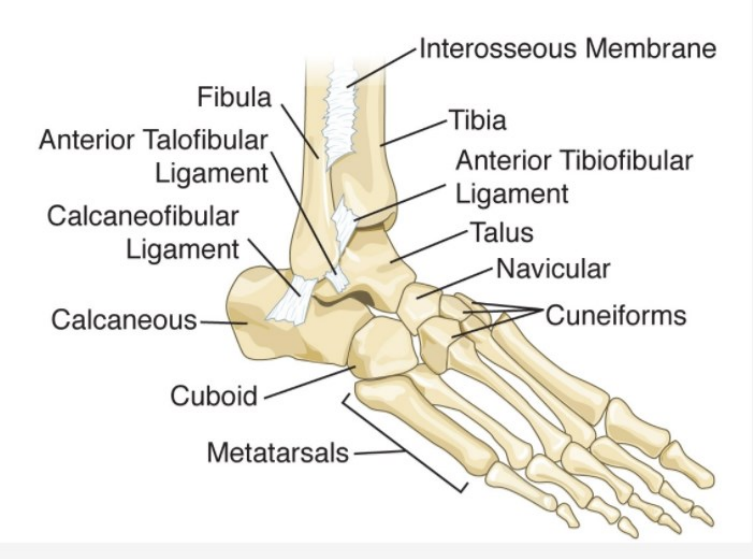

Figure 2-8 Representation of foot bones. Extracted from (Soysa et al., 2012)

In the rearfoot section of the foot sits the subtalar joint, which is formed superiorly from the talus and inferiorly by the calcaneus and navicular. The talus is the second largest bone in the foot, it supports the tibia and sits upon the calcaneus. The subtalar joint motions are linked to the ankle joint motions and to the mid-tarsal joint motions (Rockar, 1995). The midfoot contains a pyramid shaped collection of bones, constituting the arch of the foot, which includes the cuneiform bones, the cuboids bones and the navicular bones (Figure 2.8). The mid-tarsal joint rests in the midfoot section of the foot and consists of the talo-navicular and the calcaneocuboid joints (Blackwood et al., 2005). Finally, the forefoot includes the phalanges and the metatarsals, but also the metatarsophalangeal joint for each toe (Figure 2.8).

The complexity of the structures in the foot has driven multiple researchers to identify a methodology to describe motion and interplay between foot sections. By the use of multi-segment models (Simon et al., 2006) it is possible to separate the foot into

sections, or foot segment, and explore motion of each segment and interplay between them. Forces applied to the foot structure can be quantified using ground reaction force plate technology. The motion of each segment can be recorded with the use of skin mounted reflective markers, whose movement in space is recorded by a system of cameras, with 3D kinematics analysed from the traces of the marker in space (Arndt et al., 2007; Nester et al., 2014; Lundgren et al., 2008). The majority of studies on foot biomechanics focus on the investigation of inter-segment angles and motion during different types of locomotion or postural tasks (Hunt et al., 2001; Jenkyn and Nicol, 2007; Bruening et al., 2012, Arnold et al., 2013). These studies provide useful insight into foot biomechanics, but do not take into consideration the possible role of the intrinsic foot muscles.

2.4.2. Musculature of the human foot

The foot muscles can be divided into two categories: intrinsic vs extrinsic. The intrinsic foot muscles originate and insert entirely within the foot complex, whereas the extrinsic muscles originate away from the foot in the lower limb with the two compartments linked through long tendons, which extend and inserts into the foot.

2.4.2.1. Intrinsic foot muscles

The intrinsic muscles of the foot consist of one muscle on the dorsal surface and four layers of muscles on the plantar surface (Figure *2-9*). The dorsal muscles are the *Extensor digitorum brevis* and the Extensor hallucis brevis. Early studies have indicated that contraction of these muscles varied significantly between participants during walking trials (Soysa et al., 2012), therefore it was not possible to investigate their function, and very little is still known about them. On the other hand, the plantar intrinsic foot muscles

represent the majority of the muscle tissue in the foot, and due to their contribution to walking, standing and running, they have been of great interest to research and clinical investigations.

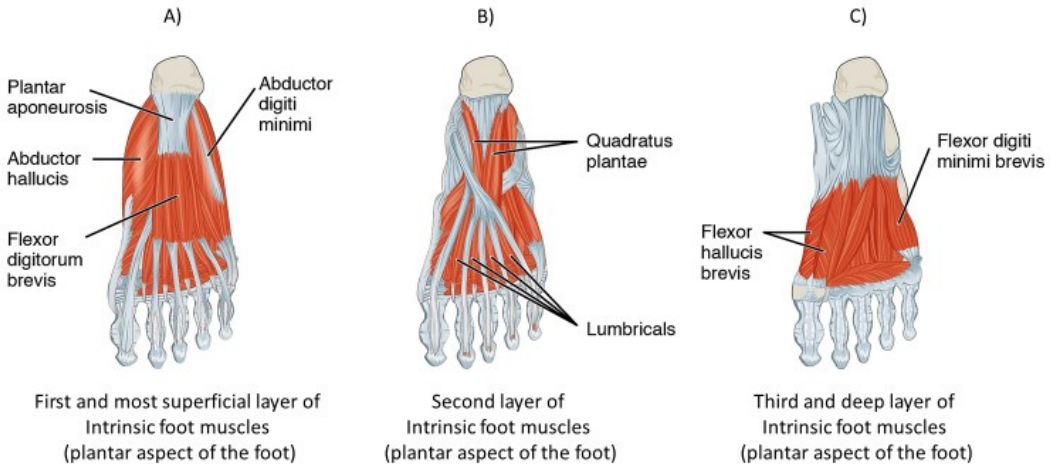

Figure 2-9 Representation of the first three layers of the intrinsic foot muscles. Panel A) shows the most superficial muscles, Panel B) shows the second layer and Panel C) the third and deep layer. The image has been amended from OpenStax (2016) down loaded from: *https://commons.wikimedia.org/wiki/File:1124_Intrinsic_Muscles_of_the_Foot.jpg*.

The following table summarises the anatomical and morphological properties of each plantar intrinsic foot muscles, from a cadaveric study on eleven dissected fresh-frozen cadaveric feet (eight males and three females) with an age range between 50 and 88 years old. All participants reported no gross abnormalities (such as severe deformities, injury), which was visually inspected prior to dissection.

Table 2-2-1 Summary of origin, insertion and proposed functions of the intrinsic foot muscle. Morphological data extracted from Kura et al (1997), where ML indicates *Muscle length* and PCSA indicates *Physiological cross-sectional area*

Muscle name	***Origin***	***Insertion***	***Action***	***Morphological data***
		First layer (superficial)		
***Abductor digiti minim*i**	lateral aspect of the proximal phalanx of the 5th toe	medial and lateral calcaneus	Abduction of 5th toe	ML: *112.8±19.1 mm* PCSA: *3.79±1.83 cm²*
Abductor hallucis	from the medial tubercle of calcaneus and the border of plantar aponeurosis	medial aspect of the base of the proximal phalanx of the hallux	Hallux abduction, assists in flexion of the hallux at the MTP joint.	ML: *115.8±4.9 mm* PCSA: *6.68±2.07 cm²*
Flexor digitorum brevis	Calcaneus	deep surface of the plantar aponeurosis	Flexion of lateral four toes	ML: *98.2±14.1 mm* PCSA: *1.5±0.6 cm²*
		Second Layer		
Quadratus plantae (medial, M and lateral, L, heads)	medial and lateral processes of the calcaneus tubercles	lateral border of the flexor digitorum longus tendon	assists flexor digitorum longus to flex the lateral toes	ML, L head: *55.3±3.9 mm* ML, M head: *81.3±20.1 mm* PCSA: *1.00 ± 0.41 cm²(*L head), *1.96 ± 0.94 cm²(*M head)
Lumbricals	tendinous slips of the flexor digitorum longus	Proximal phalanges and extensor tendons (four lateral toes)	MTP joint flexion, interphalangeal joints extension (relevant toe)	ML: *44.3±13.1 mm* PCSA: *0.26±0.17 cm²*
		Third Layer		
Adductor hallucis (transverse head, T, and oblique head, O)	bases of metatarsals II-IV (O head), ligamentous coverings of the plantar aspects of the 3rd-5th MTP joints and from the deep transverse metatarsal ligaments (T head)	Lateral aspect of the base of the proximal phalanx of the hallux	Foot adduction, assists in flexing the hallux, maintaining the transverse arch of the foot	ML: *24.8±4.2 mm (T head)*, *67.4±4.6 mm (*O head*)* PCSA: *0.62 ± 0.26 cm²* (T head), *4.94 ± 1.36 cm²* (O head)
Flexor digiti minimi brevis	plantar surface of the base metatarsal V and to the sheath of the adjacent fibularis longus tendon	base of the proximal phalanx of the 5th toe	the flexion of the 5th toe	ML: *51.0±5.3 mm* PCSA *2.00±1.02 cm²*
***Flexor hallucis brevis* (lateral head, L, and medial head, M)**	plantar surface of the cuboid and the adjacent lateral cuneiform (L head), plantar surface of the medial and intermediate cuneiform s(M head).	sides of the base of the proximal phalanx of the hallux.	Flexion of the first MTP joint	ML: *65.3±7.1 mm (L head)*, *76.0±19.8 mm (M head)* PCSA: *2.12 ± 0.84 cm²* (L head), *1.80 ± 0.75 cm²* (M head)
		Fourth layer		
Plantar interossei (3)	medial aspect of metatarsals III-V	Medial surface of the base of the proximal phalanx of the metatarsals	Toe adduction	ML: *50.5±6.8 mm* PCSA *1.34±0.56 cm²*

The intrinsic foot muscles flex and abduct/adduct the metatarsophalangeal joints and in the “foot core paradigm” (Soysa et al, 2012) they have been identified as the local stabilizers of the entire body during locomotion and postural balance maintenance. The “foot core paradigm” poses attention to the foot structure as the local stabiliser during motion, in comparison to more obvious and bigger compartments (e.g. lower limbs, trunk) considered as global stabilisers, and highlighting the foot role and importance during postural tasks or locomotion. The most commonly investigated muscles are those of the first layer (Abductor hallucis, flexor digitorum brevis, abductor digiti minimi) as they are the most superficial ones. From a cadaveric study, the abductor hallucis appeared to be the muscle with the largest cross-sectional area (Kura et al., 1997) and therefore able to produce the majority of force in abduction and flexion of the great toe. Moreover, this muscle seems to be the most important in medial arch support (Reeser et al., 1983) due its larger cross-sectional area. EMG activity in Abductor Hallucis was correlated with better balance performance, defined as smaller centre of pressure sways (Zhang et al, 2017). Soysa et al (2012) highlighted how investigation of these muscles is challenging, due to their anatomical closeness, and while cadaveric study can provide some useful information, the interplay between these muscles during live movement is required to indicate their relevance in standing and postural tasks.

2.4.2.2. Extrinsic foot muscles

Extrinsic foot muscles are part of the new “foot core paradigm”, where they have been identified as the global movers contrasting to the intrinsic foot muscles’ role as local stabilisers. Summary of anatomical features and some morphological properties is showed in the following table.

Table 2-2-2. Summary of origin, insertion and proposed actions of the extrinsic foot muscle.

Muscle Name	*Proximal origin*	*Distal attachment*	*Action*
	Anterior group		
Extensor digitorum longus	lateral condyle of the tibia and upper section of the medial surface of the fibula	tendon splitting into four parts, inserting into the 2nd and 3rd phalanges of the toes, except the hallux	Extension of phalangeal of toes
Peroneus tertius	distal part of the anterior surface of the fibula	dorsal surface of the base of the first metatarsal bone	Foot Eversion
Extensor hallucis longus	middle two-fourths of the fibula	dorsal aspect of the base of the distal phalanx of the hallux	Extension of phalanges of first ray
Tibialis anterior	lateral condyle of the lateral surface of the tibia	medial and plantar surface of the 1st cuneiform and to the base of the 1st metatarsal bone	Dorsiflexion Foot inversion
	Lateral Group		
Peroneus brevis	lower region of the lateral surface of the fibula	Styloid process of the 5th metatarsal	Foot eversion
Peroneus longus	head and upper section of the lateral surface of the fibula	lateral aspect of the base of the 1st metatarsal bone	Foot eversion
	Posterior Group		
Gastrocnemius muscle (GM) (superficial)	posterior aspects of the femoral condyles (medial aspect for medial GM and lateral aspect for lateral GM)	distal bony attachments, the Achilles' tendon (AT), inserting into the mid-portion of the posterior surface of the calcaneus	Plantar flexion
Soleus (superficial)	posterior surface of the fibular head, proximal part of the posterior surface of the fibula, and the middle third of the medial border of the tibia	distal bony attachments, the Achilles' tendon (AT), inserting into the mid-portion of the posterior surface of the calcaneus	Plantar flexion
Plantaris muscle (superficial)	lateral part of the supracondylar line of the femur	posterior part of the calcaneus	Plantar flexion
Flexor hallucis longus (deep)	lower part of the posterior surface of the body of the fibula	into the base of the terminal phalanx of the hallux	Flexion of first ray
Flexor digitorum longus (deep)	posterior side of the tibia from under the popliteal line	main tendon splits into four smaller tendons and each inserts into the bases of the distal phalanges of the 2nd-5th toes	Flexion of the phalanges of the toes
Tibialis posterior (deep)	posterior surface of the tibia and a medial segment on the upper portion of the posterior surface of the fibula	into the tuberosity of the navicular	Plantar flexion and inversion

These extrinsic muscles contribute to foot and ankle motion, by dorsi/planti flexing foot and toes or inverting/everting the foot. In contrast to the intrinsic foot muscles, the

extrinsic muscles have been investigated to a great extent in the literature. Recent studies have investigated medial and lateral gastrocnemius in humans (Bojsen-Moller, et al., 2004) and cats (Maas et al., 2010), showing how both heads of the calf muscles independently act on the ranges of ankle and knee angles during standing. In a more recent study (Vieira et al., 2010) the activities of the human MG and LG muscles were independently modulated for the control of upright stance. Moreover, in another study (Vieira et al., 2011) the recruitment of MG units occurred intermittently throughout standing (modal interval of 500 ms), with an intrinsic temporal triggering (two recruitments per second) controlling the motor unit recruitment timing in the MG muscle in standing.

The extrinsic foot muscles have been shown to play a fundamental role in standing (Vieira et al., 2010; Vieira et al., 2011) and single-leg stance (Muehlbauer et al., 2014). However, whilst there is a large array of literature related to extrinsic foot muscles it is still not clear what the level of coordination with the intrinsic foot muscles is, as the combined behaviour of these two compartments has been investigated in one study only (Zelik et al., 2015). In this study, surface EMG was recorded from one intrinsic foot muscles and four extrinsic foot muscles and EMG envelopes were used to evaluate the timing of peak muscle activity to assess whether the coordination between intrinsic and extrinsic foot muscles was either sequential or synchronous. Results seem to suggest that during the stance-to-swing transition a sequential muscle activity occurred with activation of the ankle plantarflexors, followed by the metatarsophalangeal (MTP) flexors (*Flexor digitorum brevis, Flexor digitorum longus*), MTP extensors (*Extensor hallucis brevis*, *Extensor digitorum brevis*, *Extensor hallucis longus*), and then ankle dorsiflexors. Their study showed how a relationship between these two compartments

exists and is potentially fundamental to locomotion. However, considering the importance of intrinsic foot muscles in balance and the role of extrinsic foot muscles as ankle stabilisers, it is not clear what is the relationship between these two compartments during postural tasks and therefore more investigation is needed.

Recently, intrinsic foot musculature has been shown to fulfil an active role in the adjustment of the longitudinal arch, actively stiffening it to provide a stable structure during heel-strike and push-off (Bates et al., 2013); while facilitating more compliant properties during mid-stance, allowing it to attenuate loading. In addition, an increase in vertical load causes the longitudinal arch height and length to deform significantly, resulting in stretching of musculature and in an increase in muscle activity (Kelly et al., 2014). However, this study had participants in a seated position with loading applied to the knee to simulate what happens during standing while removing the natural sway. Knowledge is therefore still missing as to what the activation patterns of intrinsic foot muscles are in scenarios including natural sways such as tasks of challenging balance. Such knowledge could help understand features of muscles activation in the context of different biomechanical demands and inform understanding of differences in foot functioning in healthy and pathological conditions.

2.5. Previous research on electromyographic activity of human intrinsic foot muscles

One of the first EMG studies on foot function (Mann and Inman, 1964) on 12 participants showed that the *Abductor digiti minimi*, *Abductor hallucis*, *Flexor digitorum brevis*, *Dorsal interossei* and lumbrical muscles were all active during the stance phase of gait and continued until toe off. However, they indicate that the bony arches of the foot have been shown to be structurally self-supporting requiring minimal muscular support during postural activities, with the foot's ligaments providing passive support to maintain the integrity of the foot during quiet standing.

Further early electromyographic studies (Basmajian and Stecko, 1963) also argued that contribution of intrinsic foot muscles is not as fundamental as muscles in the lower limb and that bones and ligaments alone are able alone to maintain the arch. Moreover, the plantar aponeurosis was widely accepted to be the primary structure responsible for arch support during rest. One study analysed muscle activation from *Gastrocnemius*, *Tibialis anterior*, *Peroneus longus*, *Flexor digitorum brevis*, *Abductor hallucis* and *Abductor digiti minimi* in a static standing position, concluding that low levels of activity was exerted by these muscles. Even though they noted that intrinsic foot muscles become very active while rising onto the toes, they concluded that this group of muscles does not play an important role in normal static support of the arches in the foot. During a second early study (Basmajian and Stecko, 1963), intramuscular EMG were collected while participants were seated, and an increasing loading was applied to the knee. They concluded that muscle activation was only noticeable when the loading reached double the participant's body weight, and, therefore that no active role was performed by the intrinsic foot muscles in normal arch support and the primary source of support are

bones and ligaments. These studies were the first to investigate the activation of intrinsic foot muscles during postural tasks, however the investigation was limited to a small selection of intrinsic foot muscles (*Abductor hallucis and flexor digitorum brevis*), using an invasive technique. The condition tested were also very limited (standing and loaded seating) and considering when these studies were performed, advancement in technology and analysis techniques could provide different results.

A later EMG study conducted by Reeser et al (1983), recorded fine wire EMG from two of the most superficial muscles (*Abductor hallucis* and *Abductor digiti minimi*) and one muscle of the second layer (*Quadratus plantae*) during a series of free exercises, that combined movement of the toes, the foot and the ankle. These movements included flexion and extension of the toes, inversion and eversion of the foot and dorsiflexion and plantarflexion of the ankle. They suggested that, contrary to what was previously stated, intrinsic foot muscles do play a fundamental role in supporting the foot structure on the foot in both posture and locomotion. This study however, applied this technique to only four participants, and an invasive approach was used in this study as well, therefore further investigation was required.

Later, Fiolkowski et al (2003) investigated the role of intrinsic foot muscles in supporting the medial longitudinal arch, with one electrode positioned in the middle portion of *Abductor hallucis* and each participant (n=10) was asked to perform a maximum voluntary contraction (MVC) for 2 seconds by plantar flexing their hallux. In the second part of the study, anaesthesia was injected into the plantar nerve, ablating the use of the intrinsic foot muscles. Results show that intrinsic musculature in the plantar aspect

of the foot has a role in supporting the medial longitudinal arch of the fully loaded foot in quiet stance. When anaesthesia was injected into the plantar nerve, authors observe an increase in the navicular drop, suggesting that the plantar musculature does support the arch and when this support is missing, the arch structure is modified.

A recent EMG study revealed a small amount of activity in *Abductor hallucis*, *Flexor digitorum brevis* and the *Quadratus plantae* muscle during relaxed standing with a significant increase in activation with increased postural demands (Kelly et al., 2012). The presence of activation in this group of muscles during quiet standing, suggests that they do provide postural support for the feet, supporting the findings of Fiolkowski et al (2003). In addition, to the static stance data presented by Fiolkowski et al (2003) and Kelly et al (2012) showed a moderate (r^2=0.5) to strong correlation (r^2>0.6) between these muscles activation and the mediolateral postural sway in single leg-stance. The synchronisation between the centre of pressure and muscle activity showed how the selected muscles reacted to sway, suggesting a contribution of these muscles in balance control.

Two other recent studies have focussed on the same three muscles to understand the function of the intrinsic foot muscles during increasing loading (Kelly et al., 2014). To understand the effect of loading on muscle activity, participants have been asked to remain still, while three levels of loading were applied to one leg. Loads ranged from 0% of body mass to 150% body mass with 25% increments. Results showed how the intrinsic foot muscles have an active role in maintaining the medial arch under these loadings. The increased vertical loading caused arch length and height deformations, which resulted in stretching of the arch musculature and increased electrical activity. It appears

that this group of muscles is able to stiffen the longitudinal arch under load, by stretching in a similar manner as the plantar aponeurosis.

While these intramuscular studies provided fundamental insights on intrinsic foot function properties and have contributed to understand the role of this group of muscles during quiet standing and postural sways, they have achieved these results by recording EMGs using an invasive methodology. If there is a need to study different patient groups as well as children, then current methodology techniques are limited. For example, balance impairment is a problem in older populations and, in many cases, older adults are on medications contra-indicated for intramuscular EMG. Moreover, understanding patterns across the intrinsic foot muscles could help in designing orthotics, which are commonly used by children and adults, but also in exploring wider aspect of foot muscles function, to enable evaluation across the widest range of people possible.

2.6. PhD thesis aims and objectives

The overarching aim of the work presented in this thesis was to investigate the potential value of non-invasively evaluating intrinsic foot muscle behaviour using multi-channel surface electrode arrays. This is achieved by investigating the feasibility of recording surface EMG from the plantar region of the foot during postural motor tasks (Chapter 4), as this approach has never been applied to intrinsic foot muscles. Considering the anatomical challenge of recording from this region, the effect of foot loading on the multi-channel system of electrodes needed to be investigated and the physiological features needed to be analysed. The result from this work revealed that the EMG signals from the plantar foot region presented amplitude and frequency features in the physiological ranges presented in the literature (Basmajian and De Luca, 1985), therefore patterns of intrinsic foot muscles activation could be investigated by analysing i) spatial parameters related to changes in the amplitude and signal complexity (SampEn) distribution during different postural motor tasks (Chapter 4), ii) the association between the mechanics of medial arch motion and the electrical response of the intrinsic foot muscles (Chapter 5), and finally iii) the structural properties of the EMG signals from intrinsic foot muscles with a novel non-linear analysis technique, to investigate how the signal structure change with postural demand and what this can reveal about the controller perceived challenge of managing postural tasks (Chapter 6).

3. General methodology

In the following chapter a description of the experimental setup, data acquisition protocol and data analysis common to the set of three experimental chapters (Chapters 4 – 6) and to the preliminary data presented in the Discussion Section (Chapter 7) is provided.

3.1. Participants

Thirty healthy participants (twenty-four males and six females, age: 44 ± 14 years, weight: 73 ± 15 kg, height: 1.7 ± 0.1 m) voluntarily took part in the study having provided informed, written consent to do so. All procedures were approved by the local ethics committee in the Faculty of Science and Engineering in Manchester Metropolitan University. Exclusion criteria for participants included foot pain or lower limb pain during the last six months.

For each experimental chapter, the number of participants differs, based on the number of trials which needed to be discarded, due to either different types of noise affecting the data or technical issues.

Table 3-1 Morphological data of the complete dataset (N=30). Participants included in each experimental study is indicated with an " X".

Participants code	Age (years)	Weight (kg)	Height (cm)	Foot size (UK)	Chapter 4 (N=25)	Chapter 5 (N=21)	Chapter 6 (N=20)	Chapter 7 (N=17)
S1	26	65	180	8.5	-	-	-	-
S2	31	93	187	11	-	-	-	-
S3	33	81	185	9	**X**	**X**	**X**	**X**
S4	29	72	182	9	**X**	**X**	**X**	**X**
S5	34	72	169	6.5	**X**	**X**	**X**	**X**
S6	36	68	162	4	**X**	**X**	**X**	**X**
S7	48	70	170	7.5	**X**	-	-	-
S8	62	109	172	6.5	**X**	**X**	**X**	**X**
S9	33	62	164	8.5	**X**	-	-	-
S10	52	106	183	10	**X**	**X**	**X**	**X**
S11	31	86	194	10.5	**X**	**X**	**X**	-
S12	48	65	177	6.5	-	-	-	-
S13	27	96	182	10	**X**	**X**	**X**	**X**
S14	23	50	157	5.5	**X**	**X**	**X**	**X**
S15	52	70	171	6.5	**X**	**X**	**X**	**X**
S16	59	73	161	6.5	**X**	-	-	-
S17	28	90	179	10.5	**X**	**X**	**X**	**X**
S18	33	71	177	8.5	**X**	**X**	**X**	-
S19	57	67	172	9	-	-	-	**X**
S20	63	65	160	8	**X**	**X**	**X**	-
S21	33	73	180	10.5	**X**	**X**	-	**X**
S22	55	75	175	9	-	-	-	-
S23	56	66	178	11	**X**	**X**	**X**	**X**
S24	73	60	155	5.5	**X**	-	-	-
S25	32	65	167	8	**X**	**X**	**X**	-
S26	61	48	159	5.5	**X**	**X**	**X**	**X**
S27	30	88	180	10.5	**X**	**X**	**X**	-
S28	63	70	180	10	**X**	**X**	**X**	**X**
S29	21	64	170	8	**X**	**X**	**X**	**X**
S30	45	70	168	9	**X**	**X**	**X**	**X**

A post-hoc analysis was carried out (α=0.05; effect size=0.5), which revealed that a sample of 27 participants would be enough to obtain a statistical power greater than 80%.

3.2. Experimental Setup

Monopolar surface EMGs were collected (sampling frequency 2048 Hz) from the intrinsic foot muscles with a high-density sEMG grid of 64 channels (ELSCH model, OT Bioelettronica, Turin, Italy), consisting of 13 rows and five columns, with one missing electrode (2 mm diameter, 8 mm inter-electrode distance in both directions). Prior to attaching the grid of electrodes, the skin of the plantar region of the right foot was lightly abraded with abrasive paste and cleaned to remove any debris. To determine the location of the electrode grid, the adipose pads at the heel and metatarsals were palpated and the grid was positioned between these regions with the columns along the longitudinal axis of the foot (Figure 3 -*1*). A conductive cream (Spesmedica, Italy) was inserted into each cavity of the grid to assure proper electrode skin interface. The reference electrode was positioned around the right ankle.

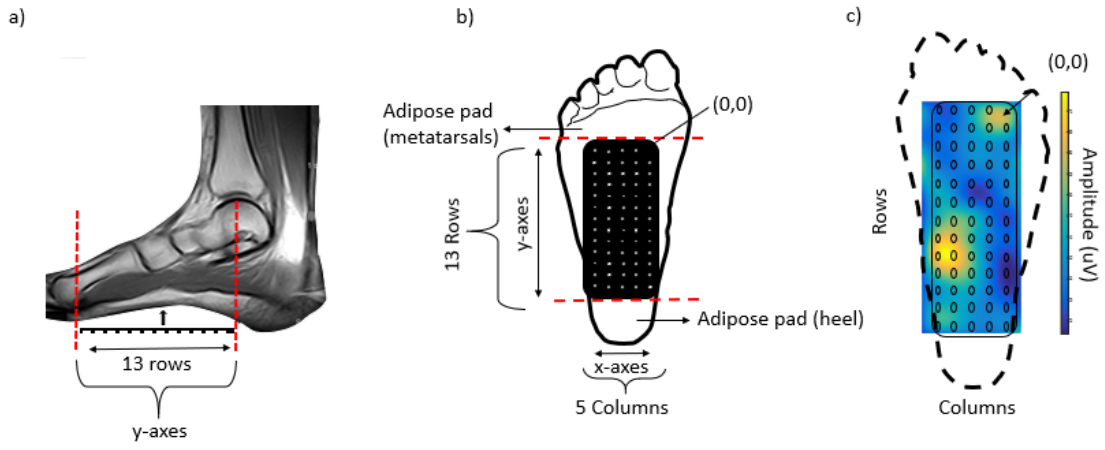

Figure 3 -1 Position of the 64-channel electrode grid on the plantar region of the foot. Panel a) shows an MR image from one participant and the representation of the sEMG grid. The MR image shows where the sEMG was positioned. Panel b) shows the whole grid on the sole of the foot, with one missing electrode at the top left corner. The grid is positioned between the adipose tissue of the metatarsal heads and the heel pad. The majority of the four layers of foot muscles is between these two regions. Panel c) a representative map of amplitude distribution across the plantar region of the foot.

Surface EMGs were also recorded from six extrinsic foot muscles in the lower limb, which included: i) medial and lateral gastrocnemius; ii) medial and lateral portions of soleus; iii) tibialis anterior; and iv) peroneus longus. Six wireless electrodes (Delsys Inc, Trigno, Boston, MA, USA) were positioned on lightly abraded and cleaned skin over each muscle belly. The muscle belly was identified by asking the participant to produce a low-level contraction allowing palpation of the muscle. The multi-channel system of electrodes was applied on one foot only according to the limitation imposed by the cables connected to the EMG amplifier. By recording from two feet would have involved the inclusion of other four cables. The length of these cables would not have allowed to maintain the amplifier outside the motion capture recording volume, which therefore could have caused hindering of markers. For these reasons, the EMG signals were recorded from one foot only.

To record body movement, three-dimensional motion data were recorded (sampling frequency 1000 Hz) using a 9-camera motion-capture system (Vicon Motion Systems, Oxford, UK) positioned around a 46 × 51 cm force plate (Advanced Mechanical Technology, Inc., AMTI, Watertown, Massachusetts, USA) which was covered with a 50mm thick Styrofoam layer to reduce electrical noise from the ground. Both feet were positioned on a single force plate, which was a result of cable length to the EMG amplifier, which reduces the distance to it. By moving the amplifier in the recording volume, it would have increased the likelihood of hindering markers on the shank or foot.

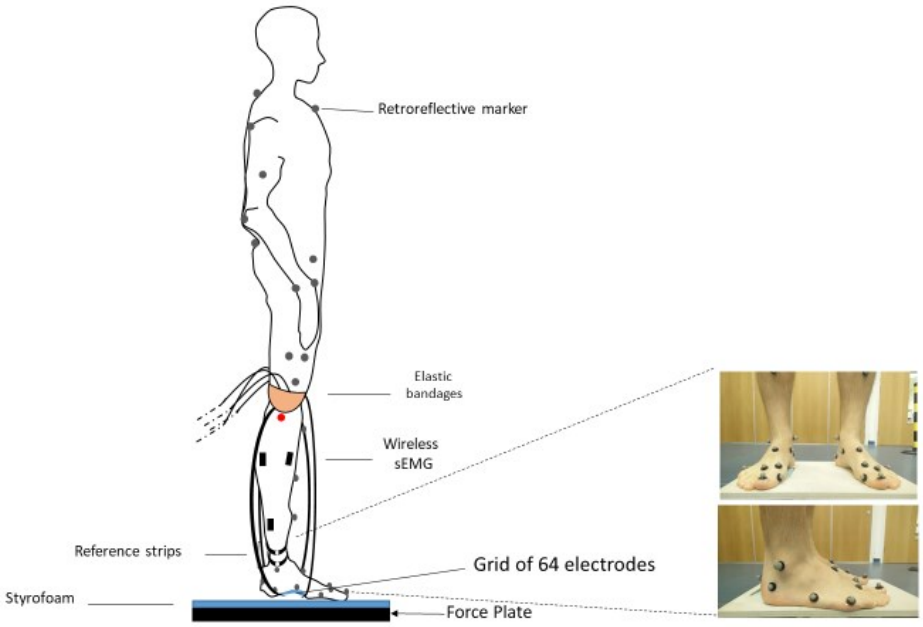

Figure 3-2. Representation of the complete marker set. The foot marker set is showed in the pictures on the right as well. Black rectangle represent the wireless sEMG sensors, the green layer represente the grid of 64 electrodes. Cables were fixed above the knee with elastic bandages.

With the use of a combined marker set, 54 reflective markers were positioned on anatomical landmarks to track whole body movement. The Plug-in Gait Marker set was utilised for anatomical landmarks on the shoulder to the epicondyle of the knee. From the tibial tuberosity to the foot a modified Heidelberg foot marker set (Simon et al., 2006) was applied (Figure 3-2), with an additional marker on the shank to reduce problems associated with marker occlusion.

3.3. Experimental Protocol

The experimental protocol was designed to include a range of movements from quasi-static to motion, which enabled the investigation of foot behaviour during different motor demands. Each participant was asked to stand at a comfortable foot width in the test area. The position of the right foot was standardised by the length of the cable connected to the EMG amplifier, whereas the left foot was positioned at a comfortable distance, trying to maintain a central position on the force plate. While participants were told to maintain their comfortable position, an indication of a standard foot width was provided to them. This was done to avoid including further constraints to participants' movement, which is already caused by the cables connected to the EMG amplifier and the laboratory environment. Moreover, it was possible to identify whether participants were drifting from their selected position, by observing the ground reaction force and they were then instructed to re-adjust their position.

Participants were then instructed to perform one of six motor tasks, including: i) bipedal standing (self-selected comfortable stance width); ii) deliberate anterior/posterior sways; iii) two-foot tiptoe standing; iv) single-leg standing; v) deliberate medial/lateral sways and vi) deliberate leaning toward three selected marks on the ground. Each task was presented three times, with the order of tasks randomised between participants. Each trial lasted thirty seconds, while participants were either maintaining a position or, in the case of sway tasks (anterior/posterior, medial/lateral and leaning), participants were instructed to sway following a metronome beating at 2 Hz. Different frequencies (speeds) were tested before selecting a 2 Hz frequency and, it was concluded that higher

frequencies would have made the performance of the task too challenging (e.g. too fast), whereas lower frequencies would have allowed more space for the interpretation of the movement, which could potentially alter the motor control response.

The selected frequency allows participants to perform the movement with precision.

Synchronisation between force plate, motion capture data and EMG signals was achieved with the use of an external trigger.

3.4. Data analysis

3.4.1. Kinematics and kinetics analysis

Kinematics and kinetics measures from motion capture data were used to calculate the Centre of pressure (CoP) and segment angles (hip joint angle, knee joint angle, ankle joint angle, medial arch angle). The CoP was calculated with Visual 3D (C-motion. Inc, Germantown, MD) and a low-pass filter was applied (Butterworth, 4th order, 6 Hz cut-off). For the purpose of Chapter 4, events corresponding to anterior and posterior sways were identified from the CoP path. The data points corresponding to these events were manually selected from the CoP trace, following manual inspection of signals. Respectively peaks and valleys of the CoP were manually selected, by visualising the transition of each participant during the task (e.g from anterior to posterior sway) (Figure *3-3*).

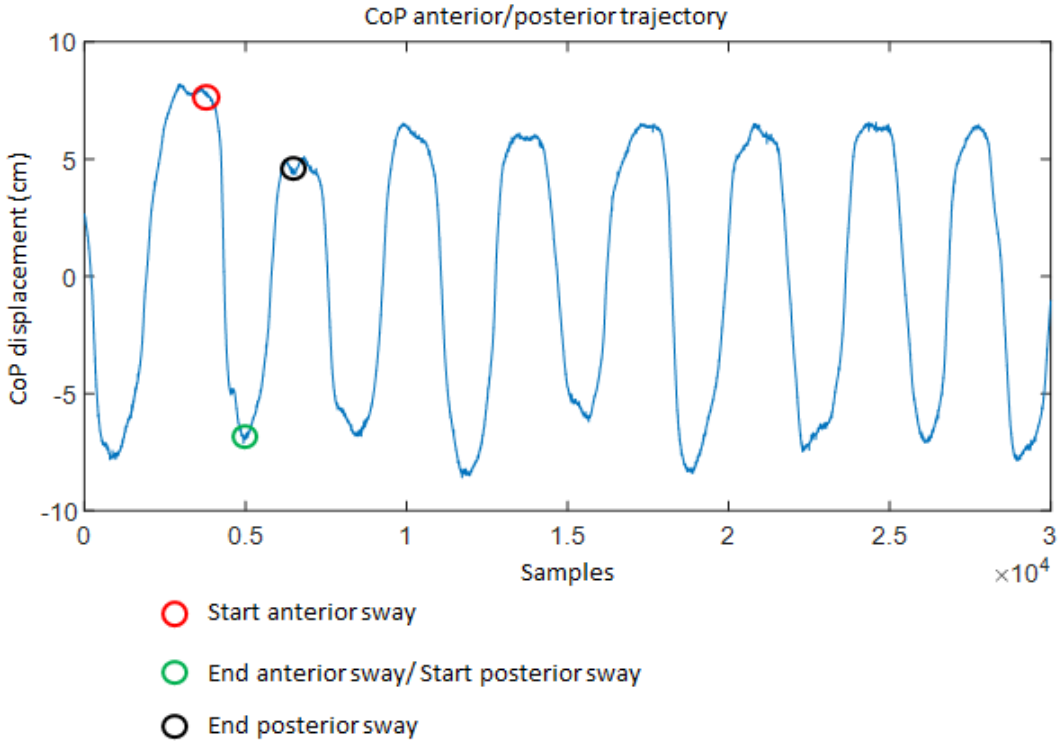

Figure 3-3 Example from one representative CoP anterior/posterior trajectory showing the manual selection of epochs in the time series. The selction of "Start anterior sway" (red circle), "End anterior sway/Start posterior sway" (green circle) and "End posterior sway" (black) was repeated until the end of the trial for each wave.

It was not possible to automate this procedure, because even though they were instructed to follow a metronome, slight differences still occurred between participants.

In Chapter 4, segment angles were also calculated based on the multi-segment models used in this study (Figure 3.2). These angles were calculated with the in-built function "Compute Model Based" in Visual3D (C-motion. Inc, Germantown, MD), where it is possible to define two segments (e.g. hip and knee to calculate knee angle) defining the angle and then the trace of the angle over time is calculated.

Medial arch angle was calculated between the hindfoot and rearfoot segments, ankle angle between foot segment and shank segment, knee between shank and thigh and hip angle between trunk and upper leg (*Figure 3-4*).

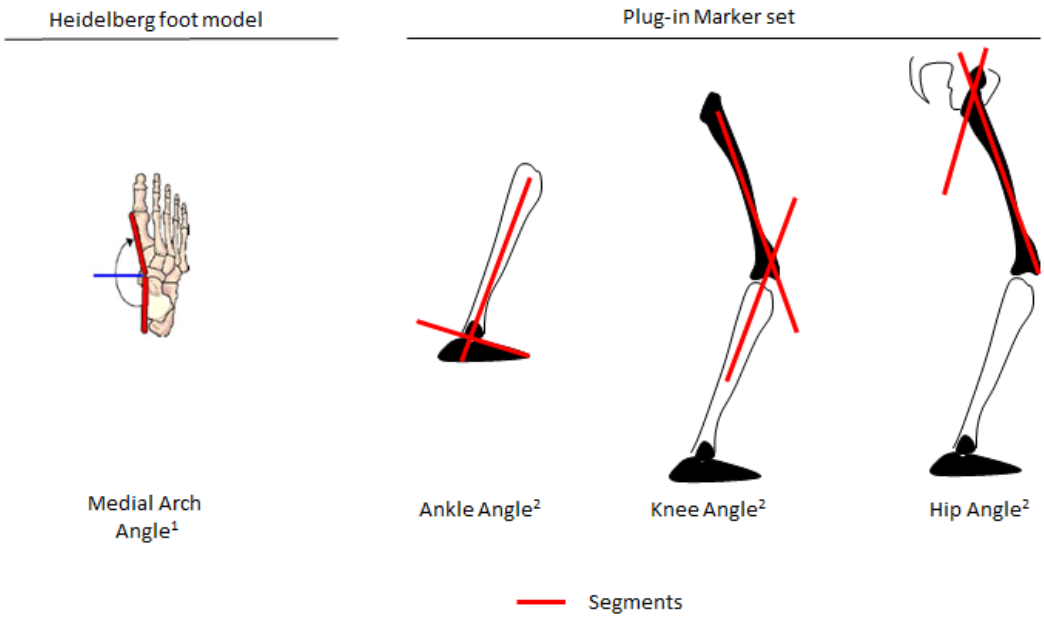

Figure 3-4 Representation of the four angles calculated in Chapter 4. The medial arch angle has been calculated based on (1) Simon et al (2006) paper, whereas ankle, knee and hip angles have been calculated base on the (2) Plug-in marker set.

The focus of the analysis for this thesis was on the processing of the EMG signal and most processing routines were common to the three experimental chapters (Chapter 4, 5, 6). Hence, in the following sections detailed description of the analysis is provided.

3.4.2. Preliminary analysis of surface EMG

Surface EMG is the superficial representation of muscle contraction (Merletti and Parker 2004) and it is referred to as an interference signal, which is the result of superposition of motor unit action potentials within the detection volume of a recording electrode. As

EMG is an electrical signal, it is easily affected by electrical noise, motion artefact and poor skin-electrode interface, which need to be identified and removed before further analysis. The quality of the surface EMG therefore needs to be assessed to discard signals or channels affected by noise, before analysis to extract important amplitude and frequency components. For this reason, recorded surface EMGs from the multi-channel grid were visually inspected and channels showing noise due to poor skin-electrode interface contact or line interference were reconstructed based on the interpolation of the signals from neighbouring channels (Gallina and Botter 2013). An example of different types of noise is presented in Figure 3.3-5, for two representative cases. Panel a) shows an example of a representative participant with clusters of signals showing different types of noise. Interpolation was not possible in this case, as neighbour channels do not show clear EMG patterns. On the other hand, Panel b) shows one channel with noise, surrounded by channels showing clean signals. In this case, it was possible to interpolate with neighbour signals and the trial was not discarded.

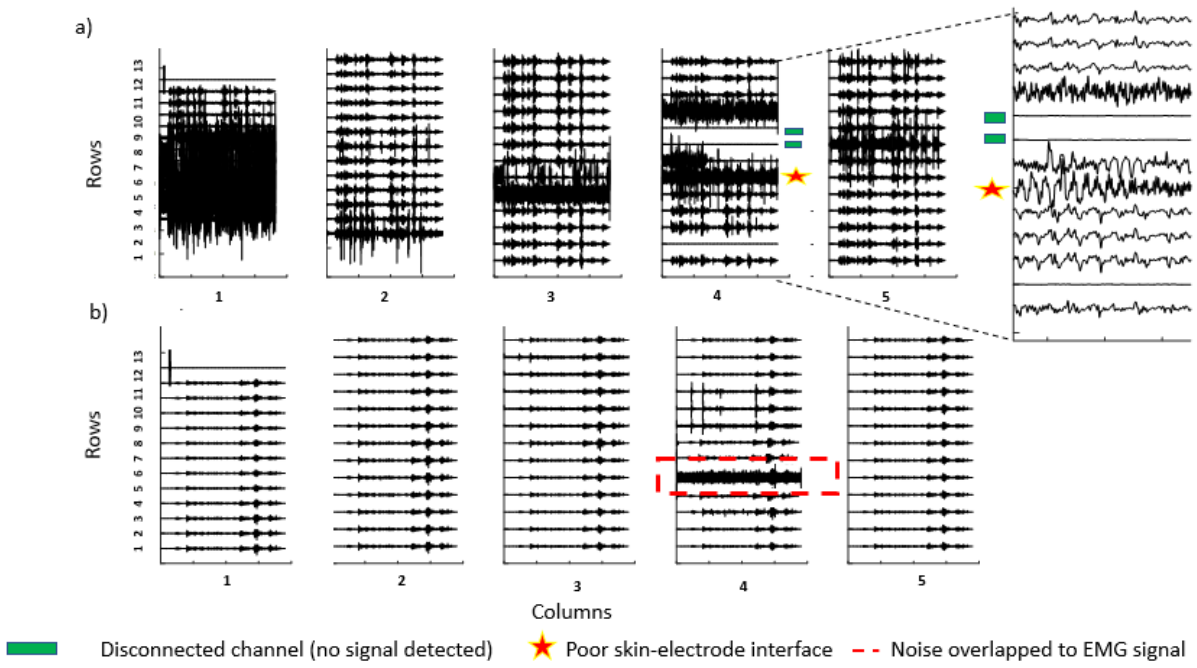

Figure 3.3-5 Representation of EMG signals collected with a 64 channels grid from two representative participants. Panel a) shows multiple channles with different types of noise. Two channels were accidentally disconnetted and therefore no signal was recorded (light blue squares). Clusters of channels present poor skin electrode interface (red star). The zoomed window shows both thypes of noises, respectively in rows 4, 5,6,7,8.

From the total of 30 participants, for each study a different number of participants was included (after discarding those reporting data collection affected by noise): 25 showed a complete data set and were therefore included in chapter 4, 21 for chapter 5, 20 for chapter 6 and 17 for chapter 8.

Next, wavelet analysis was used to process EMG signals following the protocol provided by (von Tscharner 2000), where a filter bank of *k* wavelets was selected to represent a band-pass filter for the signal, with parameters set to ensure that the original signal intensities could be approximately reconstructed from the sum of the *k*-wavelet-transformed signals. For the purpose of this study, a filter bank of 11 ($0 \leq k \leq 10$) wavelets was used to decompose the myoelectric signals from each selected trial into their intensities (Table 3.2).

Table 3.4.2 Upper and Lower bands for each wavelet, Central frequency (Hz) and Time resolution (ms).

Wavelet	Lower Frequency (Hz)	Central Frequency (Hz)	Higher Frequency (Hz)	Time resolution(ms)
0	2.34	6.90	16.41	75.63
1	10.16	19.29	33.20	50.63
2	24.22	37.71	56.25	44.38
3	44.14	62.09	84.77	34.38
4	69.92	92.36	119.53	26.88
5	101.56	128.47	160.16	23.13
6	139.06	170.39	206.64	21.25
7	182.42	218.07	258.59	18.75
8	231.25	271.49	316.41	16.88
9	285.94	330.62	380.08	16.25
10	346.48	395.44	449.22	14.38

To remove low frequency artefacts, the signal from the first wavelet was discarded so the total intensity at any given time was calculated as the sum of the intensities of the selected ($1 \leq k \leq 10$) wavelets (Hodson-Tole et al., 2012).

The total intensity from the wavelet transformed signal was used for further analysis as a measure of EMG intensity over time. The sum of total intensity approximates the description of power (von Tscharner, 2000), therefore half of the power is practically equal to the square of the root mean square (RMS) values, therefore the square root of half the power is equivalent to measures of amplitude such as RMS (von Tscharner, 2000; Wakeling et al., 2002). The total intensity was calculated for each channel, resulting in a map of 64 EMG intensities for each signal time point.

Surface EMG signals from the extrinsic foot muscles were also visually inspected, however, due to some technical problems in the sensor operating system, not all

channels were recorded properly. Due to the system almost at the end of its life, data from 13 participants was lost between recording and exporting the data on an external hard drive and, unfortunately, this was only discovered at the end of each data collection session. Seventeen participants showed at least EMG signal from two extrinsic foot muscles (tibialis anterior, lateral gastrocnemius), therefore these were included for further analysis and processed with wavelet analysis as described above.

3.4.3. EMG based Centre of Gravity

The use of a multichannel electrode grid allowed the acquisition of EMG signals from a wide region of the plantar surface of the foot, and therefore, it was possible to investigate spatial features of EMG activity within the region (Rojas-Martínez et al., 2013). The distribution of EMG intensity values (Figure 3.3) was investigated by calculating an intensity-based Centre of Gravity (CoG_E), to inform where the region with the highest amplitude signal was located and any changes in the CoG_E position over the course of a trial.

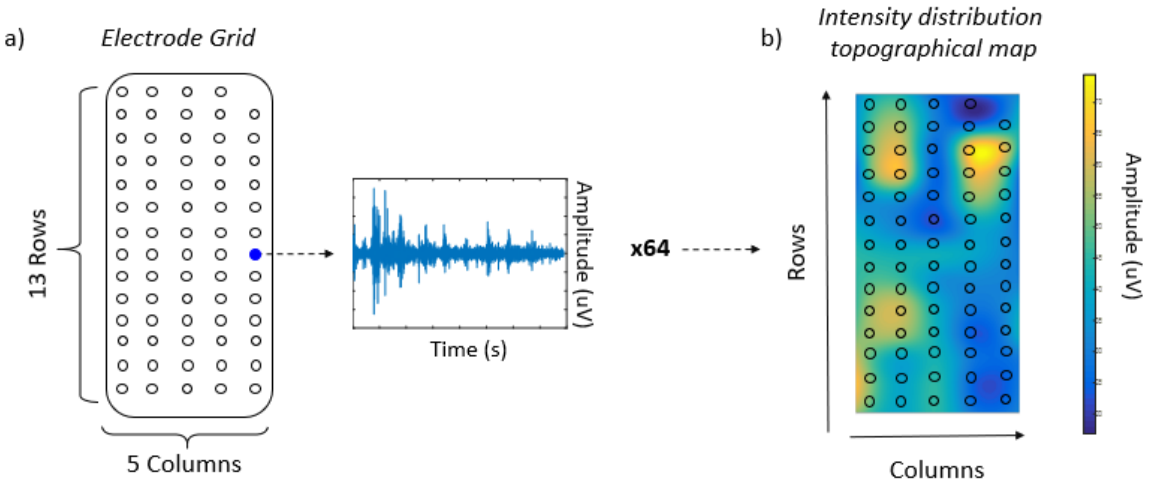

Figure 3.3 Schematic representation of the electrode grid where each channel records an EMG signal providing a total of 64 signals. Here the intensity distribution is represented with a coloured map (b), where the region with the highest intensity are yellow and the regions with the lowest intensity are in blue.

To calculate the CoG_E, clusters of channels were identified, by segmenting the region with highest amplitude (yellow regions in Figure 3.3). The segmentation used was based on Otsu's algorithm (Chen et al., 2010), which allows image segmentation without relying on potentially subjective thresholding (Figure 3.3). Otsu's segmentation works directly on the grey level histogram and finds layers by minimising the weighted within-class variance and maximising the between class variance. Layers can then be identified based on this separation between classes (Chen et al., 2010). By selecting only the most superficial layer (yellow regions in Figure 3.3) the channels showing the highest values were segmented, whereas by adding multiple layers (blue and green layers in Figure 3.3) it is possible to investigate multiple levels of the image.

Figure 3.3 shows an example segmentation applying one and two layers and the results of single and multiple thresholding. By selecting only the most superficial layer the

channels showing the highest values were segmented, whereas by adding multiple layers it is possible to investigate multiple levels of the image.

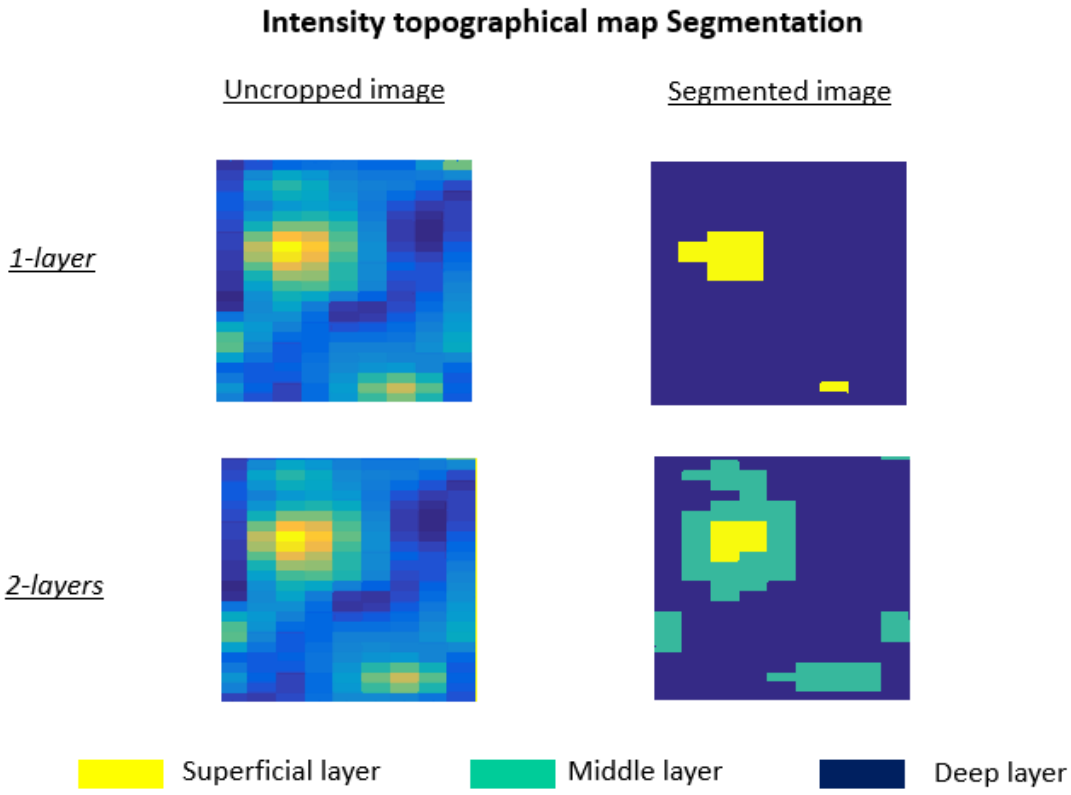

Figure 3-6 Segmentation example for a representative intensity topographical map. Top panel shows the segmentation when one layer is applied, whereas the bottom panel shows the segmentation for two-layers. The yellow regions represent the most superficial layer, corresponding to highest amplitude values, the dark blue represents the deepest layer and the light blue represents values in the middle of the most superficial and deepest layer.

For CoG_E calculation, only one layer was utilised, as it was enough to distinguish between regions with the highest levels of intensities and region with lower intensities. To include only the regions with the highest intensities, clusters of channels showing an intensity value bigger than 80% of the maximum, therefore channels representing the highest activation, were considered for the calculation of CoG_E electrode grid co-ordinates in

the medial/lateral (CoG_{Ex}) and anterior/posterior (CoG_{Ey}) direction (Equation (3.1), Equation (3.2)):

$$CoG_{Ex} = \frac{1}{\sum I(t)} \cdot x(i) \cdot I(t) \qquad (3.1)$$

$$CoG_{Ey} = \frac{1}{\sum I(t)} \cdot y(i) \cdot I(t). \qquad (3.2)$$

Where, *I* is the intensity value at t^{th} data point and *x* and *y* are the coordinates of the i^{th} channels. CoG_E were then used for investigation of distribution of intensities across the sole of the foot during the postural tasks performed in the experimental protocol. *Gx* and *Gy* coordinates for each participant were then normalised to foot length and width, to compare between participants.

Although valuable, amplitude based analysis are not able to provide information on the mechanisms underlying neuromuscular responses to motion. Therefore, non-linear analysis, based on entropy measures, have recently been applied to EMG time series to investigate the variability of the EMG signal, which can be informative on aspects of motor control process (Svendsen and Madeleine, 2010). In this work, entropy based measures were used to analyse the EMG signal to investigate the structure of the signal and potentially provide insights into control processes underpinning the postural tasks studied (Section 2.3.3.3 of Chapter 2). The processing technique took the form of Sample Entropy and Entropy Halflife, whose theory was previously introduced in Section 2.3.3.3 of the Literature Review (Chapter 2). In the following paragraphs the details of the processing technique applied to the EMG data is provided.

3.4.4. Sample Entropy analysis

The total intensity from the wavelet transformed myoelectric signal from each electrode channel was filtered with a high-pass filter (2nd order Butterworth filter, cut-off 10 Hz), to remove the slower temporal signal components related to the movement pattern and leaving components relating to short fluctuations in the envelope profile (Enders et al., 2015). SampEn was calculated using an open-source software package (Goldberger et al., 2000), with a tolerance value, *r*, of 0.2 and a segment length, *m*, equal to 2. The selection of m and r could change the result of the estimate; therefore, it is important to select these parameters appropriately, based on the data series to be investigated. Accuracy and confidence of entropy increase as the number of lengths m matches increases and this can be done by selecting short templates (small m) and wide tolerance (large r). Typical values of m can be found between 2 and 4, depending on the time series of the application (e.g. CoP. EMG, ECG,…), whereas r is defined as 0.1 to 0.25 of the standard deviation of the signal (Richman and Moorman, 2000). In some papers the values are not stated (e.g. Siddiq et al., 2016; Enders et al., 2015). Here we have empirically chosen m=2 and r=0.2, led in part by application of SampEn to EMGs previously reported (Zhang and Zhou, 2012) and that the resulting values did not tend towards zero and in part by applying values of m between 1 and 4 and observing a plateau of SampEn values at m=2 and r=0.2.

SampEn values were normalised to the SampEn value resulting from analysis of a randomly selected channel in the grid, where the data points were randomly shuffled

prior to SampEn calculation. As a random sequence of data, the result should provide the highest value of SampEn meaning all normalised values would be ≤ 1.

As with the analysis of the EMG intensities (Section 3.4.2), the sample entropy analysis also provided a map of 64 SampEn values, corresponding to the grid of electrodes. Similarly, to the intensity data, this allowed the investigation of the distribution of SampEn across the grid, through the calculation of SampEn based CoG (CoG_{SE}). In this case, the implementation of Otsu's segmentation included the use of multiple layers (Figure 3.3). This allowed the segmentation of the channels showing the lowest recorded SampEn values, represented by values of SampEn lower than 80% of the maximum value of the region representing a structured EMG signal, as well as the highest recorded SampEn values, represented by SampEn values higher than 80% of the maximum value (associated with an EMG signal characterised by more randomness). To select the lowest values, a second layer of segmentation was introduced, so the values corresponding to the layer between the maximum and the minimum SampEn values were discarded and the cluster of channels showing lowest values of SampEn was used to calculate the coordinate of the CoG_{SE}. This analysis allowed investigation of the spatial distribution of the signal complexity, indicating regions in the foot with a more structured EMG signal than others with more random EMG signal.

3.4.5. Entropy Halflife analysis

In Chapters 6, a SampEn based analysis was used, a measure called Entropy Halflife (EnHL). The use of EnHL in Chapter 6 and in the pilot experiment in Section 7.2 of the Discussion Chapter (Chapter 7) enabled the investigation of the short-term fluctuations over time of the EMG signal from the intrinsic and extrinsic foot muscles (Enders et al. 2015, Hodson-Tole and Wakeling 2017). EnHL provides information about the structure persistency during motion and potentially of underlying motor control process during simple motor tasks.

The EnHL approach is based on the reshaping of the original signal, to ensure the investigation of a time series where the order is shuffled.

$$P_i = \left[x_{i+0\times\tau}, x_{i+1\times\tau}, x_{i+2\times\tau}, x_{i+3\times\tau}, x_{i+j\times\tau}\right], \quad \text{(Eq. 3.3)}$$

Where $\{\forall j \ \in Z^{\geq 0} | j \times \tau + i \leq L\}, i = 1,2, \ldots . \tau$ and each data point *x* is reshuffled for increasing time intervals (τ).

Data points at a short time interval could potentially be associated, compared to data points at larger time scales, therefore the reshaping scale method described by Enders et al. (2015), allows quantification of the time point where the reshuffled signal transitions from being structured to being completely random. A longer EnHL suggests that a more persisting structure is present in the time series and that potentially a more regular motor unit firing patters is occurring (Enders et al., 2015), whereas a shorter EnHL suggests that the signal is more random and perhaps is the result of a more random motor unit firing patterns. Further details on the EnHL theoretical aspects has been provided in Section 2.3.3.3 of the Literature Review (Chapter 2).

The filtered wavelet transformed EMG signal was initially resampled at 1000 Hz, to provide an interval between data points of 1 ms, and then truncated by discarding the first the last 3% (corresponding to 5 s at the beginning of the trial and 5 s at the end) of data points, to ensure the EnHL analysis represented the motor task and excluded the initial and final adjustments to the task. This corresponds to the middle 20 s of the trials, where the majority of motion seemed to have occurred. This truncation also allowed EnHL to be conducted on signals of the same length, since Entropy Halflife is based on SampEn calculation, which is dependent on signal length, it might also have an effect on the EnHL values. Each truncated EMG intensity envelope was therefore reshuffled at increasingly larger time scales, ranging from 1 ms to 10 seconds, and SampEn calculated for each time scale as previously reported (Section 3.4.3). The timescale at which the normalised SampEn values were equal to 0.5 indicates the transition from a structured to a random signal and was noted as the EnHL value (Figure 2.7). As for previous analyses (Section 3.4.2 and 3.4.3) a map of 64 EnHL values was derived for each trial. Moreover, the map of EnHL enabled the investigation of the spatial distribution of EnHL across the foot region, which could potentially provide information on healthy patterns of EnHL in the foot region.

EnHL analysis was then performed on the EMG from the extrinsic foot muscles, which allowed the study of the interplay of the mechanisms underpinning motion, by investigating the relationship of EnHL from intrinsic and extrinsic foot muscles during simple motor tasks.

All processing on EMG signal and kinematic data was performed using custom written MATLAB scripts whereas the EnHL processing was performed with a Mathematica (Wolfram Mathematica 9, Wolfram Research Inc.) code.

4. SURFACE ELECTROMYOGRAPHY CAN QUANTIFY TEMPORAL AND SPATIAL PATTERNS OF ACTIVATION OF INTRINSIC HUMAN FOOT MUSCLES

This work was presented during an Oral session at the European Society of Biomechanics, July 2017 in Seville, Spain (Abstract in Appendix A).

4.1. Introduction

Commercially available electrode arrays are flat and flexible and can be applied to various body compartment. Application to intrinsic foot muscles has never been attempted, due to the anatomical challenge of their location and, therefore, the features of EMG signals from this body compartment are yet to be described. One main concern is that loading due to body weight, which could influence signal characteristics. As such, signal amplitude changes could represent the movement of electrodes toward/away from the intrinsic foot muscles, rather than the physiological neuromuscular activation. Moreover, amplitude or frequency values outside ranges reported in literature (De Luca et al,1985), might indicate that the signal content is not representative of muscle activation. Therefore, the aim of this work was to investigate whether it is possible to non-invasively quantify physiologically relevant temporal and spatial activation patterns from the plantar foot surface to provide new information about the human foot in health and disease.

4.2. Methods

4.2.1. Participants

Twenty-five healthy participants (twenty-two males and three females, age: 41 ± 15 years, weight: 73 ± 16 kg, height: 1.7 ± 0.1 m, foot length: 26.3±1.8 cm, navicular height: 5.9±1.1 cm, foot width: 9.4 ± 0.9 cm) voluntarily took part in the study having provided informed, written consent to do so.

4.2.2. Data acquisition

Recording of surface EMG from the plantar aspect of the foot is fully detailed in Section 3.2 of General Methodology Chapter (Chapter 3).

Monopolar surface EMGs were recorded with a 64 grid of electrodes from the plantar aspect of the foot, whereas whole body motion was recorded with a 54-marker set, combination of the Plug-in Marker Set (from shoulder to knee epicondyle) and the foot model described in Simon et al (2006) (Figure *4-1*).

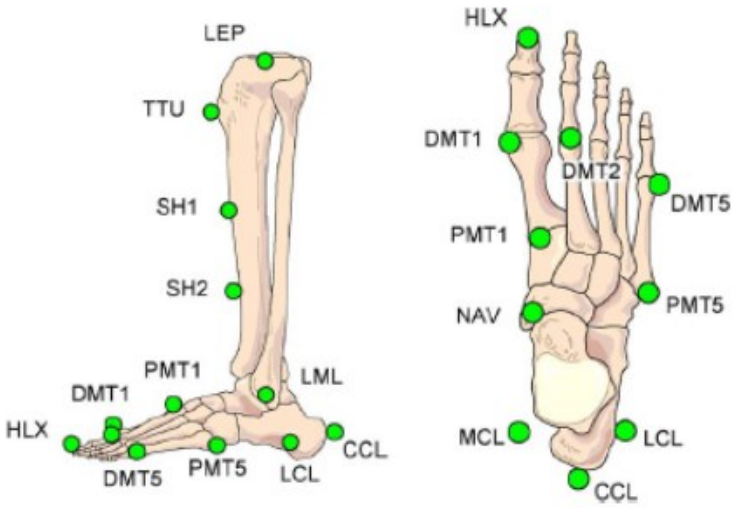

Figure 4-1 Image extracted from Simon et al (2006) showing the marker set used in this study to investigate foot kinematics.

Each participant stood in the test area and was instructed to perform three motor tasks: i) bipedal standing (self-selected comfortable stance width); ii) deliberate anterior/posterior sways (following a metronome beating at 2 Hz) and iii) two-foot continuous standing on tiptoe. These conditions were selected as they provided a range of quasi-static and motion-based conditions, and also provided one condition where there was no contact between the ground and the electrode grid meaning EMGs would be free from external loading.

4.2.3. Data analysis

Analysis of surface EMG is described fully in Section 3.4 of the General Methodology Chapter (Chapter 3). Surface EMG was processed with the wavelet analysis (von Tscharner) (Section 2.3.3.1) and to remove low frequency artefacts, the signal from the first wavelet was discarded so the total intensity at any given time was calculated as the sum of the intensities of the selected ($1 \leq k \leq 10$) wavelets (Hodson-Tole et al., 2012).

4.2.3.1. Investigation of physiological signal content

The first analysis step focused on identifying whether signals recorded were the result of physiological muscle activation and to what extent they were influenced by body weight pressure across the foot. Therefore, mean frequency and total intensity of myoelectric signals were calculated and compared to standard values presented in literature (Basmajian and De Luca, 1985).

From the wavelet transformed signal, the total intensity is used as a measure of EMG intensity over time and the sum of total intensity approximates the description of power (von Tscharner, 2000). Half of the power can be seen as practically equal to the square of the root mean square (RMS) values, therefore the square root of half the power is

equivalent to measures of amplitude such as RMS (von Tscharner, 2000; Wakeling et al., 2002). The mean frequency f_m (Wakeling et al., 2002; Hodson-Tole and Wakeling, 2007) of the intensity spectrum for each sample point is calculated from (Equation 4.1):

$$fm = \frac{\sum_k f_c(k) i_k}{\sum_k i_{j,k}} \qquad (4.1)$$

where f_c is the central frequency of each wavelet. Mean frequency was calculated for the entire length of each trial. Non-physiological signals should show frequency components outside the expected range, which usually spans from 20 Hz to 400 Hz. Peaks saturating the signal might also suggest non-physiological signal content, potentially related to skin-electrode movement. If the signals collected showed frequency and amplitude components in the range reported in the literature, it can be inferred they are the result of neuromuscular drive.

Secondly, whether EMG signal amplitudes were affected by changes in the position of the centre of pressure under the foot was investigated using trials from the anterior/posterior sway task. For this analysis, the centre of gravity (CoG_E) within the electrode grid was calculated, based on the spatial distribution of the activation intensity, and x and y co-ordinate of the maximum activation was extracted (Farina et al., 2008; Rojas-Martínez et al., 2012), as descried in Section 3.4.2. of the General Methodology Chapter (Chapter 3). If the signal amplitudes are affected by foot loading, we expect CoG_E to follow the same pattern of displacement as the biomechanical force plate derived CoP, i.e. forward movement of the CoP should correlate with forward movement of the EMG based CoG_I. If this relationship is not found, we posit that the sEMGs collected can be expected to be primarily representative of muscle activation and not predominantly the result of pressure on the electrode grid.

The CoP was calculated with Visual 3D (C-motion. Inc, Germantown, MD) and, when required, a low-pass filter was applied (Butterworth, 4^{th} order, 6 Hz cut-off) before events corresponding to anterior and posterior sways were identified from the CoP path. The corresponding filtered wavelet-transformed EMG signals were down sampled to the same frequency at which force plate data were sampled (1000 Hz) and the same three events were identified in each signal: i) start of anterior sway; ii) end of anterior sway/start of posterior sway; iii) end of posterior sway. The data points corresponding to these events were manually selected from the CoP trace. For each epoch, the 64 channels intensity map was segmented to extract the region with the highest amplitude values using Otsu's algorithm (Chen et al., 2010) (Section 3.4.2, Chapter 3). Once the CoG_E and force plate based CoP were extracted, the correlation between the two was calculated for the anterior and posterior sway epochs.

4.2.3.2. Quantifying sEMG complexity and amplitude during different movement tasks

In addition to identifying the physiological content of collected sEMG signals, we sought to investigate whether differences in movement patterns were associated with any changes in the sEMG amplitudes and complexity. Review of the biomechanical data revealed participants had completed the anterior/posterior sway trials using a variety of different strategies (i.e. swaying about the ankle joint vs around the hip joint). This variation in movement 'strategy' was therefore exploited to investigate the effects on features of recorded sEMG signals.

Firstly, to identify the movement strategy employed for each anterior and posterior sway event the ankle, knee and hip joint angles were calculated for each sway epoch. As the marker set used to track foot motion was a multi-segment model, it was also possible to calculate the angle between the rear-foot and the forefoot, corresponding to the angle from the medial longitudinal arch. A low-pass filter (Butterworth, 4^{th} order, 6 Hz cut-off) was applied to marker tracks before angle calculation, when required, to remove high frequency noise due to skin-marker contact. For each epoch, the correlation between each joint angle and the CoP was evaluated and the joint with the largest correlation co-efficient was identified as the dominant joint for that movement.

The mean sEMG intensity distribution map was calculated for each anterior/posterior sway event, with the methodology described in Section 3.4.2 (Chapter 3). The x (medial/lateral) and y (anterior/posterior) coordinates of the CoG_E were respectively normalised to the width and length of the foot for each participant (foot width measured as the distance between the first and the fifth distal metatarsal; foot length from the hallux to the calcaneus).

SampEn values were calculated for sEMG data from the same anterior/posterior sway epochs, with the methodology described in Section 3.4.3. of General Methodology. Here r=0.2 and m=2 were used. This analysis provided a map of 64 SampEn values for each epoch identified previously, corresponding to the grid of electrodes, with one map produced per anterior/posterior sway epoch. These maps were segmented using the same technique applied to the amplitude data (Section 3.4.2, Chapter 3), with the use of two layers of segmentation to distinguish the smallest and highest SampEn values. As

with the amplitude data, the x (medial/lateral) and y (anterior/posterior) coordinate of CoG_{SE}, were respectively normalised to the width and length of the foot for each participant. Finally, both amplitude and SampEn CoG values were assigned to one of four categories, defining the joint identified as dominated for the associated sway epoch, enabling comparison of activation patterns between completed movement patterns.

4.2.4. Statistical Analysis

A Kolmogorov-Smirnov normality test was performed on the resulting data and statistical analysis took the form of an ANOVA Generalised Linear Model (Minitab 16, Statistical Software (2010). State College, PA: Minitab, Inc.). A separate test was completed for each dependent factor (CoG_E,CoG_{SE}), with the random factor set as participant number and fixed factors the strategy ('HIP', 'KN','ANK', 'MA'). The critical factor was taken to be $\alpha \leq 0.05$. The location of any significant differences was identified using Bonferroni *post-hoc* analysis. Data are reported as mean ± standard deviation

4.3. Results

4.3.1. Physiological signal content

The mean frequency and intensity values for each movement task are shown in Figure 4.1 and were typical of physiological ranges reported in the literature (Basmajian and De Luca, 1985; Merletti and Parker, 2004). Intensity values were also in the range of those reported in previous studies (Kelly et al., 2012), recorded with intramuscular EMG during tasks of similar effort. Correlation between CoG_E and kinematics CoP showed no correlation during the anterior/posterior sway task (r^2=0.067±0.060), indicating no relationship between motion and shift in the myoelectric CoG_I.

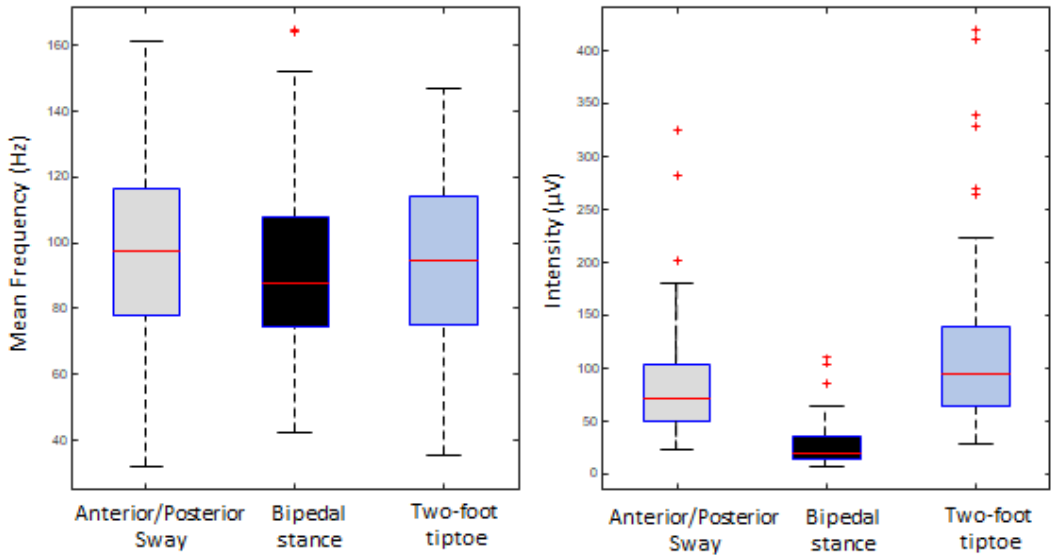

Figure 4-2 Mean ± standard deviation (N = 25) for both mean frequency (Hz) and total intensity (uV) for the three tasks: i) anterior/posterior sway (*95.76±33.17 Hz, 83.41±52.75 μV*, grey boxplot), ii) bipedal stance (*91.62±27.32 Hz, 27.20±20.27 μV*, black boxplot), iii) two-foot tiptoe (*94.17±29.32 Hz, 115.73 ± 79.24 μV*, lightblue boxplot)

4.3.2. Relationship between sway movement and sEMG patterns

The highest correlation co-efficient between the CoP and segment angles commonly differed between epochs within the same task. Across the group of 25 participants, the majority used three different dominant joints during the entire trial (one for each epoch). Table 4.1 shows the number of epochs (*n*) that each segment showed the highest correlation coefficient with the force plate CoP and the mean and standard deviation for each group. The correlation was strong for each of the four segments, but the joint most frequently identified as having the strongest correlation with CoP was the medial arch ('MA'), whereas the least frequently identified joint was the ankle ('ANK') for both sway phases.

Table 4-1 Mean ± S.D. r2 values from association (Pearson's correlation) between joint angle and CoP trace, used to define the dominant joint in each sway epoch. n indicates the number of epochs assigned to each joint.

		Medial Arch (MA)	**Ankle (ANK)**	**Knee (KN)**	**Hip (HIP)**
Anterior sways	r^2	0.896 ± 0.09 $n = 104/245$	0.855 ± 0.151 $n = 42/245$	0.891 ± 0.119 $n = 52/245$	$0.80.0092 \pm 0.035$ $n = 47/245$
	p-values	0.00005 ± 0.00002	0.0013 ± 0.0051	0.0105 ± 0.442	0.0092 ± 0.104
Posterior sways	r^2	0.895 ± 0.113 $n = 105/247$	0.891 ± 0.114 $n = 35/247$	0.909 ± 0.09 $n = 55/247$	0.909 ± 0.0852 $n = 52/247$
	p-values	0.00001 ± 0.00005	0.00007 ± 0.00025	0.0047 ± 0.0194	0.0022 ± 0.0084

Figure 4.3 shows mean and standard deviation for x and y coordinate of the location of the highest EMG activation and most structured signals for both anterior and posterior sways. For each segment both pair of coordinates moved a relatively small amount. The region with the highest activation corresponded to the region where the signal is most structured and least random. CoG_E and CoG_{SE} are both in a region between the 15-37 % of foot width and between the 14-32% of foot length, this region corresponds to the cluster of electrodes on the third column and seventh row of the grid, which is the region located towards the medial of the foot.

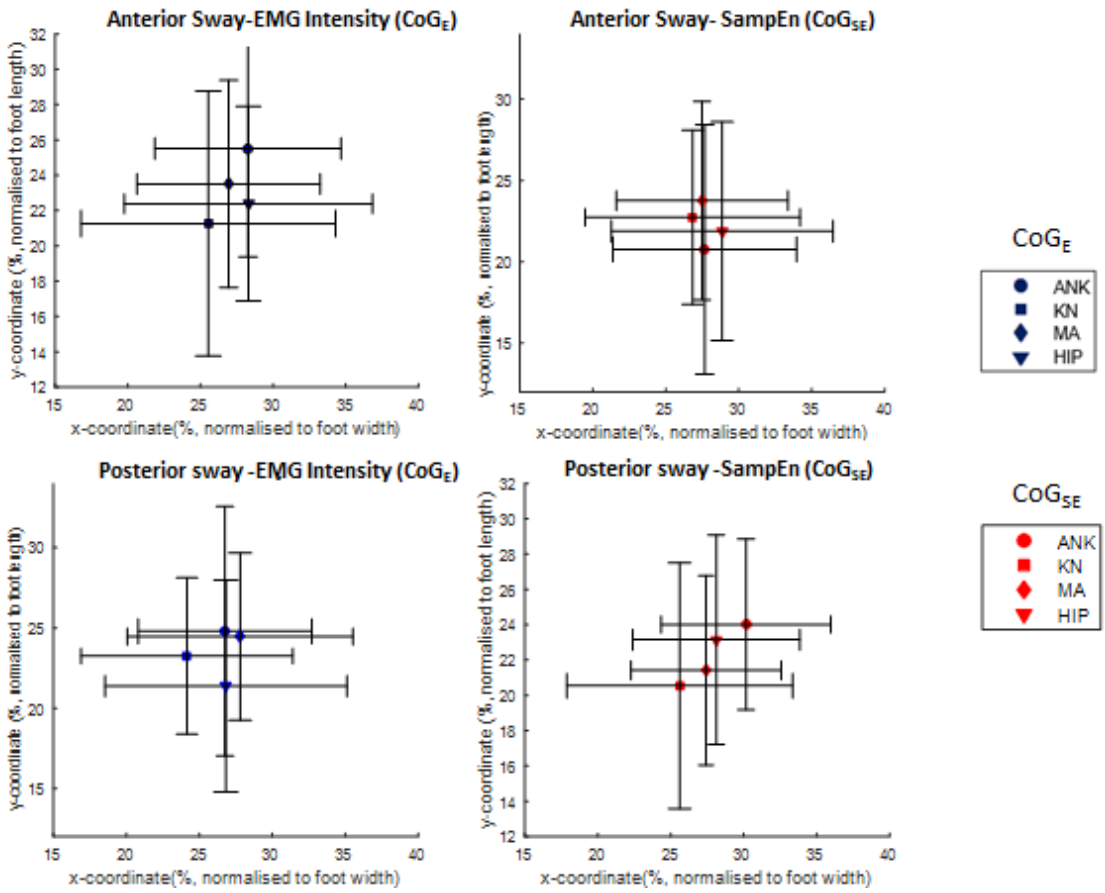

Figure 4-3 Mean and standard deviation for EMG based CoG_E and SampEn based CoG_{SE} coordinates. Red markers represent SampEn and blue markers represent sEMG. Each symbol represents a dominant segment (Ankle: 'ANK', knee: 'KN', medial arch: 'MA', hip: 'HIP'). Left column represents anterior sways. Right column posterior sways.

4.3. Discussion

This study investigated whether it was possible to collect validly physiological sEMG from intrinsic foot muscles using a multi-channel electrode array attached to the plantar surface of the foot. Features of the recorded signals (Figure 4.1) suggest that they are representative of physiological muscle activation and are not adversely influenced by pressure on the electrode grid. The signal intensity increasing with task effort is in line with previous reports (using intramuscular data) where RMS values from quiet standing

on two legs were lower than for standing on one leg (Kelly et al., 2012). The frequency values are within the physiological range (Merletti and Parker, 2004) with the highest mean frequency occurring during the anterior/posterior task. A key concern of using electrode arrays on the plantar foot surface was that signal characteristics would be significantly affected by changes in the point of pressure application under the foot. The results however clearly show no association (r^2=0.067) between CoG and CoP. In addition, the highest intensity values are for the two-foot tiptoe task, the only task where no interaction with the ground occurs, strongly indicating that the EMG signals recorded may be considered indicators of intrinsic foot muscle activation for the tasks assessed here.

During the anterior/posterior sway task participants were challenged to repeatedly and regularly change their posture. Kinematic and kinetic analysis showed that, within the same trial, the same participant commonly displayed different kinematics. Typically, the strongest association occurred between CoP and medial arch angle change (Table 4.1). In previous studies, the action of the medial arch has been suggested to be important for maintaining posture overarching the foot when performing a balancing task (Kelly et al., 2012). This could relate to the function of the intrinsic muscles as toe-flexors and, therefore, the high correlation between the sway movement and the medial arch here may reflect active gripping of the ground with the toes or passive extension/flexion of the joint with the changing centre-of-mass vector direction.

During the anterior and posterior sways, the mean position of CoG for both amplitude and SampEn did not show large differences in position, suggesting that the phase of movement nor the dominant joint had an effect on the regionalised pattern of activation in the intrinsic foot muscles. Both parameters are however grouped in one region, so the region with the highest activation and greatest signal structure coincided. The location is related to the region associated with the *Flexor Digitorum brevis* muscle, which is part of the most superficial layer of intrinsic foot muscles (Figure 4.2). The clustered nature of the data presented here would be interesting to compare against data from clinical populations to explore whether variations might be indicative of different pathologies.

Although mean values for the position of highest activation and most structured signals did not differ significantly with movement pattern, differences were seen within individual participants, an example of which is shown in Figure 4.4.

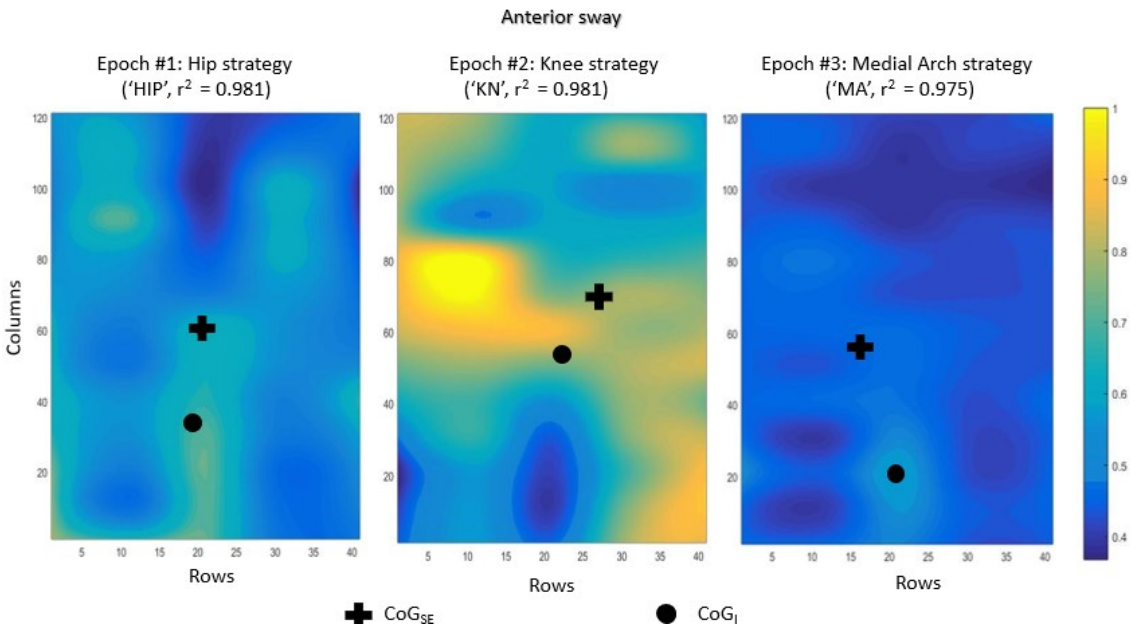

Figure 4-4 Normalised topographical maps from a representative participant during anterior sways. A different dominant joint has been used by the participant for each event.

Here the highest activation occurred during the knee and the lowest for the medial arch dominant movement. This may suggest that when flexing around the knee joint the intrinsic foot muscles actively facilitate the movement, while if the medial arch is more strongly associated with the changes in CoP, the foot is a more passive structure and extrinsic muscles may play a larger role in the task. Figure 4.5 shows the corresponding trajectories of each segment angles and the CoP for the epochs (highlighted in grey) showed in Figure 4.4. Even though the segment angles are relatively small, it allowed to identify epochs within the CoP trajectories and therefore investigate the behaviour of intrinsic foot muscles during different strategies.

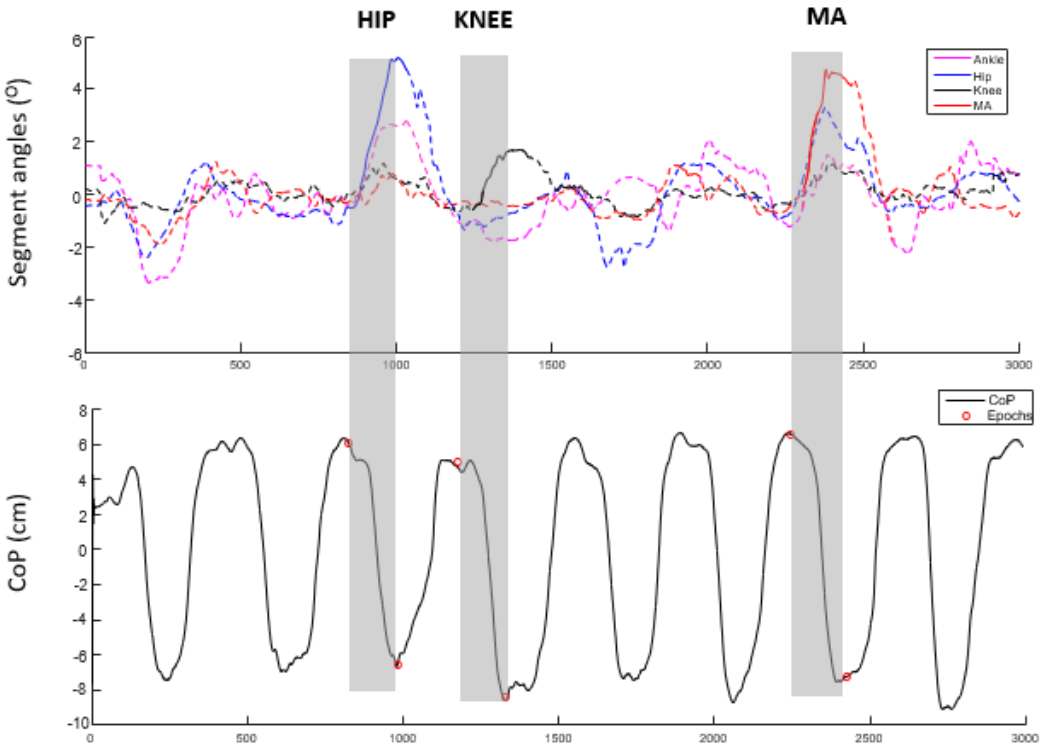

Figure 4-5 Segment angles and CoP trajectories from a representative participant showing three epochs (highligthted in grey) of anterior sway motion and the relative segment angle with the highest association (solid lines). These epochs correspond to the epochs showed in Figure 4.4.

In the group data these differences are, however, lost due to individual variation. Such variability might be related to the position of the grid on the foot with regard participant foot size or might reflect differences in foot and intrinsic muscle morphology or differences in neuromuscular activation strategies. Further investigation is therefore required to understand wider aspects of intrinsic foot muscle activation patterns across different motor tasks and participant populations.

In conclusion, this study investigated the behaviour of intrinsic foot muscles using a surface multi-channel approach, which opens opportunity to collect data from participants where the insertion of a needle is not feasible, and enables exploration of

temporal and spatial features of intrinsic foot muscle activation. It is therefore possible to non-invasively explore wider aspects of intrinsic foot muscle function to help inform understanding of foot muscle properties and function in health and disease. Future work should focus on different motion tasks, effects of pathology and the relationship between intrinsic and extrinsic foot muscles.

5. WHAT IS THE ASSOCIATION BETWEEN MEDIAL ARCH MECHANICS AND ACTIVATION PATTERNS OF INTRINSIC FOOT MUSCLES?

5.1. Introduction

The human foot is an intricate structure, acting as the base of support for the human body. Results from early studies on upright posture seem to suggest that during postural control, the majority of active muscles are located in the lower limb (Winter et al., 1995). However, a more recent biomechanical study (Menz et al., 2005) showed that the foot actively contributes to upright posture via the architecture of the arch and problems associated with this structure directly limit the ability to maintain balance.

The importance of the arch for postural control has been investigated during biomechanical studies, which indicate that the combination of bones, ligaments and plantar aponeurosis contribute to the support of the arch (Soysa et al., 2012). However, few intramuscular EMG studies (Reeser et al., 1983, Fiolkowski et al., 2003) have proposed how the intrinsic muscles provide structural support to the medial arch, as described in Section 2.5 of the Literature Review (Chapter 2), in quiet standing (Fiolkowski et al.,2003, Kelly et al, 2012). This suggests that weakness in the plantar musculature has the potential to contribute to problems standing and walking and risk of falling with significant potential to influence quality of life in affected populations of people. More recent intramuscular EMG studies (Kelly et al., 2012, Kelly et al., 2014) investigated the role of intrinsic foot muscles in maintaining balance and providing support during quiet stance. In these studies, the intensity of activation increased with the effort required by the postural task (i.e. postural demand) (Kelly et al., 2012). These

authors also showed that the activation level was strongly correlated with the mediolateral direction of movement in single leg-stance, suggesting a contribution of intrinsic foot muscles in maintaining balance control and upright posture. However, no studies have investigated association between medial arch behaviour, such as angle kinematics, and intrinsic foot muscles activation. This information could potentially inform understanding of what the response of intrinsic foot muscles is for specific postural tasks and the association with medial arch properties.

Finally, the results reported by Kelly et al. (2012) were achieved by recording muscle activation in an invasive way. This approach could cause some discomfort to the participant, who then consequently might behave in an unusual manner, caused by psychological effects or pain/discomfort associated with the invasive procedure. The invasive nature of the approach also precludes assessments of a wide range of clinical and healthy populations (e.g. diabetes due to risk of infection, children, elderly on blood thinning medication, etc). It is however possible to use non-invasive, multi-channel, surface electrodes to record myoelectric signals (Chapter 4). The advantage of using a multi-channel grid of electrodes is the possibility to investigate not only the magnitude of myoelectric features, but also the spatial distribution (Literature Review section 2.3.3.2). The aim of this chapter was therefore to quantify the effects of different postural demands on the spatial features of EMGs recorded from the intrinsic foot muscles. It was predicted that different postural tasks would result in different kinematics and centre of pressure movements (larger sway, greater changes medial arch angle) and these would be associated with changes in spatial features of the intrinsic foot muscle EMG. The following objectives were therefore set: i) recording surface EMG with a multi-channel grid of electrodes during simple postural tasks from intrinsic foot

muscles; ii) evaluating the medial arch angle and the centre of pressure; iii) quantify the EMG based CoG_E and force plate derived centre of pressure (CoP) amount of sway and medial arch angle magnitude; iv) quantify the association between EMG features and medial arch angle properties.

5.2. Methods

5.2.1. Participants

Twenty-one healthy participants (eighteen males and three females, age: 40.76 ± 14.14 years, weight: 76.76 ± 15.53 kg, height: 175.33 ± 9.39 cm) voluntarily took part in the study having provided informed, written consent to do so.

5.2.2. Data acquisition

Experimental setup and data acquisition are described in the General Methodology Section (Chapter 3). For the purpose of this investigation, data were analysed from the following four motor tasks: i) bipedal stance; ii) single-leg stance; iii) deliberate anterior/posterior sways and iv) deliberate medial/lateral sways. These conditions were selected as they provided a range of challenges to posture and maintenance of balance that enable investigation of the behaviour of intrinsic foot muscles during differing levels of centre of mass movement.

5.2.3. Data analysis

Centre of pressure (CoP) from force plate data was extracted from Visual 3D (C-motion. Inc, Germantown, MD) and further analyses was produced with custom made routines

in MATLAB (MathWorks Inc., MA, USA). Prior to all analyses mediolateral and anteroposterior CoP trajectories were detrended, by subtracting the mean from the original time series, and bi-directionally filtered (second-order low-pass Butterworth filter, cut-off frequency 12.5 Hz) (Roerdink et al., 2006; Donker et al., 2008).

As the marker set used to track foot motion was a multi-segment model, it was also possible to calculate the angle between the rear-foot and the forefoot foot segments, corresponding to the angle of the medial longitudinal arch. A low-pass filter (Butterworth, 4^{th} order, 6 Hz cut-off) was applied to marker tracks before angle calculation, when required, to remove high frequency noise due to skin-marker contact. Details of preliminary analysis of surface EMG are reported in General Methodology Chapter (Chapter 3, Section 3.4.1.). Wavelet transformed surface EMG signals were used to quantify an EMG based centre of gravity (CoG_E), which enables evaluation of the movement of the highest region of activation across the plantar region of the foot (Section 3.4.2, General Methodology). To evaluate the association between parameters, the same number of data points is needed, therefore the CoG_E was resampled to the sampling frequency of the CoP force plate derived (1000 Hz) and to the medial arch frequency (100 Hz), respectively for the relevant correlation.

5.2.4. Biomechanical parameters analysis

Postural behaviour is often assessed by means of posturography that is the quantitative analysis of COP trajectories and deviation in the location of COP measured by means of a force platform (Prieto et al., 1996; Roerdink et al., 2006; Ruhe et al., 2011). The posturography measure applied here was the calculation of the *distance* (Donker et al., 2008), which provides information about how much the CoP moved from a point of reference. This parameter was quantified by calculating the distance between the detrended trajectories, so the sway during the trial was evaluated for each time-series (Equation (5.1)):

$$d_i = \sqrt{x_i^2 + y_i^2} \qquad (5.1)$$

where $i = 1, \ldots, N$ samples in COP trajectories (Donker, Ledebt et al. 2008).

The amount of sway, *r*, is quantified by calculating the mean value of the *d* time series. This approach was applied to both the CoP trajectories and the medial arch (MA) angle trajectories, resulting in calculation of MA amount of sway (r_{MA}) and CoP amount of sway (r_{CoP}).

5.2.5. Surface EMG Parameters

CoG_E was calculated for each data point of the time series, resulting in trajectories similar to the CoP describing the movement of the highest intensity over time during the postural task. This allowed the application of the same posturography measures applied to the CoP and MA angle trajectories (Section 5.2.4), facilitating investigation of the association between the two parameters. The distance was quantified by applying

Equation (5.1) and the amount of sway for the CoG_E distance (r_{CoGE}) was then calculated as the mean of the distance time series.

5.2.6. Cross-correlation between CoG_E and respectively CoP and medial arch angle

To investigate the association between mechanical behaviour and response of the intrinsic foot muscle activation, cross-correlation between CoP (representing whole body motion), and medial arch angle (medial arch motion), with CoG_E was quantified. Cross-correlation was used to quantify the timing information between the mechanical and electrical aspect of motion (Nelson-Wong et al., 2009). Prior to the cross-correlation being calculated, envelope of trajectories from the CoP, CoG_E and MA were quantified, by applying a low-pass filter (Butterworth, 2nd order, 2 Hz cut-off) to the absolute value of each of the trajectories (Nelson-Wong et al., 2009). An embedded function in MATLAB (xcorr) was used to investigate the cross-correlation and to quantify the time difference between trajectories, also known as *lag*. The reference signal was fixed to be the CoG_E, whereas the signal to be compared was respectively CoP and MA. A negative lag means that either the CoP or the MA changed before the CoP, whereas a positive lag suggests that the CoG_E changed before CoP or MA. Table 5.1 shows the cross-correlation analyses performed for each trajectory of each time series (CoP, CoG_E and MA).

Table 5-1 Summary of cross-correlation performed. For COG and CoP X refers to medio-lateral (M/L) direction and Y refers to anteroposterior (A/P) directions. For MA X refers to inversion-eversion (I/E) and Y refers to flexion-extension (F/E).

	XX	**XY**	**YX**	**YY**
CoG_E -MA	*CoG_{Ex}* (M/L direction) and *MAx* (I/E)	*CoG_{Ex}* (M/L direction) and *MAy* (F/E)	*CoG_{Ey}* (A/P direction) and *MAx* (I/E)	CoG_{Ey} (A/P direction) and MAy (F/E)
CoGE-CoP	CoG_{Ex} (M/L direction) and CoPx (M/L direction)	CoG_{Ex} (M/L direction) and CoPy (A/P direction)	CoG_{Ey} (A/P direction) and CoPx (M/L direction)	CoG_{Ey} (A/P direction) and CoPy (A/P direction)

The relationship of the lag between CoP and CoG_E and the lag between CoG_E and MA for each pair of trajectories analysed (Table 5.1, XX, XY, YX, YY) was quantified by applying the major axis technique (Sokal and Rohlf, 1995) to obtained lag values. The major axis method is usually applied when the relationship between the two variables is not clear (which one is the regressor and the dependant) and they are subject to error. This method involved calculation of regression values in the linear model, the confidence interval and the eigenvalues of the axes. This allowed identification of the relationship between the cross-correlation between CoP and CoG_E. and the cross-correlation between CoG_E and MA.

The goodness of fit (r-squared values) enabled identification of any strong relationships between the response of the mechanical variables (CoP, MA) and the intrinsic foot muscles activation, while the slope of the major axis can predict time delays between CoG_E and CoP, if CoG_E and MA are known. If the lines of best fit have a positive slope,

shorter time delay between CoG_E and MA movement are associated with shorter time delays between CoG_E and CoP movement

5.2.7. Statistical analysis

A Kolmogorov-Smirnov normality test was performed on the resulting data and statistical analysis took the form of an ANOVA Generalised Linear Model (Minitab 16, Statistical Software (2010). State College, PA: Minitab, Inc.). A separate test was completed for each dependent factor (r_{COP}, r_{COGE}, r_{MA}), with the random factor set as participant number, as the analysis will not estimate the effect of each participants, and fixed factors the type of task. The critical factor was taken to be $\alpha \leq 0.05$. The location of any significant differences was identified using Bonferroni *post-hoc* analysis. Data are reported as mean ± standard deviation.

5.3. Results

5.3.1. Difference in Biomechanical and EMG parameters between postural tasks

Figure 5.1-A), shows the amount of movement (r_{CoP}) for each task. The greatest r_{CoP} occurred during the mediolateral sway (7.81±1.61 cm) and the smallest for the bipedal stance (0.64±0.28 cm). Statistical difference was found between all four tasks (*p*-value <0.05) for the r_{CoP}, with a goodness of fit of the model of 94.84% (R-sq).

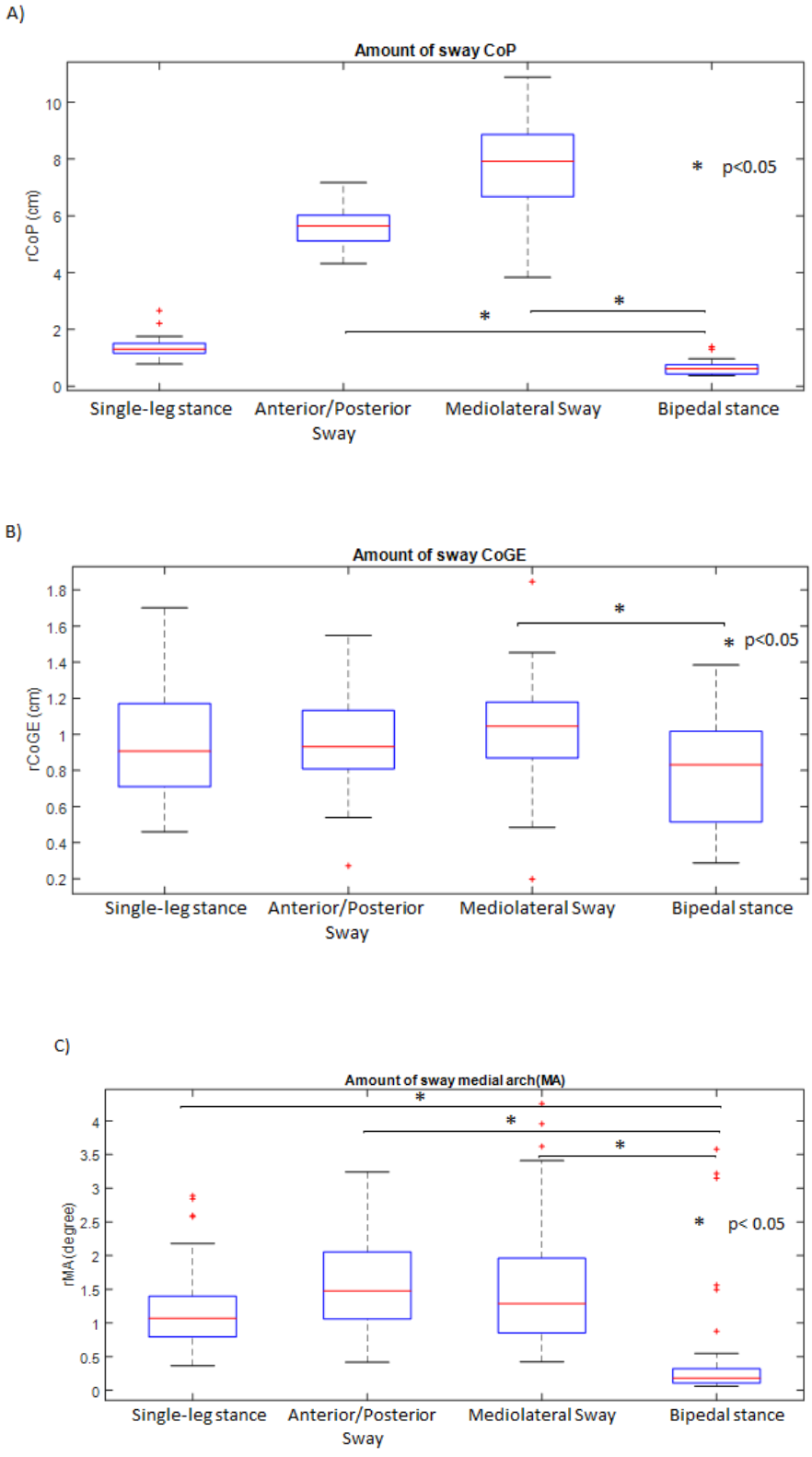

Figure 5. 5-1 Distribution of amount of sway for COP (r_{CoP}), CoG_E (r_{CoGE}) and MA (r_{MA}) values for the four postural tasks. Significant difference ($p<0.05$) in r_{CoP}, r_{CoGE}, r_{MA}, are presented (bracket and asterisk); The biggest r_{CoP} and r_{CoGE} was showed by the mediolateral sway task and the smallest during bipedal stance, whereas the biggest r_{MA} was showed by the anterior/posterior sway.

Figure 5.1-B), shows the amount of movement (r_{CoGE}) for each task for CoG_E. The r_{CoGE} was the highest for the medio-lateral sway (1.00±0.37 cm) and the smallest for bipedal stance (0.78 ±0.40 cm). For r_{CoGE} statistical difference was found between the bipedal stance (*p*-value<0.05) and the three motion tasks, with a goodness of fit of the model of 73.43 %. (R-sq).

Figure 5.1-C), shows the amount of movement of the MA angle (r_{MA}) for each task. The r_{MA} was highest for the anterior-posterior sway (1.57±0.65 degrees and the smallest for bipedal quiet stance (0.41 ±0.73 cm). For r_{MA} the statistical difference was found between the bipedal stance (*p*-value<0.05) and the three motion tasks, with a goodness of fit of the model of 28.67 % (R-sq).

5.3.3. Cross-correlation between myoelectric parameters and biomechanical parameters

The strongest association was found from the cross-correlation of both CoG_E-MA and CoG_E -CoP in the XX combination (mediolateral direction movement for CoG_E and CoP and the inversion/eversion movement for the MA angle), during the tasks of anterior/posterior sway (r^2=0.76) and mediolateral sway (r^2=0.67) (Figure 5.2, Panel A) and Panel B))

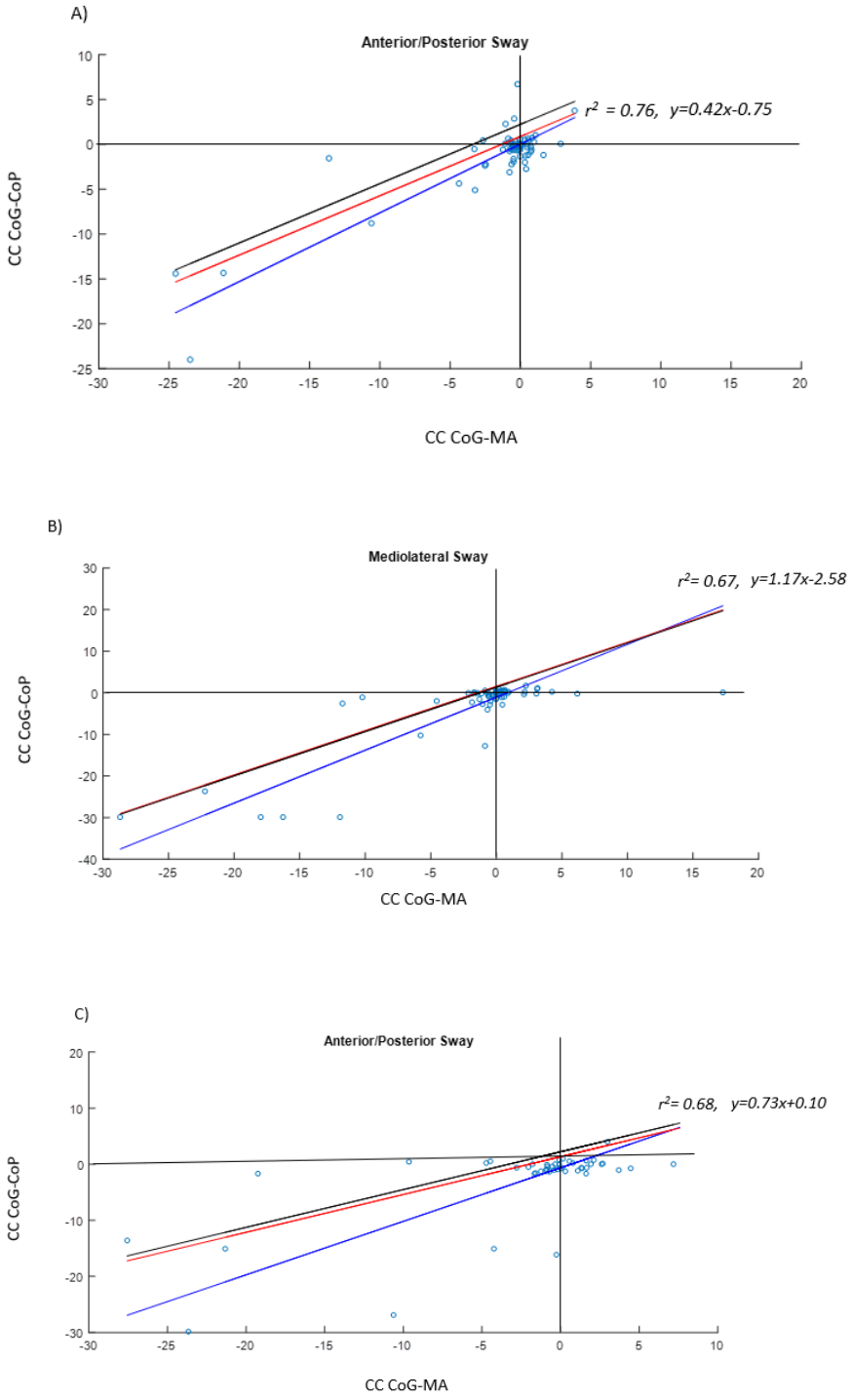

Figure 5-2 Correlation between time delays (lags) for the cross-correlation between CoG and MA and CoG and CoP. Red line is the best fit for the data, blue line is the lower confidence interval, black line is the upper confidence interval. Panel A) and B) shows the correlation for the combination XX, whereas Panel C) shows correlation for the combination XY

In addition, for the anterior-posterior sway the XY combination (mediolateral direction movement for CoG_E and CoP and flexion/extension for MA angle) also showed a strong

correlation (r^2=0.68) (Figure 5.2, Panel C). For each case, the majority of data points were located around the origin, however, the biggest portion of the line of best fit was in the negative quadrant. The other combinations of cross-correlation tested did not show strong associations, however the r^2 values are reported in Table 5.2 for completeness.

Table 5-2 Summary of r-squared values for each combination of cross-correlation

	XX	**XY**	**YX**	**YY**
Single-leg stance	0.15	0.01	-0.05	0.02
Bipedal stance	0.19	0.16	0.50	0.20
Mediolateral Sway	0.67	0.23	0.37	0.42
Anterior-Posterior Sway	0.76	0.68	0.42	0.20

5.4. Discussion

The aim of this study was to investigate the association between medial arch and body movement mechanics and the response of EMG signals recorded from the intrinsic foot muscles in a non-invasive way during postural tasks. For this group of healthy participants, the largest amount of sway occurred during the mediolateral sway task (Figure 5. 5-1, A). The same pattern was reflected in the amount of sway for CoG_E (Figure 5. 5-1, B) where there was a significant difference between the mediolateral sway and the bipedal stance task. It seems to suggest that for this task where participants were instructed to regularly shift bodyweight in the mediolateral direction, they engaged the intrinsic foot muscles at a higher level in respect to the other motion tasks.

For the medial arch the smallest amount of movement occurred in the bipedal stance task, while the largest amount of movement occurred during the anterior-posterior sway (Figure 5. 5-1, C), where the foot arches in the sagittal plane. A lot of outliers are present in the bipedal stance task, with angle magnitude values similar to those from the anterior-posterior sway task. During quiet standing this group presented large changes in medial arch angle, but with small changes in the CoP (no outliers are present Figure 5.1A). This might suggest that in some people there are large changed in the MA angle even if larger sways do not occur, which could indicate the additional arching of the foot to maintain balance.

The results presented here are in line to previous studies (Kelly et al., 2012) with the greater motion during medio-lateral sway seeming to have a stronger effect on intrinsic foot muscle activation. This suggests that during a mediolateral sway there were more changes in the CoG_E, suggesting more contribution of the intrinsic foot muscles. These

could act to stiffen the foot and limit the changes in MA. During anterior-posterior sway there is less contribution of intrinsic foot muscles, so the foot is more compliant with the type of task and MA produces more movement.

This might suggest that even if during mediolateral sway the CoG_E produces a higher amount of sway and therefore contribute to balance, it may also suggest that in order to activate the intrinsic foot muscles, the CoP needs to reach a threshold needing more balance. This result might then differ in participants where balance is impaired due to foot muscles weakness and there may produce a different pattern.

The relationship between time delays between the mechanical parameters (COP and MA) and CoG_E revealed that there are three conditions where a strong association occurs between the delays between CoP and CoG_E movement and between MA and CoG movement. These conditions belong mainly to motion in the mediolateral direction for the CoG_E for the mediolateral sway and anterior-posterior sway tasks, which again supports what Kelly et al. (2012) stated. For the anterior-posterior sway the strong correlation is also with flexion and extension of the medial arch angle (Figure 5.2, C). The positive slope showed by the lines of best fit suggests that shorter time delays between CoG_E and MA movement are associated with shorter time delays between CoG_E and CoP movement. The slope value is close to unity in two cases (Anterior-posterior XY, Figure 5.2.C and mediolateral sway XX, Figure 5.2.B) could indicate a synchronicity between the changes in the biomechanics parameters and CoG. In the third case (Figure 5.2,A), the slope of the line is less than 1 (0.42), which could indicate that a large change in the time delay between CoG and MA produces a relatively small change in the timing between CoG and CoP. This relationship seems to differ depending on the task or variables being

measured. This could potentially suggest flexibility in the motor control strategy, where the nervous system responds to a challenge (task) in a specific manner and depending on the association recorded can choose to either act synchronously (first two cases) or sequentially (last case).

The direction of motion generated a specific response both in biomechanics of the foot (CoP, MA) and intrinsic foot muscles activation (CoG_E). The difference can be seen between the mediolateral and anteroposterior direction of movement. Mediolateral sway caused more motion in the CoP and as a result more motion in the CoG, whereas in anterior-posterior sways participants produce a smaller amount of CoP sway (Figure 5.1, A), with bigger medial arch angles potentially related to an overarching of the foot. This behaviour can also be seen in the cross-correlation where the mediolateral direction (X) is the one where the strongest relationship were found (Figure 5.1.).

However, the variable nature of these data set caused a number of outliers in the cross-correlation (Figure 5.2) and if these values are removed, the correlation values drop to weak values ($r^2<0.5$). By having larger variability in the data, the ability to detect statistical significance is reduced. The post hoc analysis indicated a sample size of 27 participants was appropriate, however the variability in these data may have increased the risk of a type II error (no significance when there is one).

Nevertheless, variability could be interesting as, traditionally, it is identified as noise. Previous studies have indicated how most researchers ignore individual variability, by averaging group data, which could hinder difference in muscle activation and individual strategies (Hug and Tucker, 2017). Variability should therefore be addressed and considered as one of the most common feature of human movement and variation of

this feature could be an indicator of pathological or healthy states. (Stergiou et al, 2011). Moreover, more recently it is becoming apparent that important information may be contained in the temporal organisation of the variability.

As the variability in these results does not allow conclusions to be drawn on the dynamics between the biomechanics features (CoP and MA) and the CoG during simple motor tasks, by evaluating the structure of the signal variability with entropy-based analysis, rather than magnitude based, it could potentially provide insights into the motor control to movement and intrinsic foot muscles.

Therefore, it was decided to exploit the collected set further and evaluate the structure of the signal variability with a view of understanding more about neural drive to the IFMs.

Further investigations should therefore focus in the non-linear analysis of intrinsic foot muscles activity during postural tasks, to investigate the drive to these muscles and investigate how much these muscles are actually engaged. This knowledge could help inform on control mechanisms of both healthy and clinical population for the design of rehabilitation protocols or insole design.

6. HOW DOES POSTURAL TASKS AFFECT THE ENTROPIC HALFLIFE OF SURFACE EMGs FROM INTRINSIC FOOT MUSCLES?

6.1. Introduction

Human movement is the result of an intricate system of muscles, bones and joints working in a combined way to achieve motion (Prieto et al., 1996). Muscles contribute to movement by contracting, and pulling tendons attached to bony structures in the body. Investigating the features of human muscle activation is therefore fundamental to understand the mechanisms underpinning movement.

Muscle groups associated with the long bones of the lower limbs are more clearly involved in human movement (e.g. tibialis anterior or the triceps surae muscles) and they have been often studied in the past (Rainoldi et al., 2016; Winter, 2009; Vieira et al., 2011; Vieira et al., 2013). In contrast, other less obvious muscles contributing to motion, such as the thin layers of intrinsic muscles within the foot, are often disregarded from studies involving the investigation of balance, locomotion or postural control. However, recent studies have shown that this group of muscles in the plantar aspect of the foot play a fundamental role during quiet stance and balancing tasks, by stiffening the foot structure and supporting the arch (Fiolkowski et al., 2003, Kelly et al., 2012, Kelly et al., 2014). These studies investigate intrinsic foot muscle activation by analysing linear parameters of the myoelectric signal. For example, amplitude based measures (e.g. RMS, ARV,..) of the EMG signal, can be considered to indicate the effort level of the

muscles during a task; while frequency analysis (e.g. MNF, MDF,…)(Merletti and Parker, 2004) can provide insights on the frequency components of the signal or fatigue (Falla et al., 2003; Troiano et al., 2008). These measures do not however provide information on how challenging the task may actually be for the control process. To understand the changes in the controller approach, it is necessary to investigate the structure of the EMG signal. Non-linear analysis, such as entropy-based analysis (Richman and Moorman, 2000), can provide understanding on the structure and complexity of the myoelectric signal, features that have been shown to provide information into the factors underlying control processes (Rathleff et al., 2011;Roerdink et al., 2006; Donker et al., 2008) and could potentially provide insights into the features of the neuromuscular control process. One entropy based measure is called Sample Entropy (SampEn) (Richman and Moorman, 2000) and values from this analysis can indicate the level of randomness or structure of a time series, such as the EMG signal. Higher values of SampEn represent a more random time series, whereas lower values of SampEn suggest a more structured time series. A recent study (Zandiyeh and von Tscharner, 2013) introduced a new tool, called Entropic Halflife (EnHL), based on SampEn analysis, which is able to identify the time point representing a transition from SampEn values reflecting order to those reflecting randomness within a signal and is fully described in Section 2.3.3.3. of the Literature Review (Chapter 2). This methodology is based on a rescaling of the original signal, by reorganising the time series over multiple numbers of data points to determine the time scale over which subsequent data points remain associated to one another. This reshape scale approach provides a means of quantifying short-term fluctuations in a signal that can describe adjustments in the underlying signal process, and are applicable to studying neuromuscular function during motor tasks. This

tool allows the assessment of the EMG structure, which may provide insight into the perceived challenge (i.e. complexity) of the task. A longer EnHL suggests the order of the signal is maintained for a longer period of time, compared to shorter EnHL representing a signal losing the order and transitioning to random at a shorter period of time. This has been shown in studies of cycling (Enders et al., 2015) and running (Hodson-Tole and Wakeling 2017) where changes in task demand related to load and velocity are significant influencing factors. The neural drive to the intrinsic foot muscles has not been previously investigated using this approach and, during postural tasks, EnHL has the potential to provide insights into how long information in the signal remains relevant to the current state of order. Therefore, for more challenging tasks it is predicted that longer periods of the signal will remain affiliated (longer EnHL), for less challenging tasks more variation occurs and hence the affiliated portions of the signal will occur over shorter time periods. The first aim of this study was to therefore quantify EnHL for the intrinsic foot muscles and identify the typical range of EnHL values during postural tasks. This aim was achieved by: i) quantifying the EnHL of surface EMG signals recorded from the intrinsic foot muscles using a multi-channel surface electrode array during three postural tasks; ii) evaluate EnHL for surrogate, phase randomised signals to confirm EnHL in original signals were dependent on signal structure; iii) compare the values of EnHL with previous studies.

The second aim was to exploit the spatial information provided by the electrode array and investigate the variation in EnHL values between the array channels. Results from the study presented in Chapter 4 showed a EMG intensity distribution pattern across the array, with the highest intensity corresponding to the portion of the foot associated with the *flexor digitorum brevi*s. As previous results indicated EnHLs were longer at

higher effort levels (Enders et al., 2015; Hodson-Tole and Wakeling 2017), and potentially higher EMG intensity, it was hypothesised that electrode channels associated with the highest myoelectric intensity would correspond to longer EnHLs.

6.2. Methods

6.2.1. Participants

Twenty healthy participants (seventeen males and three females, age: 39.1 ± 13. 4 years, weight: 74.3 ± 14.3 kg, height: 175.7 ± 9.4 cm) voluntarily took part in the study having provided informed, written consent to do so.

6.2.2. Data acquisition

Surface EMGs were recorded with a 64-channel grid of electrodes as described in Section 3.2 of the General Methodology chapter (Chapter 3). Each participant was asked to stand in the test area and instructed to perform three motor tasks: i) bipedal stance; ii) one-foot stance; iii) two-foot tiptoe stance. These conditions were selected as they provided a baseline (bipedal standing) and two more challenging tasks that induce larger amplitude natural sways in both anterior/posterior (two-foot tiptoe) and mediolateral (one leg stance) directions. Participants completed three trials of each condition, and all trials were taken forward for further analysis.

6.2.3. Data analysis

The preliminary analysis of recorded surface EMGs is described in section 3.4.1. of the General Methodology chapter (Chapter 3). The total intensity from the wavelet

transformed myoelectric signal was filtered with a high-pass filter (2nd order Butterworth filter, cut-off 10 Hz), as it was suggested in previous EnHL studies to remove the slower temporal signal components, leaving components relating to oscillations in the envelope profile (Enders et al., 2015). The filtered wavelet transformed signal was then used to calculate the EnHL of the myoelectric signal from the trials.

Before applying the EnHL algorithm, each wavelet transformed myoelectric signal was resampled to 1000 Hz, so that the time difference between data points was 1 ms (Zandiyeh and von Tscharner, 2013). The middle twenty seconds of the task was selected for analysis (Hodson-Tole and Wakeling, 2017), to avoid inclusion of data points relating to initiation or termination of the task. This truncation also ensured all trials were the same length, an important consideration as EnHL is based on SampEn calculation, which may be influenced by the number of data points included in the analysis (Richman and Moorman 2000).

Based on previous results the threshold EnHL representing neuromuscular drive and affected by task demand is predicted to be approximately 40 ms (Enders et al., 2015, Hodson-Tole and Wakeling, 2017), whereas longer values do not represent physiological response to motion. Preliminary inspection of the EnHL values revealed that in some cases very long EnHL values were calculated. These were identified as sporadic channels, with values up to two times the order of magnitude of the majority of the other simultaneously recorded signals from the electrode grid. Therefore, it was decided to consider these sporadic channels as noise/non-physiological and disregard them from further analysis. In 10% of the trials (15 out of 135 trials) it was evident that sporadic electrodes showed unexpectedly long EnHL. Of these, in 14 trials the number of

channels affected was more than 20%. This accounts for more than 12 channels out of 64, making interpolation of values across channels unreliable and hence these trials were disregarded from further analysis. In the remaining 121 trials, less than 12 channels were affected, therefore it was possible to interpolate a EnHL value based on physiologically realistic surrounding signals. For these trials interpolation was completed, and they were retained in the statistical analysis.

To determine whether the EnHL values truly reflected structure of recorded signals, they were also compared with EnHLs calculated from surrogate signals (Enders et al., 2015). The surrogate signals were generated from 53 (39% of the complete data set) randomly selected trials, and corresponded to the time series containing the power information of the selected signal, but with the phase randomized. If the EnHL in the original signals was related to the signal structure EnHL values of physiological signals should be greater than the EnHL from the surrogate signals.

Once the range of EnHL values were described, maps of EnHL were analysed in terms of the spatial distribution of EnHL across the array. For each trial, the centre of gravity of the cluster of channels showing longer and shorter EnHL was calculated, by segmenting the EnHL map with two threshold levels. Channels showing EnHL values bigger than 90% of the maximum were included in the cluster of longer EnHL, whereas channels with EnHL shorter than 90 % of the minimum were included in the cluster of channels representing the region with shorter EnHL. Considering that EnHL values come from clean and interpolated EMG signals, it was possible to select a very narrow segmentation threshold (90%) to include the most divergent conditions. This has been done with Otsu's segmentation as described in Section 3.4.2. of the Methodology Chapter (Chapter

3). Finally, the regions in the array and plantar region of the foot comprising the set of CoGs (one for each trial) corresponding to respectively longer and shorter EnHL were then characterized by calculating the area. The position of each area and its distribution can therefore be considered to describe the spatial regionalisation of EnHL values across a map of the electrode grid.

6.2.4. Statistical analysis

EnHL values were tested for normality with a *Kolmogorov-Smirnov* normality test. The variance across the groups of EnHL was tested with a *Levene*'s test. These results showed that these data were normally distributed with equal variance between the groups, therefore statistical analysis took the form of a General Linear Model ANOVA (Minitab 16, Statistical Software (2010). State College, PA: Minitab, Inc.). A test was completed with the EnHL as the dependent factor, random factor participant number and fixed factors the type of task. The location of any significant difference was identified using Bonferroni corrected *post-hoc* analysis. For all analyses the critical factor was taken to be $\alpha \leq 0.05$.

A mixed effects model was completed for both the shorter and longer EnHL CoGs, with the random factor being the participant number, the fixed factor the type of task and the dependant factor the CoG coordinate. The test was computed separately for each condition (shorter and longer EnHL), once for the medial/lateral coordinate (CoG_{Ex}) and once for the anterior/posterior coordinate (CoG_{Ey})

6.3. Results

EnHL values for the intrinsic foot muscles showed a total range of: 12 ms and 38 ms for the two-foot tiptoe; 11 ms and 35 ms for single-leg stance; and 8 ms and 28 ms for bipedal stance. EnHL values are also greater than those from the surrogate signals, with a significant difference between the two groups (p<0.05). The EnHL values for the surrogate signals were in the ranges: i) 8 ms – 12 ms for the two-foot tiptoe; ii) 8 ms – 16 ms for the single-leg stance; and iii) 9 ms – 14 ms for the bipedal stance.

Figure 6-1 shows the distribution of EnHL values for each postural task, with the lowest median values occurring during bipedal stance and the highest during two-foot tiptoe. The bipedal stance task had the most outliers. There was a statistically significant difference between each task (p<0.05).

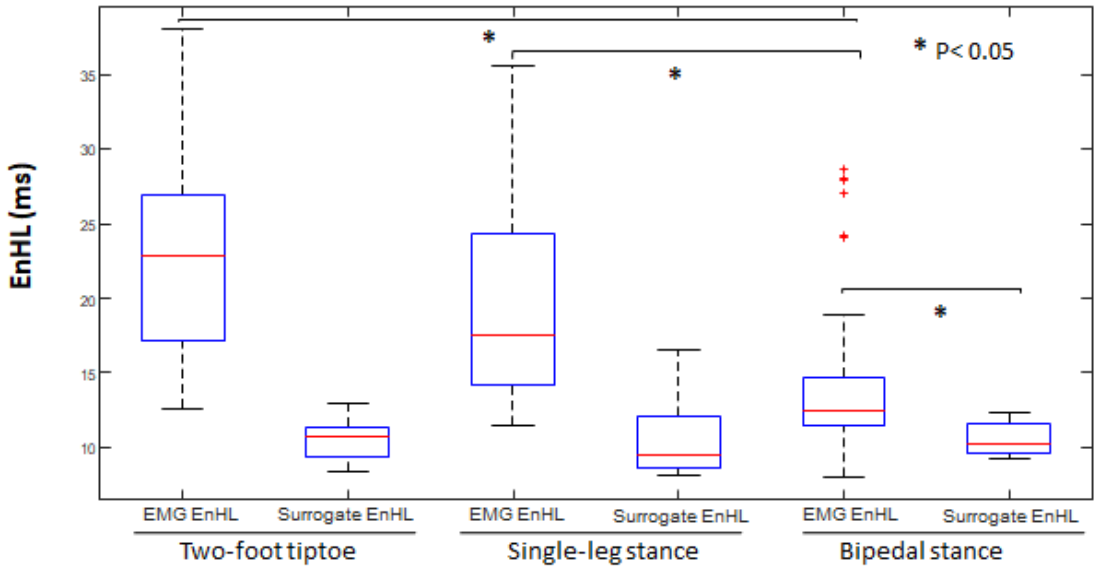

Figure 6-1 Entropy Halflife values distribution for two-leg stance, single-leg stance and two-foot tiptoe for EMG signal (EMG EnHL) and surrogate signal (Surrogate EnHL). A statistical difference was found between tasks and between EMG EnHL and surrogate EnHL.

Figure 6.2 shows the distribution of the CoG over the sole of the foot for the regions with longer and shorter EnHL. Both regions are composed of a group of CoG points (each dot representing a trial) and a perimeter encasing the set of CoGs, black for the longer EnHL and blue for shorter EnHL. For the bipedal stance the longer EnHL region (inside the black perimeter) is found in the central portion of the shorter EnHL region. During one-foot stance the longer EnHL is in a similar position, but the shorter EnHL is slightly shifted to the lateral aspect of the electrode array (e.g. the foot). Finally, for the two-foot tiptoe the shorter EnHL region does not incorporate the longer EnHL region, but both regions are in the central aspect of the array, in a confined and overlapping compartment. The location of both regions for the three tasks is confined between the 10-60 % of the width of the foot and the 5-50% of the length of the foot. (Figure 6.2, Panel A, shaded area)

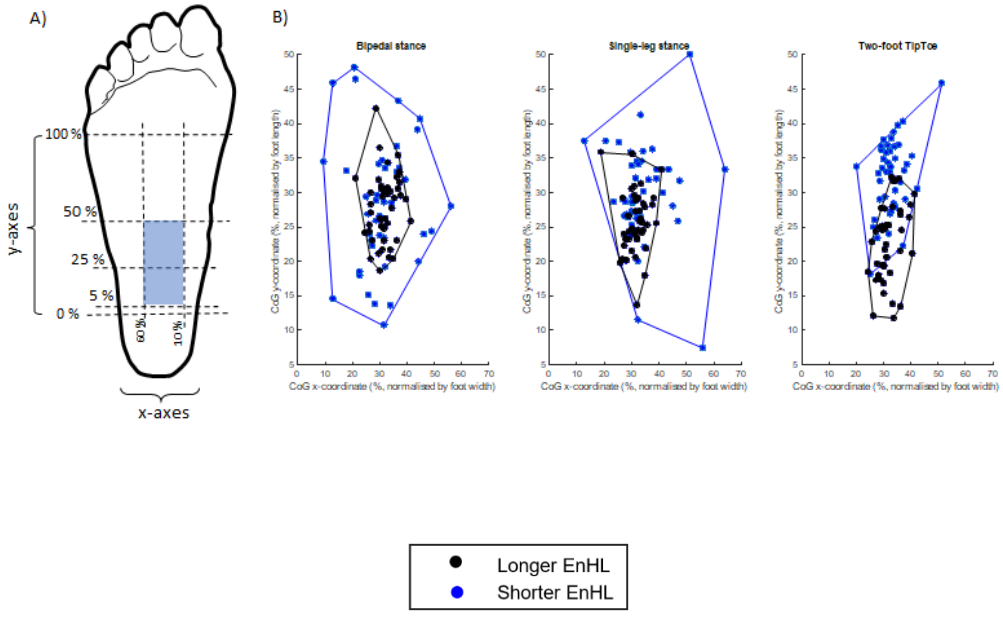

Figure 6-2 Centre of Gravity coordinates of respectively the region with the longest EnHL (black dots) and the region with the shortest EnHL (blue dots) for each participant. Each dot represents a trial. CoG coordinates were normalised by foot width (CoGx) and foot length (CoGy). The area comprising the group of CoG corresponding to highest EnHL is circled in black and the area comprising the group of CoG corresponding to shorter EnHL is circled in blue.

The mixed effects statistical model showed that the only condition where participants and type of task affected the CoG was for the shorter EnHL region, with a significant difference in the CoG x-coordinate (smaller values) for the two-foot tiptoe task.

Table 6.1 shows that the smallest areas, for both longer and shorter EnHL is for the two-foot tiptoe task, when both regions are more confined than in the other two tasks. The largest area of the shorter EnHL occurred during the bipedal stance task, whereas the biggest area for the longer EnHL occurred during one-foot stance.

Table 6-1 Area in cm^2 for regions representing shorter and longer EnHL

	BIPEDAL STANCE	**SINGLE-LEG STANCE**	**TWO-FOOT TIPTOE**
AREA SHORTER ENHL(CM^2)	2.934	2.595	0.793
AREA LONGER ENHL (CM^2)	0.607	0.716	0.349

6.4. Discussion

The aims of this study were for the first time to i) investigate values of EnHL for EMG signals from intrinsic foot muscles during postural tasks and ii) investigate the distribution of EnHL across the foot region.

The values for EMG signals from intrinsic foot muscles for all three postural tasks, are in a similar range to those found for both synthetic (6.68 ms and 10.96 ms) and physiological data, (8 ms and 25 ms for treadmill walking, depending on the frequency

component of the signal investigated)(Hodson-Tole and Wakeling 2017) Importantly, EnHL values were higher than the values from the surrogate signals, showing that the phase order is important for EnHL and therefore there is information in the physiological signal that could potentially be related to the neural drive. Understanding the temporal structure of surface EMG could potentially help understand the functioning of the underlying motor control (Baltich et al., 2014)

Previous results showed how EnHL increases for more challenging mechanical demands, i.e. pedalling at a higher load (Enders et al., 2015), running at faster velocities (Hodson-Tole and Wakeling, 2017). When comparing EnHL from these results for the three postural tasks studied, Figure 6.1 shows how the median value of EnHL was affected by the task performed. EnHL increased with the postural effort, with the highest value during the two-foot tiptoe standing. The difference between tasks suggests that the demand placed on the neuromuscular control process differs, with the two-foot tip-toe being the most challenging task. Enders et al stated that when motor tasks are more challenging, there is a more confined solution space on how to achieve this movement, which results in a longer EnHL, meaning the structure of the signal increases. In these results, based on the EnHL values, it appears that the most challenging task is the two-foot tiptoe, showing the longest EnHL and the least challenging the bipedal stance.

EnHL has never been applied to EMG signal recorded during postural tasks, therefore there are no other studies against which direct comparisons can be made. There is, however, a study of EnHL applied to CoP path during different postural task (Federolf et al., 2013). Results from this study show that during bipedal stance, the EnHL of CoP is longer than during single-leg standing. This differs to results here, where the bipedal

stance resulted in the shortest EnHL for the EMG signals. The differences in EnHL change may reflect the fact that EnHL applied to CoP includes a lot of motor control events, not only the muscle contraction pattern. Federolf et al. (2013), propose that shorter CoP EnHL could reflect a combination of more frequent interventions by the neuromuscular system and greater tolerance of variability in the mechanical configuration. In contrast, longer EMG EnHL is thought to reflect greater structure and neural drive. The fact that longer EMG EnHLs corresponded to the shorter CoP EnHLs could therefore support the proposal that CoP EnHLs are related to altered neuromuscular system interventions.

In Figure 6.1 there are a number of outliers present in the bipedal stance data with EnHLs longer than the median values of both two-foot tiptoe and one-foot stance. Taking into consideration the study on CoP EnHL, the CoP of this sub-group of participants was investigated, with the prediction that greater fluctuations in CoP would be associated with these longer EnHLs (Figure 6.3).

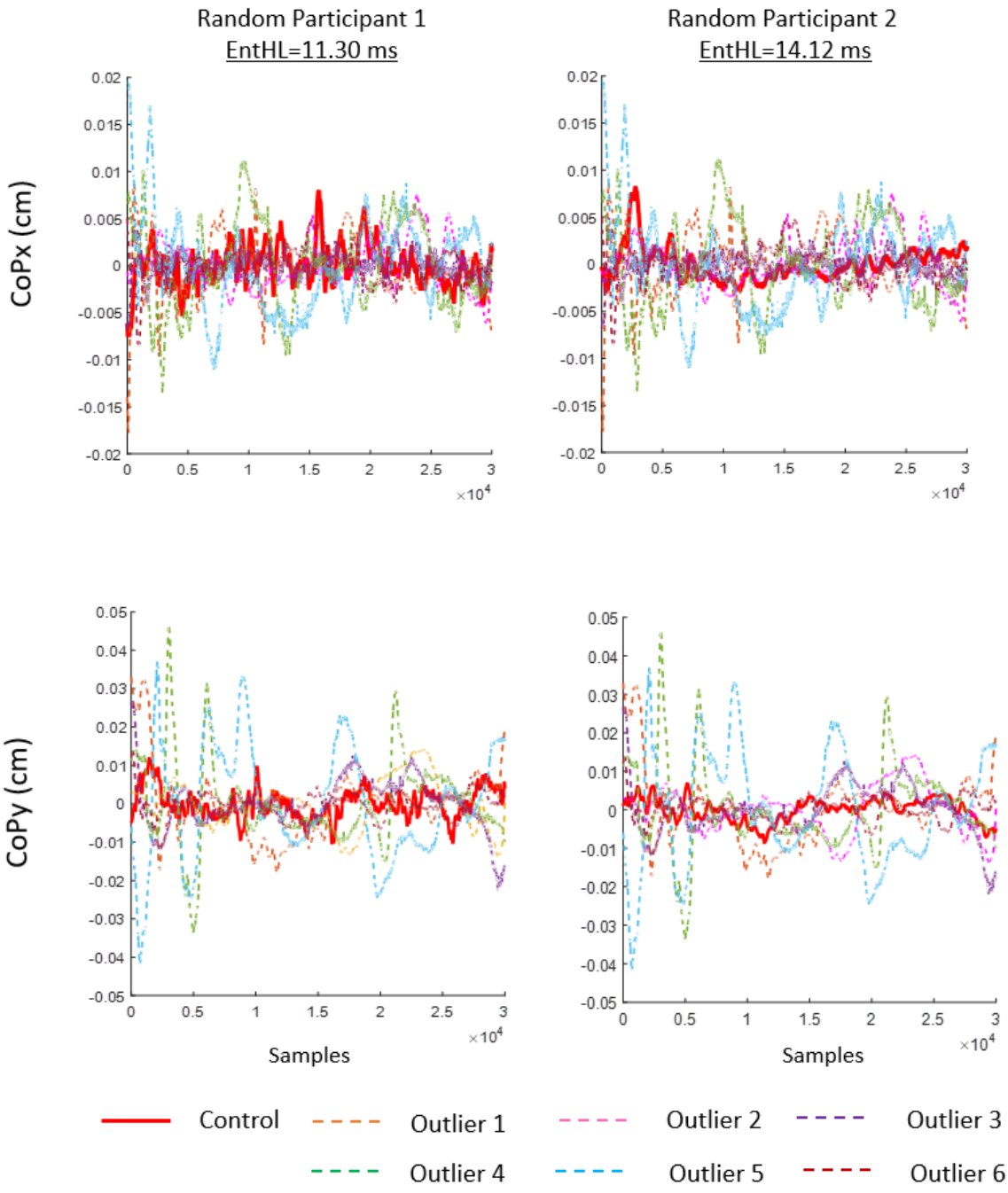

Figure 6-3 Centre of pressure (CoP)paths in the medial/lateral direction (CoPx) and in the anterior/posterior direction (CoPy) for six outliers (each colour is an outlier) and one randomly selected control participant (think red path).

Figure 6.3 shows the detrended CoP path of each outlier (six trials from a total of four participants) compared to two control participants ("Control"), who were randomly selected between the group of participants showing a EnHL value in the range identified as physiological for the bipedal stance task (Figure 6-1). For the mediolateral direction

(CoP_x), the path from the outliers and from the control participant is showing a similar trend, suggesting that natural sways in the mediolateral direction had similar ranges and temporal characteristics. However, for the anterior/posterior direction (CoP_y), the path for the control participants has smaller amplitude and higher frequency components than the data path from the outliers. The longer EnHL in this group of participants, seems to suggest that they have adjusted their position frequently to maintain the upright posture (Baltich et al., 2014). As maintaining quiet stance seemed to be more challenging for this group of participants, with sways in the anterior/posterior direction with different feature, this might have influenced the neural control, with a more variable EMG signal and longer EnHL.

It is clear there was more structure in the EMG signals recorded in the outlier trials (Figure 6-1). This may suggests these participants found standing more challenging compared to the other participants. Previous studies (Baltich et al., 2014; Federolf et al., 2013) have also stated that CoP EnHL is influenced by the degrees of freedom the nervous system can rely on or the number of cognitive functions utilised to accomplish a task. Therefore, a longer EnHL might also be the reflection of a task with more states (or strategies on how to perform it) available compared to a task where the less states are available. Considering the sways in the anterior/posterior direction recorded here during the simple task of standing, for this sub-group of participants the number of strategies available to accomplish the task were multiple or similar to those required for what are assumed to be more challenging tasks (i.e. two-foot tiptoe), resulting in longer EMG EnHLs.

Alternative explanations for the differences in EMG EnHL that should be considered are: i) there are longer scale temporal components in the EMGs that were not removed by the applied high pass filter (Section 3.4.4. General Methodology Chapter); ii) that there were fluctuations in the signal activation duration and/or duty cycle (Hodson-Tole and Wakeling, 2017); iii) or in the raw EMG firing statistics (Wakeling and Hodson-Tole, Under Review) and these differences in the characteristics of the EMG signal influenced the EnHL values. As the application of EnHL analysis to the study of EMG signal and neuromuscular control characteristics is in its infancy further work is required to appropriately interpret these findings. Included in this should be consideration of possible ways of combining non-linear analysis of CoP and EMG time series, using approaches such as cross approximate entropy.

A final consideration for the outliers is that, this group of participants did not have any morphological common feature (i.e. age, weight, height, …), which could have been a factor influencing the EnHL. The only morphological feature, which may be a relevant factor to consider is foot size, as one participant presents the smallest foot size in the group and a second one the biggest foot size. However, the small sample size means it is not possible to directly link these morphological traits to factors influencing task performance, a topic that could be the focus of future work.

In terms of spatial variation of EnHL, Figure 6.2 shows how for only the two-foot tiptoe task, showing the longest EnHL values, the region of longer EnHL and shorter EnHL share only partly the central portion of the foot. For the three tasks, the region with longer EnHL is in a similar location and also the area presents similar values (Table 6.1). Results

from a previous study (presented in Chapter 4) showed that during postural tasks, there is a region in the foot (around the third column and seventh row of the grid) where the highest activation levels occur (see Results of Chapter 4). The region corresponds to the *flexor digitorum brevis* and it corresponds to the location where the longer EnHL CoG can be observed in these results. For what it concerns the shorter EnHL region, the type of task has an effect only for the two-foot tiptoe ($p<0.05$). During two-foot tiptoe, the shorter EnHL region shrinks to the region corresponding to the highest activation (Figure 6.2), compared to the area of the other two postural tasks. Previous results applying EnHL to EMG signal (Enders et al., 2015, Hodson-Tole and Wakeling, 2017) suggest that the motor unit (MU) firing information presents structured components, proposing that an increase in MU firing patterns, suggests an increase in the regularity of MU discharge and, as a result, EMG signal and short-term fluctuations become more regular. This suggests a synchronisation in the MU firing patterns, which is an important factor in muscle activation and force development and it is in accordance with the common drive concept (De Luca and Erim, 1994), which states that the MU in a single pool receive the same net drive from the central nervous system. Even though it is not possible to talk about individual MU properties as these results were collected from surface EMG, both Enders et al. (2015) and the results from the present study, showed how increasing the effort (respectively, power of cycling and challenge of postural task), produced an increase in the EnHL, which could potentially be linked to an increase in MU pattern regularity and muscle activation. In this study, the narrowing of the region of shorter EnHL to a similar foot portion of the foot, suggests that where the highest activation occurs, is also where variation in EnHL occur. Moreover, the *Flexor digitorum brevis* muscle belly is found in the posterior aspect of the foot (McKeon et al., 2015)

(originating from the calcaneus), which seemingly seems to correspond to the region with longer EnHL. Whereas towards the metatarsals, the *Flexor digitorum brevis* splits into four heads which each insert onto a metatarsal. This region could potentially correspond to the shorter EnHL region, which could potentially be involved less during two-foot tiptoe.

6.5. Conclusion

This study shows a baseline range of EnHL during postural tasks, which might be used as reference for future investigation. Further investigation is needed, to understand which factors of performing a postural task could potentially affect the EnHL and therefore the structure of the signal. Further analysis, should also focus on the relationship between the structure of EMG signal from intrinsic foot muscles and extrinsic foot muscles, as this might reveal potential information of coordination between these two compartments fundamental for standing and locomotion. There is scope for this tool to be applied to clinical populations, where the control mechanisms may be additionally challenged by pathology. Here the EnHL could reveal how different populations achieve similar tasks and which parameters affect neural drive. This is a particular possible strength of the approach as it provides a time-based measure that enables comparison between studies/populations that the current sample entropy based analyses do not afford.

7. Discussion

The overarching aim of the work presented in this thesis was to investigate the potential value of non-invasively evaluating intrinsic foot muscle behaviour using multi-channel surface electrode arrays. The first objective of this work was to investigate the feasibility of collecting surface EMG from a portion of the plantar region of the foot with a non-invasive methodology. There are some potential difficulties in collecting surface EMG from a region loaded with body weight; for example, the grid needs to be flexible and soft enough for the participant to stand on it, but on the other hand both body weight and the movement on the grid could affect the EMG signal collected. The results in Chapter 4 showed that the loading of body weight on the surface EMG grid does not interfere with the acquisition of physiological EMG signals. Both amplitude and frequency components were in the physiological ranges (Figure 4.1), reported in literature with frequency values between 20 Hz and 400 Hz and amplitude values up to 1 mV. It was therefore concluded that it is possible to record physiological surface EMG from the plantar aspect of the foot in a non-invasive way, which opens new opportunity to gain more knowledge on spatial activation features of intrinsic foot muscles in a healthy group of people. In fact, it was also possible to quantify spatial features of both amplitude and signal structure (SampEn) of the activation from the sole of the foot. The results showed that the region with the highest activation is the portion of the foot corresponding to the *Flexor digitorum brevis* (Figure 4.2). Moreover, the same region presented the most structured signal, suggesting the presence of a more ordered signal at higher effort (i.e. higher intensity). The interesting aspect was that for the group of participants studied here, the region over which this pattern was observed was really

confined, therefore any behaviour outside this portion could potentially represent participants showing a different neuromuscular behaviour, perhaps representing a different motion control strategy or indicative of a pathology. Future work could focus on the investigation of these patterns in clinical populations, such as peripheral neuropathy or in aging, where standing might be achieved with different control strategies.

The second objective of the thesis was to use the activation patterns from the plantar aspect of the foot and evaluate the response of their spatial features to mechanical behaviour during postural tasks (Chapter 5). Specifically, the support of the medial arch is one of the main functions of the intrinsic foot muscles (Reeser et al., 1983; Fiolkowski et al., 2003), therefore the association between the medial arch angle, force plate derived CoP changes and EMG patterns could inform understanding of the behaviour of this group of muscles, linked with the mechanical behaviour of the foot. The main findings showed that a task comprising mediolateral sways causes greater motion of the CoP and of the spatial features of the EMG, whereas an anterior/posterior motion task causes the medial arch angle to change the most with relatively small changes in EMG spatial features (Figure 5.1). With these results it was possible to show how the direction of motion generates a specific response both in biomechanics of the foot (CoP, MA) and intrinsic foot muscles activation (CoG_E). This behaviour could also be seen in the cross-correlation between the time delays of biomechanics parameters (CoP, MA) and time delays of intrinsic foot muscles spatial features (CoG) where the mediolateral direction (X) is the one majorly involved (Figure 5.2). This could potentially suggest flexibility in the motor control strategy, where the nervous system responds to a challenge (task) in a specific manner and depending on the association recorded can choose to either act

synchronously (mediolateral sway) or sequentially (anterior posterior sway). This could be useful in designing of rehabilitation protocols or shoe insoles, knowing that this region is mainly activated during sways in the mediolateral direction. This could also help in the treatment of ankle sprain, which happen in the sagittal plane and could potentially be the result of intrinsic foot muscles weakness (Mickle et al., 2009; Soysa et al., 2012).

However, the variability of the results in Chapter 5 (Figure 5.2) generated a large number of outliers and therefore, by removing these outliers, the association were not as strong as with the outliers (Chapter 5). While variability could be an indicator of a different strategy applied to motion, it does not allow to provide a valid explanation of the timing and association between the biomechanics parameters and the intrinsic foot muscles activation. However, these data were analysed with linear analysis, which are based on the magnitude of the signal, independent of any temporal information, and potentially it is not the best way to process these types of data. Therefore, the use of non-linear methodology, could potentially reveal relation of the motor control which are hindered with linear analysis.

The third and final objective of this thesis was, therefore, to investigate the EMG signal from the intrinsic foot muscles with a novel non-linear analysis tool, called Entropic Halflife, which enables the analysis of the neuromuscular drive during motion. In Chapter 6, this methodology was, for the first time, applied to EMG from intrinsic foot muscles recorded during a range of postural tasks. New findings from this chapter, showed that EnHL from intrinsic foot muscles are in the range of 8 ms and 28 ms for quiet stance, 12 ms and 38 ms for two-foot tiptoe and 11 ms and 35 ms for single-leg stance (Figure 6.1). These range of values are similar to previous results (Hodson-Tole

and Wakeling, 2017, Enders et al., 2015) and represent baseline values for the intrinsic foot muscles during postural tasks that could be used as reference for further studies. EnHL values from this Chapter also showed, what was previously found in other studies, that longer EnHL are indicative of a higher balance demand of the task. In addition, the spatial distribution of the EnHL across the foot suggests that it is affected by the type of task and the more persistent signal appears to be in the same region where the highest activation was found (Figure 6.2).

In conclusion, results from Chapter 4, Chapter 5 and Chapter 6 show that it is possible to non-invasively collect multi-channel surface EMG and draw new knowledge from the muscles on the plantar aspect of the foot relating to spatial activation features, signal structure properties and neuromuscular drive. These results could therefore help and have an impact on understating foot muscle behaviour in populations where balance is challenged or in the design of rehabilitation protocols and shoe insoles.

7.1. Limitations of the study

Limitations of each experimental study are described in the relevant chapters, however there are some general limitations, which will be addressed here.

One overall limitation of the work presented is the number of participants who took part in the data collection. While the total number is reasonable (30 participants), the number of participants for the single chapters decreased due to either issues associated with noise in the EMG signal or technical problems, which caused some of the participants' trials to be discarded. The pool of participants also included a very variable age range (21 to 73 years old) and most of the participants were under 40 years old with very few over 40 years, which did not allow comparison between groups based on age.

Future work should consider assessment of a wider age range, especially as ageing is associated with a loss of balance and increased falls risk. Recent work has also shown that thermoregulation in the foot during walking exercise differs between young adults and those over 40 years of age (Reddy et al., 2017) which given the role of skeletal muscles in thermoregulation (Rowland et al., 2015), may also reflect differences in foot muscles properties that warrant further investigation. Moreover, the pool of participants was made up more of males than females, which might have influenced the results, considering the effect of gender on joint kinematic (McLean et al, 2004).

Another limitation is the size of the EMG electrode array applied to the plantar aspect of the foot. The dimension of the 64 channels array could not cover consistently the same portion of the foot, because of the different foot sizes. For the majority of the data set collected, no EMG signal was recorded from the *Abductor hallucis* or from the *Abductor digiti minimi brevis,* which are two of the biggest muscles in the foot, but located on the medial and lateral aspects outside the edge of the electrode grid. Future work should consider development of custom designs for different foot sizes or optimising the positioning of a smaller number of electrodes to consistently capture more muscles from all participants.

Taken together the age range of the participants and the range of foot sizes, may have influenced the variability seen in the results of the experimental chapters. This can be especially seen in the variability of the EMG signal amplitude and frequency (Chapter 4-Figure 4.1) and in the cross-correlation results (Chapter 5-Figure 5.2). However, it does not seem to have affected the EnHL results (Chapter 6 - Figure 6.1), which in itself is interesting, as EnHL provides insights into signal structure, rather than the magnitude of

the data. Non-linear analysis, such as entropy-based measures, could potentially be more suitable for such a variable data set, as it is able to provide more consistent insights into intrinsic foot muscles motor control.

7.2. Future work

This study opens new opportunity of investigating non-invasively surface EMG from the plantar surface of the foot. However, there are still some aspects which need further investigation, such as the relationship between the intrinsic foot muscles and the extrinsic foot muscles compartment.

The intrinsic foot muscles are believed to work in conjunction with the extrinsic foot muscles compartment (Zelik et al., 2015). The intrinsic and extrinsic foot muscles form the foot muscles compartment. The extrinsic and intrinsic foot muscles are usually evaluated separately, and as far as current literature goes, only one study investigated the co-ordination of these two groups of muscles locomotion (Zelik et al., 2015). There surface EMG was recorded from muscles contributing to metatarsophalangeal (MTP) flexion and extension. Intrinsic foot muscles were *Extensor hallucis brevis* (EHB), *Extensor digitorum brevis* (EDB) and *Flexor digitorum brevis* (FDB), were the first two muscles are on the dorsal aspect of the foot and only the last one belongs to the plantar aspect of the foot. Extrinsic foot muscles were *Extensor hallucis longus* (EHL) and *Flexor digitorum hallucis longus* (FDHL) and EMG envelopes were used to evaluate the timing of peak muscle activity to assess whether the type of coordination between intrinsic and extrinsic foot muscles was either sequential or synchronous (as defined by Zelik et al, 2014). Their results seem to suggest that during locomotion a sequential activation occurs during walking with activation of the ankle plantar flexors, followed by the

metatarsophalangeal (MTP) flexors (*Flexor digitorum brevis, Flexor digitorum longus*), MTP extensors (*Extensor hallucis brevis*, *Extensor digitorum brevis*, *Extensor hallucis longus*), and then ankle dorsiflexors. However, during other motion tasks (such as side-ways walking, tiptoe) this pattern was not consistent, showing a synchronous pattern. Their study showed that a relationship between these two compartments exists and is potentially fundamental to understand the interplay between these two compartments during postural tasks and locomotion, but considering the promising results from Chapter 6, this interplay can be investigated with the EnHL, to understand the underlying mechanisms during motor control. From the work in this thesis, several interesting questions with regard how posture is controlled, and the role of the intrinsic and extrinsic foot muscles arise. Due to technical issues with the data collected in this work, it was not possible to fully address these within the scope of the current thesis, however it was possible to provide some preliminary insight which are detailed below.

8. Interplay between body sway and intrinsic foot muscles activation for postural balance control in humans

From the total 30 volunteers, as described in section 3.1 of General Methodology, EnHL was calculated from EMG signals recorded from seventeen healthy participants (fourteen males and three females, age: 39.1 ± 13. 4 years, weight: 74.3 ± 14.3 kg, height: 175.7 ± 9.4 cm) during three motor tasks: i) bipedal stance; ii) single-leg stance; iii) two-foot tiptoe stance.

Due to a technical problem with the electrode sensors which was only identified at the end of the data collection period, not all participants had a full data set of sEMG from the six extrinsic muscles. Therefore, it was decided to pick the channel on the tibialis anterior, which was present for the complete set of participants, and one antagonist muscle. For the majority of participants (16/17 participants) the EMG from the lateral gastrocnemius was always properly recorded, whereas for the remaining participant the lateral soleus was usable. Considering the percentage of participants showing EMGs from the lateral gastrocnemius, signals from antagonist muscles were grouped into a single group, referred to from this point on as the antagonist muscle. Wavelet analysis was used to process these extrinsic EMGs, with the same procedure used for the intrinsic EMGs described in Section 3.4.1 of the General Methodology (Chapter 3). The filtered wavelet transformed EMGs from the extrinsic foot muscles were then used to calculate the EnHL of the myoelectric signal from the trials.

To determine whether the EnHL values found truly reflected structure of recorded signals, they were also compared with EnHLs calculated from surrogate signals (Enders

et al., 2015). The surrogate signals were generated from 29 (43 % of the complete data set) randomly selected trials, and corresponded to the time series containing the power information of the selected signal, but with the phase randomized. If the EnHL in the original signals was related to the signal structure EnHL values of physiological signals should be greater than the EnHL from the surrogate signals. In addition, EnHL was also evaluated for the CoP of the same three postural tasks, to link the neuromuscular drive to the CoP with the EMG.

The results showed values of EnHL for the extrinsic foot muscles differed between tasks, with the highest EnHL occurring for single-leg stance. However, the surrogate values were similar to those from the EMG values for the majority of cases (except single-leg stance *Tibialis anterior*), which suggests that these values need to be considered with caution as similar values between EMG and Surrogate EnHL suggest that the frequency content rather than the signal structure (i.e. order of the data points) could be dominating the pattern observed (Figure 7.1).

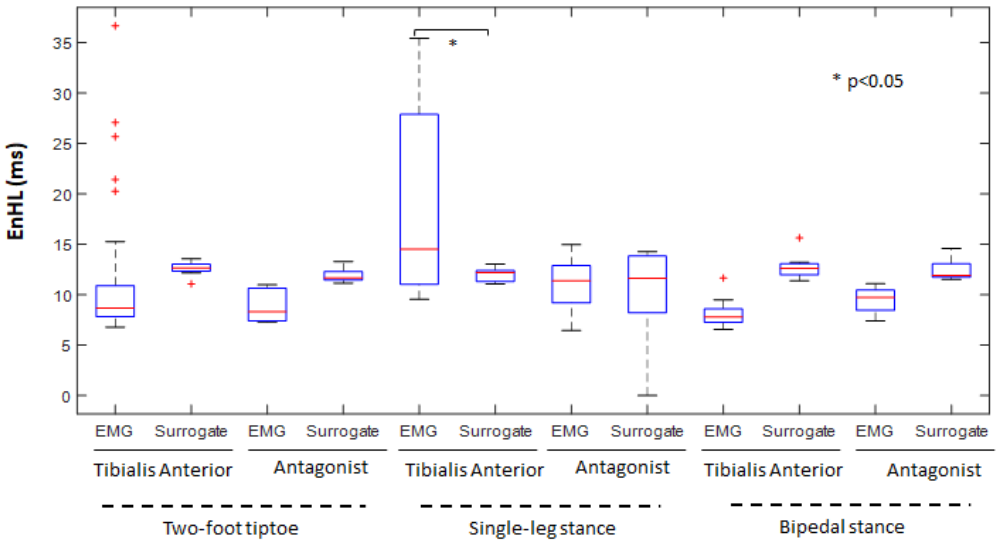

Figure 8-1 EnHL distribution for the three postural tasks (two-foot tiptoe, single-leg stance, bipedal stance) for Tibialis anterior and the antagonist muscle.

Comparison between intrinsic and extrinsic foot muscles EnHL showed that, during the three postural tasks EnHL from extrinsic foot muscles were shorter than EnHL from the intrinsic foot muscles, (Figure 7.2). Previous studies have stated that EnHL is associated with the motor demand, with longer EnHL for tasks requiring more effort (Enders et al., 2015). In addition, mechanical demands of the movement can influence the number and population of motor units recruited during the activation phase (Hodson-Tole et al., 2009). In the present study, for the extrinsic foot muscle (TA) and only during single-leg stance, EnHL was longer than the surrogate signal. This factor could be the result of the involvement of TA in foot inversion as it wraps round and inserts on the medial cuneiform and first meta-tarsal, therefore its activation will be linked to controlling medio-lateral shape of the foot. For the rest of the tasks, the similarity of EnHL values to those from the surrogate signal, suggests that the structure of the signal was not

there to be detected. This could mean there is a minimum level of activation or motor unit firing that is required for the EMG signal to become structured and therefore to be detected by EnHL analysis. Moreover, the region on the extrinsic muscles, over which the EMG signal was recorded, was small compared to the dimension of the extrinsic foot muscles bellies, therefore the EnHLs as presented here might not be a true reflection of the true behaviour of the whole muscle (Vieira et al., 2015).

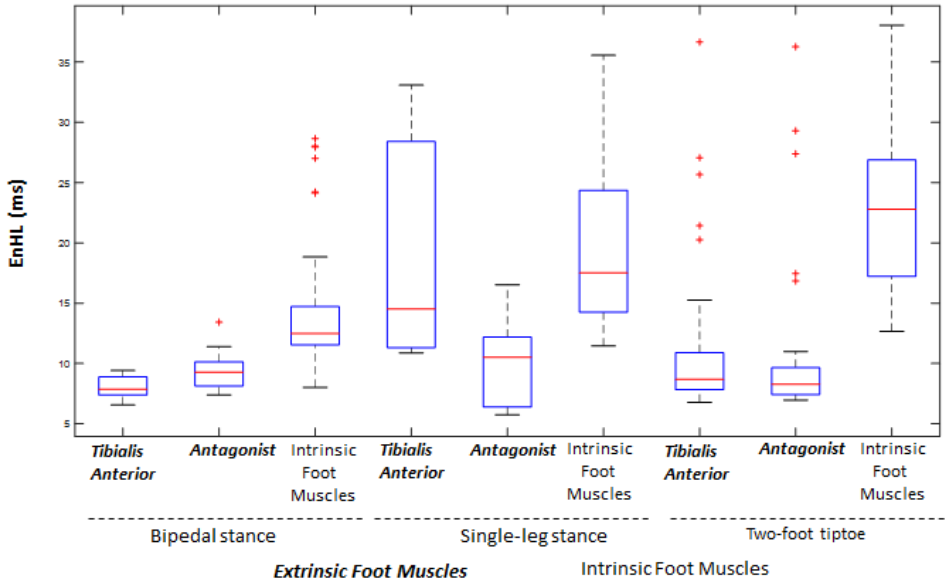

Figure 8-2 EnHL distribution for extrinsic (EnHL TA, EnHL Ant, in bold characters) and intrinsic foot muscles (EnHL IFM) for the three postural tasks.

Comparison of the EnHL for the CoP shows that during dynamic tasks, specifically for two-foot tiptoe, more control is driven to the intrinsic foot muscles, with less control to the CoP, meaning shorter EnHL values. This also applies to the extrinsic foot muscles, with the exemption of TA during single-leg stance, suggesting also more control to this muscle (particularly for the plantar flexors). During quiet stance, less drive to the

intrinsic foot muscles, but with an increase in stability of the CoP (longer EnHL), especially in the anterior-posterior direction (Figure7.2, Figure 7.3).

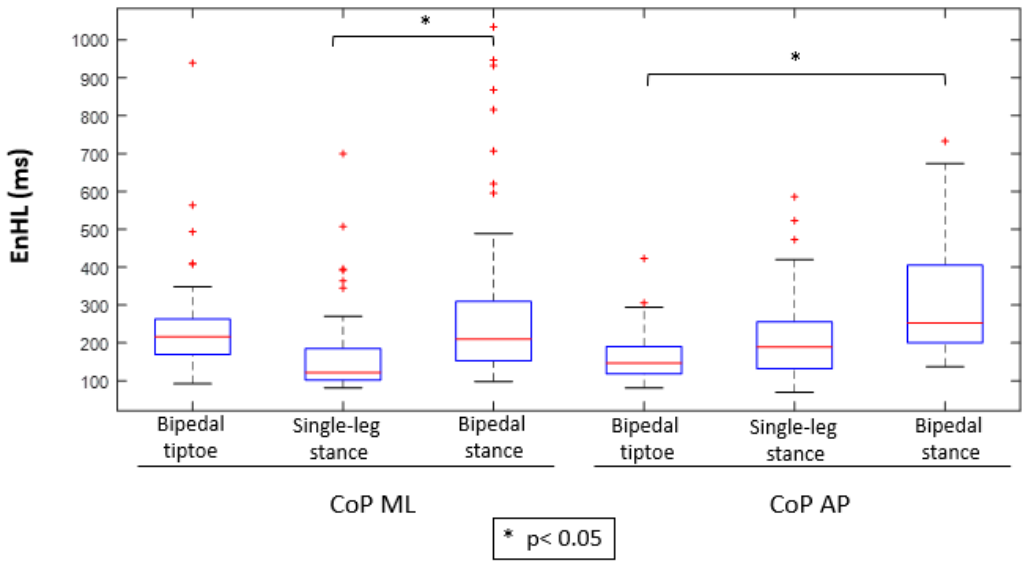

Figure 8-3. EnHL distribution for CoP mediolateral trajectory (x) and antero-posterior trajectory (y) for the postural tasks (Two-foot tiptoe, bipedal stance, single-leg stance).

This could potentially suggest that the extrinsic foot muscles maintain the drive to keep upright stance, while the intrinsic foot muscles seem to make short-term adjustments to maintain the posture. The interplay between the intrinsic and extrinsic foot muscles compartment seems to suggest that when the balance is distributed between both legs and feet (two-foot tiptoe and bipedal stance), the EMG signal from the intrinsic foot muscles is structured over longer periods of time, whereas when equilibrium is shifted on one side (single-leg stance), the extrinsic foot muscles are also involved in the motor task, with longer EnHL. Moreover, it appears to be more control to the CoP during more static tasks, which might suggest the system needs to make fewer short-time adjustments to maintain the upright posture.

However, one main limitation of this study was the recording of EMG signal from one antagonist extrinsic foot muscles only, due to the technical problem which did not allow to record from all six muscles identified. The involvement of the medial gastrocnemius or the soleus could not be investigated in this study. Further analysis is therefore needed to understand the level of contribution of other extrinsic foot muscles during simple motor tasks. There is however scope to further investigate on how much the level of activation influences the neuromuscular drive, which could lead to further insights into the analysis of biological time series with non-linear analysis.

9. Conclusion

In conclusion, this thesis has documented the potential *and* value of collecting surface EMG from the intrinsic foot muscles non-invasively; hence, this work contributes knowledge of the *in vivo* behaviour of the intrinsic foot muscles during postural tasks. The insights on the spatial and temporal patterns of activation and signal structure suggest that a localised region in the foot is engaged more during postural tasks in health participants. Hence, any difference in these patterns could potentially function as indicator of different motor strategies, motor impairment or foot deformities and should be investigated more widely in future.

In addition, the work highlighted the potential of applying non-linear analysis to EMG time series, where there is more consideration of the temporal evolution of movement patterns and the associated variability. This approach has the potential of informing new understanding of the mechanisms underpinning motor control in different clinical populations. The new findings of this work could therefore help in the design of new orthosis and rehabilitation protocols, with the novel methodological approach enabling this to be done across any clinical populations.

10. References

Adrian, E. D. and Bronk, D. W. (1929) 'The discharge of impulses in motor nerve fibres: Part II. The frequency of discharge in reflex and voluntary contractions.' *The Journal of Physiology*, 67(2) pp. i3-151.

Arndt, A., Wolf, P., Liu, A., Nester, C., Stacoff, A., Jones, R., Lundgren, P. and Lundberg, A. (2007) 'Intrinsic foot kinematics measured in vivo during the stance phase of slow running.' *J Biomech*, 40(12) pp. 2672-2678.

Arnold, J. B., Mackintosh, S., Jones, S. and Thewlis, D. (2013) 'Repeatability of stance phase kinematics from a multi-segment foot model in people aged 50 years and older.' *Gait Posture Gait Posture*, 38

Baltich, J., von Tscharner, V., Zandiyeh, P. and Nigg, B. M. (2014) 'Quantification and reliability of center of pressure movement during balance tasks of varying difficulty.' *Gait Posture.*, 40(2), Jun, pp. 327-332. doi: 310.1016/j.gaitpost.2014.1004.1208. Epub 2014 May 1019.

Basmajian, J. V. and Stecko, G. (1963) 'The Role of Muscles in Arch Support of the Foot.' *The Journal of Bone & Joint Surgery*, 45(6) pp. 1184-1190.

Basmajian, J. V. and De Luca, C. J. (1985) *Muscles alive : their functions revealed by electromyography.*

Blackwood, C. B., Yuen Tj Fau - Sangeorzan, B. J., Sangeorzan Bj Fau - Ledoux, W. R. and Ledoux, W. R. (2005), 'The midtarsal joint locking mechanism.' (1071-1007 (Print))

Bojsen-Moller, J., Hansen, P., Aagaard, P., Svantesson, U., Kjaer, M. and Magnusson, P. (2004) 'Differential displacement of the human soleus and medial gastrocnemius aponeuroses during isometric plantar flexor contractions in vivo.' *J Appl Physiol*, 97 pp. 1908-1914.

Bonato, P., Roy, S. H., Knaflitz, M. and De Luca, C. J. (2001) 'Time-frequency parameters of the surface myoelectric signal for assessing muscle fatigue during cyclic dynamic contractions.' *IEEE Trans Biomed Eng*, 48(7), Jul, pp. 745-753.

Bruening, D. A., Cooney, K. M. and Buczek, F. L. (2012) 'Analysis of a kinetic multi-segment foot model. Part I: Model repeatability and kinematic validity.' *Gait Posture*, 35

Chen, Y., Chen, D.-r., Li, Y. and Chen, L. (2010) *Otsu's thresholding method based on gray level-gradient two-dimensional histogram.* Vol. 3 6-7 March 2010.

Crompton, R. H., Vereecke, E. E. and Thorpe, S. K. (2008) 'Locomotion and posture from the common hominoid ancestor to fully modern hominins, with special reference to the last common panin/hominin ancestor.' *J Anat*, 212(4), Apr, pp. 501-543.

De Luca, C. J. and Erim, Z. (1994) 'Common drive of motor units in regulation of muscle force.' *Trends Neurosci.*, 17(7), Jul, pp. 299-305.

Donker, S. F., Ledebt, A., Roerdink, M., Savelsbergh, G. J. and Beek, P. J. (2008) 'Children with cerebral palsy exhibit greater and more regular postural sway than typically developing children.' *Exp Brain Res*, 184(3), Jan, pp. 363-370.

Enders, H., Von Tscharner V Fau - Nigg, B. M. and Nigg, B. M. 'Neuromuscular Strategies during Cycling at Different Muscular Demands.' (1530-0315 (Electronic)), 20150619 DCOM- 20160301,

Executive, H. a. S. (2009-2010) *Health and Safety statistics.*

Falla, D. and Farina D. (2008) 'Motor units in cranial and caudal regions of the upper trapezius muscle have different discharge rates during brief static contractions.' *Acta Physiology*, 192 pp. 551-558.

Falla, D. and Farina, D. (2008) 'Non-uniform adaptation of motor unit discharge rates during sustained static contraction of the upper trapezius muscle.' *Exp Brain Res*, 191 pp. 363-370.

Falla, D., Rainoldi, A., Merletti, R. and Jull, G. (2003) 'Myoeletric manifestations of sternocleidomastoid and anterior scalene muscle fatigue in chronic neck pain patients.'

Farina D, Leclerc F, Arendt-Nielsen L, Buttelli O and Madeleine P (2008) 'The change in spatial distribution of upper trapezius muscle activity is correlated to contraction duration.' *Journal of Electromyography and Kinesiology*, 18 pp. 16-25.

Federolf, P., Roos, L. and Nigg, B. M. (2013) 'Analysis of the multi-segmental postural movement strategies utilized in bipedal, tandem and one-leg stance as quantified by a principal component decomposition of marker coordinates.' *J Biomech.*, 46(15).

Federolf, P., Zandiyeh, P. and von Tscharner, V. (2015) 'Time scale dependence of the center of pressure entropy: What characteristics of the neuromuscular postural control system influence stabilographic entropic half-life?' *Exp Brain Res.*, 233(12).

Fiolkowski, P., Brunt, D., Bishop, M., Woo, R. and Horodyski, M. (2003) 'Intrinsic pedal musculature support of the medial longitudinal arch: an electromyography study.' *J Foot Ankle Surg*, 42(6), Nov-Dec, pp. 327-333.

Gallina, A. and Botter, A. (2013) 'Spatial localization of electromyographic amplitude distributions associated to the activation of dorsal forearm muscles.' *Frontiers in Physiology*, 4 p. 367.

Germann, W. and Stanfield, C. (2003) *Principles of Human Physiology.* Benjamin-Cummings Publishing Company, S. o. A. W. L., Inc and edition, s. I. (eds.) 1st ed.

Goldberger, A. L., Amaral, L. A., Glass, L., Hausdorff, J. M., Ivanov, P. C., Mark, R. G., Mietus, J. E., Moody, G. B., Peng, C. K. and Stanley, H. E. (2000) 'PhysioBank, PhysioToolkit, and PhysioNet: components of a new research resource for complex physiologic signals.' *Circulation*, 101(23), Jun 13, pp. E215-220.

Harcourt-Smith, W. E. H. and Aiello, L. C. (2004) 'Fossils, feet and the evolution of human bipedal locomotion.' *Journal of Anatomy*, 204(5) pp. 403-416.

Harris, C. M. and Wolpert, D. M. (1998) 'Signal-dependent noise determines motor planning.' *Nature*, 394, 08/20/online, p. 780.

Henneman, E. and Olson, C. B. (1965) 'RELATIONS BETWEEN STRUCTURE AND FUNCTION IN THE DESIGN OF SKELETAL MUSCLES.' *Journal of neurophysiology*, 28 pp. 581-598.

Herzog, W., Powers, K., Johnston, K. and Duvall, M. (2015) 'A new paradigm for muscle contraction.' *Frontiers in Physiology*, 6, 06/10

Hodson-Tole, E. F. and Wakeling, J. M. (2007) 'Variations in motor unit recruitment patterns occur within and between muscles in the running rat (Rattus norvegicus).' *J Exp Biol*, 210(Pt 13), Jul, pp. 2333-2345.

Hodson-Tole, E. F. and Wakeling, J. M. (2009) 'Motor unit recruitment for dynamic tasks: current understanding and future directions.' *J Comp Physiol B.*, 179(1), Jan, pp. 57-66. doi: 10.1007/s00360-00008-00289-00361. Epub 02008 Jul 00363.

Hodson-Tole, E. F. and Wakeling, J. M. (2017) 'Movement Complexity and Neuromechanical Factors Affect the Entropic Half-Life of Myoelectric Signals.' *Frontiers in Physiology*, 8, 09/19

Hodson-Tole, E. F., Pantall, A., Maas, H., Farrell, B., Gregor, R. J. and Prilutsky, B. I. (2012) 'Task-dependent activity of motor unit populations in feline ankle extensor muscles.' *The Journal of Experimental Biology*, 215(21) pp. 3711-3722.

Holtermann, A., Roeleveld, K. and Karlsson, J. S. (2005) 'Inhomogeneities in muscle activation reveal motor unit recruitment.' *J Electromyogr Kinesiol*, 15

Hunt, A. E., Smith, R. M., Torode, M. and Keenan, A. M. (2001) 'Inter-segment foot motion and ground reaction forces over the stance phase of walking.' *Clin Biomech*, 16

Huxley, A. F. (1957) 'Muscle structure and theories of contraction.' *Prog Biophys Biophys Chem*, 7 pp. 255-318.

Jenkyn, T. R. and Nicol, A. C. (2007) 'A multi-segment kinematic model of the foot with a novel definition of forefoot motion for use in clinical gait analysis during walking.' *J Biomech*, 40

Kelly, L. A., Kuitunen, S., Racinais, S. and Cresswell, A. G. (2012) 'Recruitment of the plantar intrinsic foot muscles with increasing postural demand.' *Clin Biomech (Bristol, Avon)*, 27(1), Jan, pp. 46-51.

Kelly, L. A., Cresswell, A. G., Racinais, S., Whiteley, R. and Lichtwark, G. (2014) 'Intrinsic foot muscles have the capacity to control deformation of the longitudinal arch.' *Journal of The Royal Society Interface*, 11(93)

Kleine, B. U., van Dijk, J. P., Lapatki, B. G., Zwarts, M. J. and Stegeman, D. F. (2007) 'Using two-dimensional spatial information in decomposition of surface EMG signals.' *J Electromyogr Kinesiol*, 17

Kura, H., Luo, Z. P., Kitaoka, H. B. and An, K. N. (1997) 'Quantitative analysis of the intrinsic muscles of the foot.' *Anat Rec*, 249(1), Sep, pp. 143-151.

Leardini, A., Sawacha, Z., Paolini, G., Ingrosso, S., Nativo, R. and Benedetti, M. G. 'A new anatomically based protocol for gait analysis in children.' *Gait & Posture*, 26(4) pp. 560-571.

Lee, S. S. M., de Boef Miara, M., Arnold, A. S., Biewener, A. A. and Wakeling, J. M. (2011) 'EMG analysis tuned for determining the timing and level of activation in different motor units.' *Journal of electromyography and kinesiology : official journal of the International Society of Electrophysiological Kinesiology*, 21(4) pp. 557-565.

Lindstrom, L., Magnusson, R. and Petersen, I. (1970) 'Muscular fatigue and action potential conduction velocity changes studied with frequency analysis of EMG signals.' *Electromyography*, 10(4), Nov-Dec, pp. 341-356.

Lindstrom, L. H. and Magnusson, R. I. (1977) 'Interpretation of myoelectric power spectra: A model and its applications.' *Proceedings of the IEEE*, 65(5) pp. 653-662.

Lundgren, P., Nester, C., Liu, A., Arndt, A., Jones, R., Stacoff, A., Wolf, P. and Lundberg, A. (2008) 'Invasive in vivo measurement of rear-, mid- and forefoot motion during walking.' *Gait Posture*, 28

Maas, H., Gregor, R. J., Hodson-Tole, E. F., Farrell, B. J., English, A. W. and Prilutsky, B. I. (2010) 'Locomotor changes in length and EMG activity of feline medial gastrocnemius muscle following paralysis of two synergists.' *Experimental Brain Research. Experimentelle Hirnforschung. Experimentation Cerebrale*, 203(4), 05/11

Mann, R. and Inman, V. T. (1964) 'PHASIC ACTIVITY OF INTRINSIC MUSCLES OF THE FOOT.' *J Bone Joint Surg Am*, 46, Apr, pp. 469-481.

Masuda, T. and Sadoyama, T. 'Skeletal muscles from which the propagation of motor unit action potentials is detectable with a surface electrode array.' *Clinical Neurophysiology*, 67(5) pp. 421-427.

McGinnis, P. *Biomechanics of Sport and Exercise.* 3rd edition ed.

McKeon, P. O., Hertel, J., Bramble, D. and Davis, I. (2015) 'The foot core system: a new paradigm for understanding intrinsic foot muscle function.' *British Journal of Sports Medicine*, 49(5) pp. 290-290.

McLean, S. G., Lipfert, S. W., and van den Bogert, A. J., (2004), "Effect of Gender and Defensive Opponent on the Biomechanics of Sidestep Cutting," Medicine & Science in Sports & Exercise, 36(6), pp. 1008 - 1016.

Menz, H. B., Morris, M. E. and Lord, S. R. (2005) 'Foot and ankle characteristics associated with impaired balance and functional ability in older people.' *J Gerontol A Biol Sci Med Sci*, 60(12), Dec, pp. 1546-1552.

Merletti, R. and Parker, P. (2004) *Electromyography, Physiology, Engineering and Non-invasive Applications.*

Merletti, R., Holobar, A. and Farina, D. (2008) 'Analysis of motor units with high-density surface electromyography.' *J Electromyogr Kinesiol*, 18

Mickle, K. J., Munro, B. J., Lord, S. R., Menz, H. B. and Steele, J. R. (2009) 'ISB Clinical Biomechanics Award 2009: toe weakness and deformity increase the risk of falls in older people.' *Clin Biomech (Bristol, Avon)*, 24(10), Dec, pp. 787-791.

Muehlbauer, T., Mettler, C., Roth, R. and Granacher, U. (2014) 'One-Leg Standing Performance and Muscle Activity: Are There Limb Differences?' *Journal of Applied Biomechanics*, 30(3), 2014/06/01, pp. 407-414.

Nelson-Wong, E., Howarth S Fau - Winter, D. A., Winter Da Fau - Callaghan, J. P. and Callaghan, J. P. 'Application of autocorrelation and cross-correlation analyses in human movement and rehabilitation research.' (0190-6011 (Print))

Nester, C. J., Jarvis, H. L., Jones, R. K., Bowden, P. D. and Liu, A. (2014) 'Movement of the human foot in 100 pain free individuals aged 18–45: implications for understanding normal foot function.' *Journal of Foot and Ankle Research*, 7(1), November 28, p. 51.

Pandy, M. 'Biomechanics of the Musculo-Skeletal System 2nd edition.' *Journal of Biomechanics*, 33(10) p. 1340.

Pincus, S. M. (1991) 'Approximate Entropy as a measure of system complexity.' *Proc. Natl. Acad. Sci USA*, 88 pp. 2297-2301.

Prieto, T. E., Myklebust, J. B., Hoffmann, R. G., Lovett, E. G. and Myklebust, B. M. (1996) 'Measures of postural steadiness: differences between healthy young and elderly adults.' *IEEE Trans Biomed Eng*, 43(9), Sep, pp. 956-966.

Rainoldi, A., Moritani, T. and Boccia, G. (2016), 'EMG in Exercise Physiology and Sports.'

Ramdani, S., Seigle, B., Lagarde, J., Bouchara, F. and Bernard, P. L. (2009) 'On the use of sample entropy to analyze human postural sway data.' *Med Eng Phys*, 31(8), Oct, pp. 1023-1031.

Rathleff, M. S., Samani, A., Olesen, C. G., Kersting, U. G. and Madeleine, P. (2011) 'Inverse relationship between the complexity of midfoot kinematics and muscle activation in patients with medial tibial stress syndrome.' *J Electromyogr Kinesiol*, 21(4), Aug, pp. 638-644.

Reddy, P. N., Cooper, G., Weightman, A., Hodson-Tole, E. and Reeves, N. D. 'Walking cadence affects rate of plantar foot temperature change but not final temperature in younger and older adults.' *Gait & Posture*, 52 pp. 272-279.

Reeser, L. A., Susman, R. L. and Stern, J. T., Jr. (1983) 'Electromyographic studies of the human foot: experimental approaches to hominid evolution.' *Foot Ankle*, 3(6), May-Jun, pp. 391-407.

Richman, J. S. and Moorman, J. R. (2000) 'Physiological time-series analysis using approximate entropy and sample entropy.' *Am J Physiol Heart Circ Physiol*, 278(6), Jun, pp. H2039-2049.

Rockar, P. A., Jr. (1995) 'The subtalar joint: anatomy and joint motion.' *J Orthop Sports Phys Ther*, 21(6), Jun, pp. 361-372.

RODRIGUEZ-SANZ, D et al (2018) 'Foot health and quality of life among university students: cross-sectional study'. Sao Paulo Med. J., vol.136, n.2, pp.123-128.

Roerdink, M., De Haart, M., Daffertshofer, A., Donker, S. F., Geurts, A. C. and Beek, P. J. (2006) 'Dynamical structure of center-of-pressure trajectories in patients recovering from stroke.' *Exp Brain Res*, 174(2), Sep, pp. 256-269.

Rojas-Martínez, M., Mañanas, M. A. and Alonso, J. F. (2012) 'High-density surface EMG maps from upper-arm and forearm muscles.' *Journal of NeuroEngineering and Rehabilitation*, 9(1) p. 85.

Rojas-Martínez, M., Mañanas, M. A., Alonso, J. F. and Merletti, R. (2013) 'Identification of isometric contractions based on High Density EMG maps.' 23(1) pp. 33-42.

Rowland, L. A., Bal, N. C. and Periasamy, M. (2015) 'The role of skeletal-muscle-based thermogenic mechanisms in vertebrate endothermy.' *Biological reviews of the Cambridge Philosophical Society*, 90(4), 11/25, pp. 1279-1297.

Ruhe, A., Fejer, R. and Walker, B. (2011) 'Center of pressure excursion as a measure of balance performance in patients with non-specific low back pain compared to healthy controls: a systematic review of the literature.' *Eur Spine J*, 20(3), Mar, pp. 358-368.

Schiaffino, S. and Reggiani, C. (2011) 'Fiber types in mammalian skeletal muscles.' (1522-1210 (Electronic))

Sherrington, C. S. (1925) 'Remarks on some aspects of reflex inhibition.' *Proc. R. Soc. Lond.*, 97 pp. 519-545.

Simon, J., Doederlein, L., McIntosh, A. S., Metaxiotis, D., Bock, H. G. and Wolf, S. I. (2006) 'The Heidelberg foot measurement method: development, description and assessment.' *Gait Posture*, 23(4), Jun, pp. 411-424.

Slifkin, A. B. and Newell, K. M. (1999) 'Noise, information transmission, and force variability.' *Journal of Experimental Psychology: Human Perception and Performance*, 25(3) pp. 837-851.

Sokal, R. R. and Rohlf, F. J. (1995) *Biometry: The Principles and Practice of Statistics in Biological Research.* Co., W. H. F. a. (ed.) 3rd ed.

Soysa, A., Hiller, C., Refshauge, K. and Burns, J. (2012) 'Importance and challenges of measuring intrinsic foot muscle strength.' *Journal of Foot and Ankle Research*, 5, 11/26

Stashuk, D. W. (1999) 'Decomposition and quantitative analysis of clinical electromyographic signals.' *Medical Engineering & Physics*, 21 pp. 389-404.

Suda, E. Y., Madeleine, P., Hirata, R. P., Samani, A., Kawamura, T. T. and Sacco, I. C. N. 'Reduced complexity of force and muscle activity during low level isometric contractions of the ankle in diabetic individuals.' *Clinical Biomechanics*, 42 pp. 38-46.

Svendsen, J. H. and Madeleine, P. (2010) 'Amount and structure of force variability during short, ramp and sustained contractions in males and females.' *Hum Mov Sci*, 29(1), Feb, pp. 35-47.

Troiano, A., Naddeo, F., Sosso, E., Camarota, G., Merletti, R. and Mesin, L. (2008) 'Assessment of force and fatigue in isometric contractions of the upper trapezius muscle by surface EMG signal and perceived exertion scale.' *In Gait Posture*. Vol. 28. Netherlandspp. 179-186.

Tucker, K., Falla, D., Graven-Nielsen, T. and Farina, D. (2009) 'Electromyographic mapping of the erector spinae muscle with varying load and during sustained contraction.' *J Electromyogr Kinesiol*, 19

Vieira, T., Loram, I., Muceli, S., Merletti, R. and Farina, D. (2011) 'Postural activation of the human medial gastrocnemius muscle:are the muscle units spatially localised?' *J Physiol*, 589.2 pp. 431-443.

Vieira, T. M., Botter, A., Minetto, M. A. and Hodson-Tole, E. F. (2015) 'Spatial variation of compound muscle action potentials across human gastrocnemius medialis.' *J Neurophysiol*, 114(3), Sep, pp. 1617-1627.

Vieira, T. M. M., Windhorst, U. and Merletti, R. (2010) 'Is the stabilization of quiet upright stance in humans driven by synchronized modulations of the activity of medial and lateral gastrocnemius muscles?' *Journal of Applied Physiology*, 108(1) pp. 85-97.

Vieira, T. M. M., Minetto, M. A., Hodson-Tole, E. F., Botter, A. and (2013) 'How much does the human medial gastrocnemius muscle contribute to ankle torques outside the sagittal plane?' *Human Movement Science*, 32 pp. 753-767.

von Tscharner, V. (2000) 'Intensity analysis in time-frequency space of surface myoelectric signals by wavelets of specified resolution.' *In J Electromyogr Kinesiol*. Vol. 10. Englandpp. 433-445.

Wakeling, J. M., Kaya, M., Temple, G. K., Johnston, I. A. and Herzog, W. (2002) 'Determining patterns of motor recruitment during locomotion.' *J Exp Biol*, 205(Pt 3), Feb, pp. 359-369.

Wakeling and Hodson-Tole, (2017), " How do the mechanical demands of cycling affect the information content of the EMG?", Medicine and science in sports and exercise-Under Review-

Winter, D. (2009) *Biomechanics and Motor Control of Human Movement.* Fourth ed.

Yang, D. D., Hou, W. S., Wu, X. Y., Zheng, X. L., Zheng, J. and Jiang, Y. T. (2011) *Changes in spatial distribution of flexor digitorum superficialis muscle activity is correlated to finger's action.* Aug. 30 2011-Sept. 3 2011.

Yentes, J. M., Hunt, N., Schmid, K. K., Kaipust, J. P., McGrath, D. and Stergiou, N. (2013) 'The appropriate use of approximate entropy and sample entropy with short data sets.' *Ann Biomed Eng*, 41(2), Feb, pp. 349-365.

Zandiyeh, P. and von Tscharner, V. (2013) 'Reshape scale method: A novel multi scale entropic analysis approach.' *Physica A: Statistical Mechanics and its Applications*, 392(24), 2013/12/15/, pp. 6265-6272.

Zelik, K. E., La Scaleia, V., Ivanenko, Y. P. and Lacquaniti, F. (2015) 'Coordination of intrinsic and extrinsic foot muscles during walking.' *European Journal of Applied Physiology*, 115(4), 2015//, pp. 691-701.

Zhang, X., Schutte, K. H. and Vanwanseele, B. 'Foot muscle morphology is related to center of pressure sway and control mechanisms during single-leg standing.' (1879-2219 (Electronic))

Zhang, X., Ren, X., Gao, X., Chen, X. and Zhou, P. 'Complexity Analysis of Surface EMG for Overcoming ECG Interference toward Proportional Myoelectric Control.'

Appendix A

Is it possible to quantify temporal and spatial patterns of activation of human intrinsic foot muscles?

Elisabetta Ferrari [(1)], Glen Cooper [(2)], Neil D. Reeves [(1)], Emma Hodson-Tole [(1)]
(1) School of Healthcare Science, Manchester Metropolitan University, Manchester, UK
(2) Manchester University, Manchester, UK

Introduction

Pathologies and deformities that affect foot functioning can have major impact on a person's quality of life, with significant associated costs for healthcare providers. Although foot anatomy is complex, previous studies of function usually focus on one sub-portion (e.g. one muscle), so, it is not clear how a number of muscles within the foot interact in healthy individuals. Therefore, the aim of this study was to investigate whether it is possible to quantify physiologically relevant temporal and spatial activation patterns of the intrinsic foot muscles, from the plantar foot surface.

Methods

All procedure were approved by the local ethics committee. Surface EMGs (sEMG) were collected from twenty-two healthy participants (mean±sd:age 41.77±15.08 years, body mass 73.68±16.13 kg, height 173.68±10.67 cm), who completed simple postural tasks. Participants stood on a force plate with a 64-channel grid of electrodes on the plantar surface of the right foot and a whole body 54 marker set applied for kinematics data. sEMG from the intrinsic foot muscles were initially investigated visually to discard channels showing poor contact or high levels of noise. Frequency and amplitude components were extracted to explore whether the signals were the result of physiological muscle activation. Median frequencies and root mean square (RMS) amplitude were calculated for three tasks: two foot quiet standing, deliberate anterior-posterior sways and two foot standing on tiptoe, enabling comparison of sEMG features between a quasi-static and motion based conditions and while there was no contact between the ground and the grid. To investigate whether signals were affected by the shift in foot pressure during movement, RMS values for each channel of the grid were calculated for epochs of anterior and posterior sway. Entropy (measure of uniformity) was computed to evaluate spatial distribution in muscle activation [1]. Regions showing highest activation were segmented and the centre of gravity (CoG) in medial/lateral and anterior/posterior directions calculated [1]. Correlations between force plate measures of centre of pressure (CoP) and CoG were calculated.

Results

The lowest RMS values occurred during quiet standing. The task involving deliberate sways showed intermediate RMS values and the task involving standing on two foot tiptoe showed the highest. Median frequency was highest during quiet standing and lower during the other two tasks. Both median frequency and RMS values for the three conditions were within physiological ranges [2][3]. The r^2 values from the correlation between the CoG and CoP were in the range of 0.0607 ±0.0601, indicating no correlation. Entropy values showed different levels of uniformity between tasks, with more uniform distribution during motion.

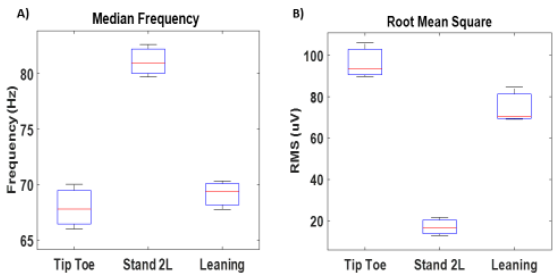

Figure 0-1 Median frequency (A) and root mean square (B) for quiet standing (Stand 2L), anterior/posterior sways (Leaning); two foot standing on tiptoe (Tip Toe)

Discussion

Both median frequency and RMS values indicate the EMG signals recorded are representative of physiological muscle activation. Moreover, the RMS values show the highest activation while the grid was not in contact with the floor (tiptoe), suggesting that foot pressure does not influence the amplitude of the signal (Fig. 1). Also, no correlation between the centre of gravity calculated from surface EMG amplitude and the centre of pressure from the force plate suggests that the EMG signals from the intrinsic foot muscles are not the representation of the shift of foot pressure on the grid and may therefore be considered as indicators of neuromuscular function. It is therefore possible to investigate spatial and temporal features of intrinsic foot muscle activation patterns non-invasively, which could help inform understanding of foot muscle properties and function in health and disease.

References

1. Farina D et al, JEK, 18:16-25, 2008.
2. De Luca C.J. et al , J Biomech , 45:1573-1579, 2010.
3. Farina D et al, J Appl Phys,11: 1215-1230,2014

Appendix B

IS IT POSSIBLE TO QUANTIFY TEMPORAL AND SPATIAL PATTERNS OF ACTIVATION OF INTRINSIC HUMAN FOOT MUSCLES?

Ferrari E[1], Cooper G[2], Reeves N[1], Weightman A[2], Hodson-Tole E[1]

[1]Manchester Metropolitan University, Manchester, UK

[2]University of Manchester, Manchester, UK

Science and Engineering Symposium, Manchester Metropolitan University, September 2016

The human foot is critical for locomotion and posture, therefore pathologies and deformities, which affect its functioning, can have relevant impact on a person's quality of life, with significant associated costs for healthcare providers. Although the anatomy

of the foot is very complex, with four layers of muscles in a narrow compartment, previous studies of function usually focus on one sub-portion (e.g. one muscle), which is not descriptive of the overall biomechanical behaviour; moreover, how intrinsic foot muscles activate to achieve motion is still not clear. Therefore, the aim of this study is to quantify patterns of intrinsic foot muscle activation, by recording temporal and spatial activation across the plantar foot surface.

Surface EMG was collected from twenty-two healthy participants (40±13 years old). Participants stood with a 64-channels grid of electrodes on the plantar surface of the foot, while performing simple motor tasks. Each surface EMG trace was divided in 1s non-overlapping epochs and root mean square values were calculated for each channel, resulting in a 64-root mean square map for each epoch. The entropy of the activation pattern across the 64-channels for each epoch was quantified to provide information about changes in activation uniformity over time (Farina et al. 2008). Preliminary results are showing promise for this technique.

These methods could provide a tool that can evaluate functional significance of muscle activation patterns, adding basic understanding of foot function by investigating patterns from different populations (e.g. trained people), and also clinical indicators of pathology which may have diagnostic and monitoring value (e.g. preventing foot ulceration in diabetes patients)

Farina D, Leclerc F, Arendt-Nielsen L, Buttelli O and Madeleine P (2008). "The change in spatial distribution of upper trapezius muscle activity is correlated to contraction duration." Journal of Electromyography and Kinesiology **18**: 16-25.